

Molecular tuning of DNA framework-programmed silicification by cationic silica cluster attachment

Xinxin Jing^{1,2,8}, Haozhi Wang^{1,8}, Jianxiang Huang^{3,4,8}, Yingying Liu^{1,8}, Zimu Li¹, Jielin Chen¹, Yiqun Xu¹, Lingyun Li¹, Yunxiao Lin¹, Damiano Buratto^{3,4}, Qinglin Xia⁵, Muchen Pan⁵, Yue Wang⁵, Mingqiang Li¹, Ruhong Zhou^{3,4,*}, Xiaoguo Liu^{1,*}, Stephen Mann^{6,7,*} and Chunhai Fan^{1,*}

1. School of Chemistry and Chemical Engineering, New Cornerstone Science Laboratory, Frontiers Science Center for Transformative Molecules, Zhangjiang Institute for Advanced Study and National Center for Translational Medicine, Shanghai Jiao Tong University, Shanghai 200240, China.

2. Institute of Molecular Medicine, Shanghai Key Laboratory for Nucleic Acid Chemistry and Nanomedicine, Renji Hospital, School of Medicine, Shanghai Jiao Tong University, Shanghai, China.

3. Institute of Quantitative Biology, College of Life Sciences, and Department of Physics, Zhejiang University, Hangzhou, China.

4. Shanghai Institute for Advanced Study, Zhejiang University, Shanghai, China.

5. Division of Physical Biology, CAS Key Laboratory of Interfacial Physics and Technology, Shanghai Institute of Applied Physics, Chinese Academy of Sciences, Shanghai 201800, China.

6. School of Materials Science and Engineering, Shanghai Jiao Tong University, Shanghai 200240, China.

7. Max Planck-Bristol Centre for Minimal Biology, School of Chemistry, University of Bristol, Bristol BS8 1TS, United Kingdom.

8. These authors contribute equally, Xinxin Jing, Haozhi Wang, Jianxiang Huang and Yingying Liu.

*e-mails: rz24@columbia.edu, liuxiaoguo@sjtu.edu.cn, s.mann@bristol.ac.uk, and fanchunhai@sjtu.edu.cn

Abstract

The organizational complexity of biominerals has long fascinated scientists seeking to understand biological programming and implement new developments in biomimetic materials chemistry. Nonclassical crystallization pathways have been observed and analyzed in typical crystalline biominerals, involving the controlled attachment and reconfiguration of nanoparticles and clusters on organic templates. However, the understanding of templated amorphous silica mineralization remains limited, hindering the rational design of complex silica-based materials. Here, we present a systematic study on the stabilization of self-capping cationic silica cluster (CSC) and their assembly dynamics using DNA nanostructures as programmable attachment templates. By tuning the composition and structure of CSC, we demonstrate high-fidelity silicification at single-cluster resolution, revealing a process of “adaptive templating” involving cooperative adjustments of both the DNA framework and cluster morphology. Our results provide a unified model of silicification by cluster attachment and pave the way towards the molecular tuning of pre- and post-nucleation stages of sol-gel reactions. Overall, our findings provide new insights for the design of silica-based materials with controlled organization and functionality, bridging the gap between biomineralization principles and the rational design of biomimetic material.

Introduction

Nature has created a wide range of biominerals with evolutionary lineage, hierarchical structuration and adaptive functionality¹⁻⁷. The organizational complexity of biominerals across multiple length scales has long intrigued researchers interested in the biological programming of inorganic materials and the potential abstraction of these concepts in biomimetic materials chemistry^{8,9}. Recent studies on crystalline biominerals such as bones¹⁰, teeth¹¹ and shells¹² have advocated a nonclassical crystallization pathway involving the controlled attachment of non-crystalline nanoparticles and clusters to preformed organic templates followed by *in situ* reconfiguration to initiate crystal nucleation and directional growth on the organic matrix⁴. This novel crystallization mechanism has also been demonstrated in a range of biomimetic systems including anatase (TiO_2)¹³, calcium carbonate (CaCO_3)¹⁴⁻¹⁷, hydroxyapatite ($\text{Ca}_{10}(\text{PO}_4)_6(\text{OH})_2$)^{18,19}, lead selenide (PbSe)^{20,21} and magnetite (Fe_3O_4)^{22,23}.

Amongst the wide diversity of biominerals, silica is the most abundant amorphous phase. It is naturally deposited in diatoms²⁴, sea sponges²⁵, radiolaria²⁶ and plants²⁷ via highly controlled and programmed processes involving the *in vivo* condensation of silicic acid in the presence of specific proteins to produce exquisite complex microarchitectures with unusual mechanical properties. For example, the axial filament at the center of the silica spicule of the demosponge *T. aurantium*^{5,28} consists of an integrated hybrid structure consisting of specific enzymes (silicateins) packed in a hexagonal superstructure with amorphous silica occupying the interstitial spaces among the protein units. Much effort has been undertaken to synthesize various types of microscopically ordered amorphous silica by integrating classical sol-gel processes with supramolecular templates based on surfactant, protein or DNA self-assembly²⁹⁻³², or through the use of positive charged proteins and polyamines to control silica nucleation and growth³³. Nevertheless, the general lack of a unified theoretical model hampers the microscopic understanding of templated silicification, thereby constraining the rational design of new silica-based materials with complex microscopic organization and functionality.

Silica sol-gel reactions are typically undertaken via a successive process involving the hydrolysis of silicon alkoxides to produce silanol monomers, linear and cyclic oligomers, and pre-nucleation clusters ~1.0 nm in size, which give rise to primary silica nanoparticles that associate into orderless gels or sols depending on the extent of crosslinking and condensation, respectively (**Extended Data Fig. 1a**)^{34,35}. Although this polymerization mechanism is distinctly different from the classical models of crystallization, in principle the transitioning from primary nanoparticles to 3D networks or colloidal dispersions resembles particle attachment mechanisms of non-classical crystallization in which disordered pre-nucleation clusters serve as reconfigurable building units for the formation of crystalline phases³⁶. However, elucidation of the pre- and post-nucleation stages of silicification is difficult because of the transient nature of siloxane oligomers and their rapid dehydration and progressive polymerization into large structures.

To address this challenge, we tuned the composition, structure and arrested growth of silica pre-nucleation clusters by controlling the co-condensation of N-trimethoxysilylpropyl-N,N,N-trimethylammonium chloride (TMAPS) and tetraethyl orthosilicate (TEOS) to generate monodisperse suspensions of ultrastable self-capping cationic silica cluster (CSC) (**Extended Data Fig. 1b**) which are characterized using a combination of cryogenic transmission electron microscopy (cryo-EM), synchrotron-based small angle X-ray scattering (SAXS), dynamic light scattering (DLS), high-speed atomic force microscopy (HS-AFM), matrix-assisted laser desorption ionization mass spectrometry (MALDI MS), solid-state magic angle spinning ^{13}C and ^{29}Si nuclear magnetic resonance (MAS NMR), ion trap mass spectrometer (IT MS) and Monte Carlo/molecule dynamics (MC/MD) hybrid simulations. Our results imply a general mechanism for the widespread presence of template-directed amorphous mineralization in natural and synthetic systems and provide a step to programmable biomimetic silica-based hybrid materials.

Results

Synthesis and characterization of cationic silica clusters (CSC)

CSC were discovered at pH 8 by co-condensation of mixed aqueous solutions of TMAPS and TEOS. By tuning the TMAPS/TEOS ratio in TE-MgCl₂ buffer, we obtained a series of size-controlled CSC after 6-day maturation of the mixture (**Fig. 1a, Supplementary Fig. 1 to 3, Supplementary Table 1**), which indicated that the size of the CSC increased as the TMAPS/TEOS ratio was decreased. Synchrotron SAXS measurements showed highly uniform diameters of gyration (D_g) for these CSC, from ~6.8 nm ~4.7 nm ~3.9 nm to ~1.3 nm (**Fig. 1b and 1c**). We used the D_g values to designate the different samples obtained under different molar ratios, eg. 3.9 nm-CSC. In each case, the aqueous CSC dispersions displayed a ζ -potential typically between +30 to +40 mV and were stable for at least two months. Binary phase diagrams of hydrodynamic size plotted for different TMAPS/TEOS molar ratios indicated that the sizes of the CSC were primarily dependent on TMAPS concentration (**Fig. 1d, Supplementary Table 2**). Cluster sizes smaller than 1.0 nm were determined for TMAPS concentrations exceeding 61.6 mM, suggesting that high concentrations of TMAPS inhibited the polymerization process. Corresponding phase maps of conductivity (**Fig. 1e**) and ζ -potential (**Supplementary Fig. 4, Supplementary Table 3**) showed analogous increases in the positive surface charge along with a stepwise increase in the conductivity with increasing TMAPS concentration. A progressive decrease in pH from an initial value of 8.0 occurred as the TMAPS or TEOS concentrations decreased or increased, respectively, due to increased consumption of hydroxide ions during the sol-gel process (**Supplementary Fig. 5**). Corresponding cryo-EM images indicated that the generation of homogeneous CSC at pH 8 was replaced with a heterogeneous mixture of silica pre-nucleation clusters and CSC at an initial pH of 6 due to the rate of silicon alkoxide hydrolysis being higher than the condensation rate under acidic conditions (**Supplementary Fig. 6**). Taken together, the results were consistent with the presence of positively charged trimethylammonium side chains at the

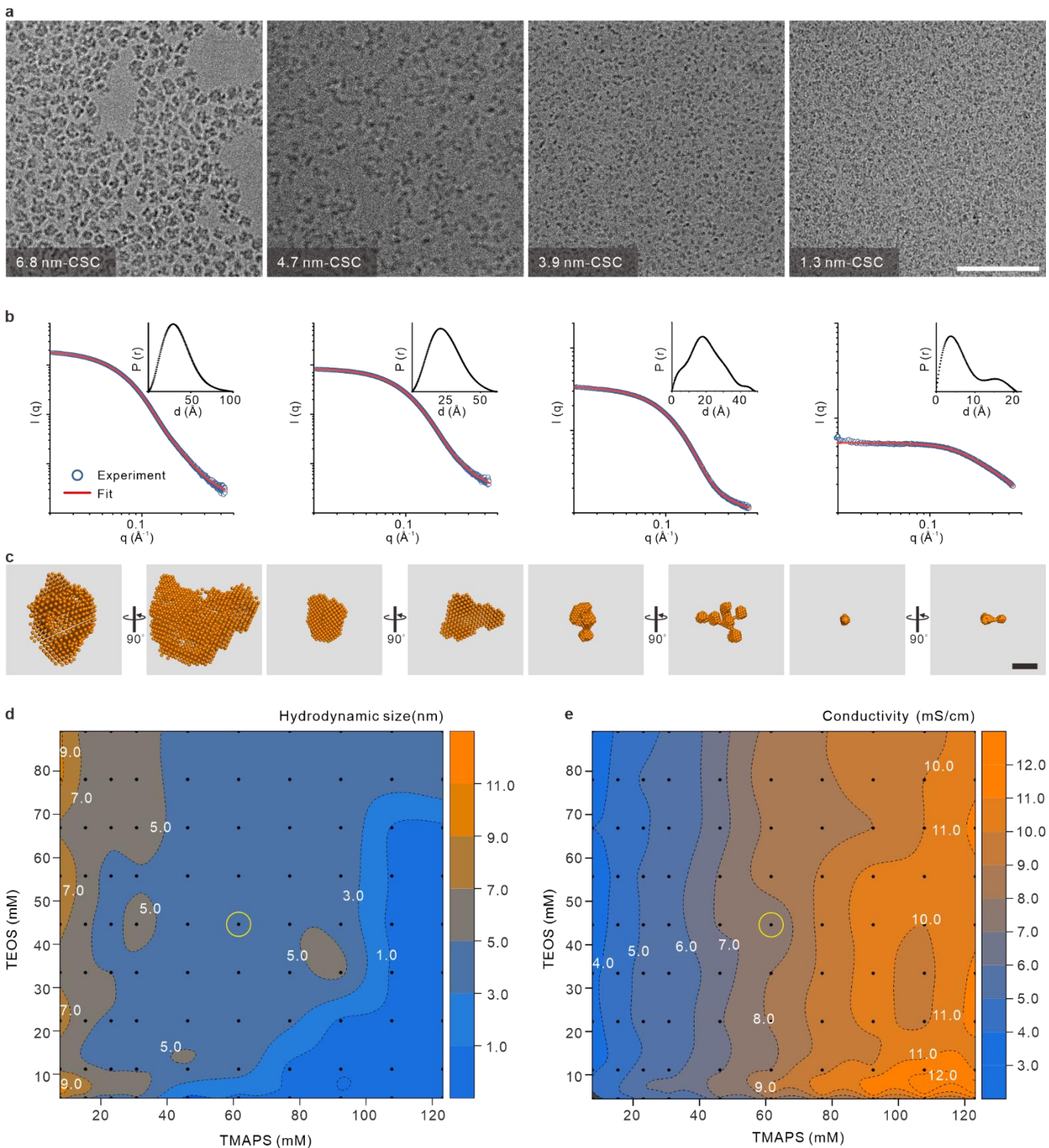


Fig. 1 | Morphology, size and conductivity of typical CSC. **a.** Cryo-EM images for typical CSC with calculated diameters of gyration (D_g) of 6.8 nm, 4.7 nm, 3.9 nm and 1.3 nm. Scale bar, 50 nm. **b.** SAXS 2D profiles and Pair Distance Distribution Function (PDDF, $P(r)$) plots of these CSC. In each case, the SAXS profiles revealed monodisperse populations of CSC. The PDDF plots of 6.8 nm- and 4.7 nm-CSC showed characteristic deflected Gaussian Distribution features, indicating ellipsoidal structures. Interestingly, the PDDF plots of 3.9 nm-CSC showed multiple shoulder peaks at $\sim 5 \text{ \AA}$, $\sim 30 \text{ \AA}$ and $\sim 45 \text{ \AA}$, indicating a branched necklace or random coil-like structure. The PDDF plots of 1.3 nm-CSC showed bimodal distributions with different peak intensities, indicating a dumbbell shape with different sphere sizes. **c.** *Ab initio* calculations of the molecular envelopes from the SAXS data revealed that 3.9 nm-CSC were composed of seven subunits with diameters of $\sim 1 \text{ nm}$. Scale bar, 2 nm. **d** and **e**, Hydrodynamic size and conductivity binary phase diagrams of CSC ($N = 90$). The yellow circles highlight the TMAPS/TEOS ratio for 3.9 nm-CSC.

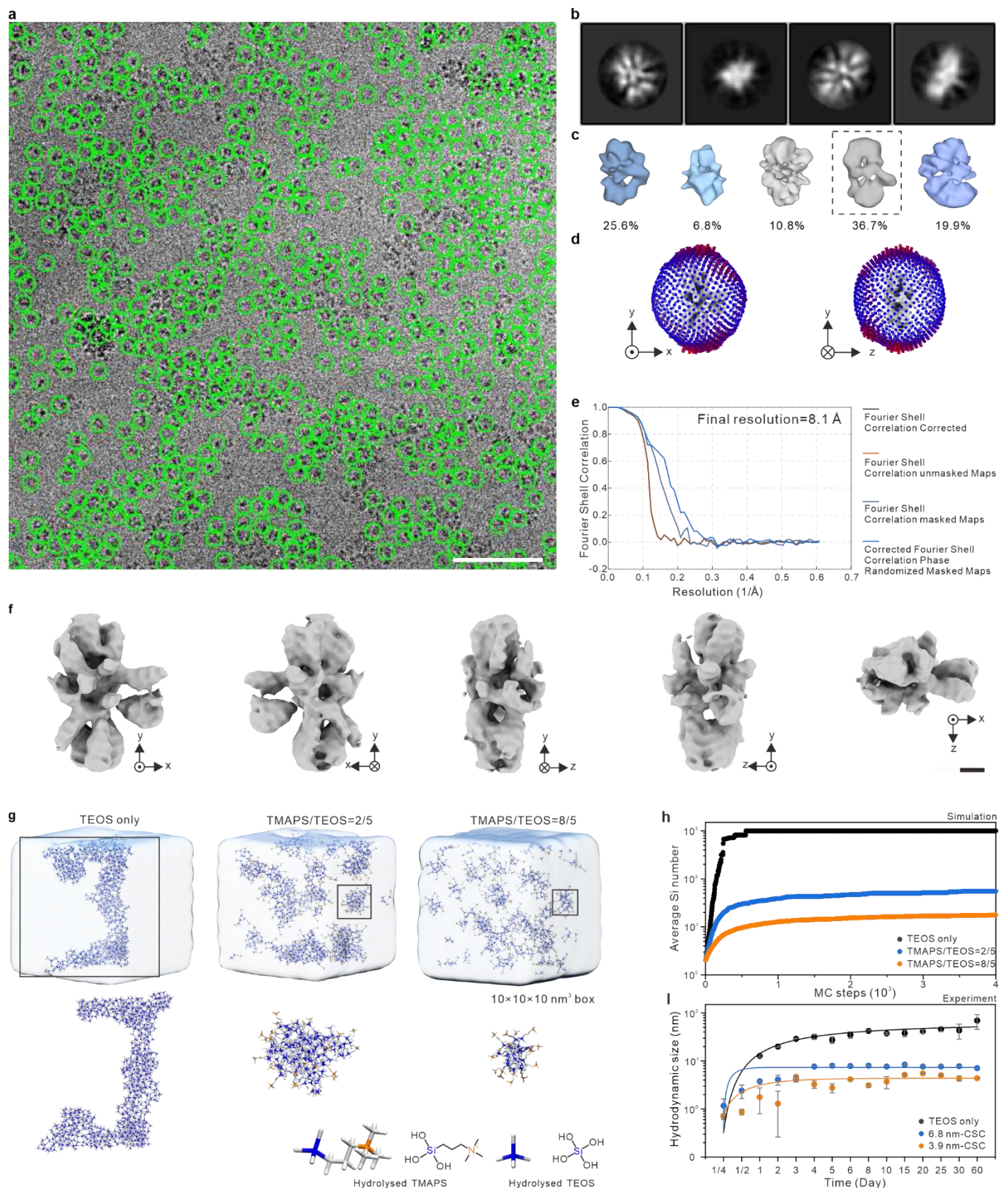


Fig. 2 | Single-particle analysis and MC/MD simulations of 3.9 nm-CSC. **a**, Representative image. The green circles highlight the auto-picked CSC particles. Scale bar, 50 nm. **b**, Representative 2D class averages. **c**, Representative 3D class averages. **d**, Histogram representing the orientational distribution of the particles from the 36.7% class. **e**, Fourier shell correlation plots. **f**, Five different views of the electron density maps of the particles from the 36.7% class. Scale bar, 1 nm. **g**, MC/MD simulations of the initial stages in silica sol-gel condensation. The presence of TMAPS interrupts the continuous polymerization of hydrolyzed TEOS to produce ultrastable CSC (middle and right) with sizes determined by the TMAPS/TEOS molar ratio. Top images; total simulation systems using a $10 \times 10 \times 10 \text{ nm}^3$ water box. Bottom images; representative polymerized silica clusters for three different TMAPS/TEOS ratios; Si atoms (blue), N atoms (orange), O atoms (gray) and H atoms (white). **h**, Calculated average Si atom numbers of single clusters formed by condensation of TEOS alone or TMAPS/TEOS at ratios of 0.4 or 1.6 for increasing MC steps. **d**, Corresponding experiments using TEOS alone or TMAPS/TEOS ratios of 0.4 and 1.6 showed time-dependent changes in cluster hydrodynamic size. In the TEOS only system, the silica particles increased continuously to 100 nm after 60 days while the CSC reached their maximum sizes after 4 days and remained stable for at least 60 days when prepared from mixtures of TMAPS and TEOS.

surface of the co-condensed silica clusters that acted as self-capping agents for constrained polymerization and stabilization of the CSC.

High-resolution cryo-EM images of samples prepared at a TMAPS/TEOS ratio of 1.40 showed highly monodisperse CSC with a size distribution of 3.3 ± 0.7 nm (**Fig. 2a**). The reconstructed electron density 3D model of discrete 3.9 nm-CSC revealed non-spherical and loosely packed features, with a maximum 3D spatial resolution of 0.96 nm (**Fig. 2b-f**). This was consistent with DLS and synchrotron SAXS measurements that gave a hydrodynamic diameter and calculated D_g of 3.6 ± 0.1 nm and ~ 3.9 nm, respectively.

To reveal the structural features of the 3.9 nm-CSC, we performed *ab initio* calculations of the molecular envelopes derived from the SAXS data, which revealed a hierarchically arrangement of seven loosely packed primary units of ~ 1.2 nm (**Fig. 1c**). The Kratky plots from the SAXS 2D profiles of CSC prepared at lower TMAPS/TEOS molar ratios indicated that the clusters increased in density as their size increased (**Extended Data Fig. 2**). We identified distinctive curves including linear divergence (1.3 nm-CSC, TMAPS/TEOS = 2.80), partial parabolic convergence (3.9 nm-CSC, TMAPS/TEOS = 1.40) and parabolic convergence (4.7 nm- and 6.8 nm-CSC, TMAPS/TEOS = 0.70 and 0.35, respectively)³⁷, which reflected the structural evolution of the CSC from linear to random-coil to spherical, according to the *Porod* rule and *Power law*³⁸ ($I(q) \propto q^{-n}$). These structural changes imply that the 3.9 nm-CSC consist of a flexible chain of corner-shared organosiloxane/siloxane tetrahedral that can be readily deformed or compressed.

The ability to tune the molecular structure of the CSC via changes in the TMAPS/TEOS molar ratio was demonstrated by hybrid MC/MD simulations of the early stages of silicification. For this, we simulated the initial co-condensation behavior in mixed solutions of TMAPS and TEOS placed in a weakly alkaline buffer ($pH = 8.0 \pm 0.1$) within a water box of 10 nm^3 (**Fig. 2g**). The simulations confirmed an effective self-capping effect of TMAPS side chains in which the positively charged $-N^+(CH_3)_3$ groups preferentially covered the surface of the silica clusters. Potential mean force (PMF) analysis performed on two different CSC showed that the outward projection of $-N^+(CH_3)_3$ groups provided both repulsive coulombic forces and steric hindrance that inhibited inter-cluster aggregation and successive polycondensation (**Extended Data Fig. 3**). By contrast, in the absence of TMAPS, simulations of the silica clusters resulted in rapid growth into particles that attained the size limitation of the water box. The MC/MD simulations also demonstrated that the size of the CSC was inversely dependent on the TMAPS/TEOS molar ratio (**Fig. 2h and 2i**). For example, the calculated average number of Si atoms in two typical CSC were 53 ± 3 (TMAPS/TEOS = 2/5) and 18 ± 1 (TMAPS/TEOS = 8/5).

SAXS volume of correlation (V_c)³⁸ and MALDI MS were used to determine the molecular weights (M_w) of the CSC prepared at different TMAPS/TEOS molar ratios. The $V_c M_w$ values of the different CSC were 1,500, 8,300, 18,100 and 46,000 Da, which correlated with the corresponding MALDI MS m/z values of 1,221.1, 8,262.2, 18,001.5 and 52,011.3 (**Fig. 3a and 3b**).

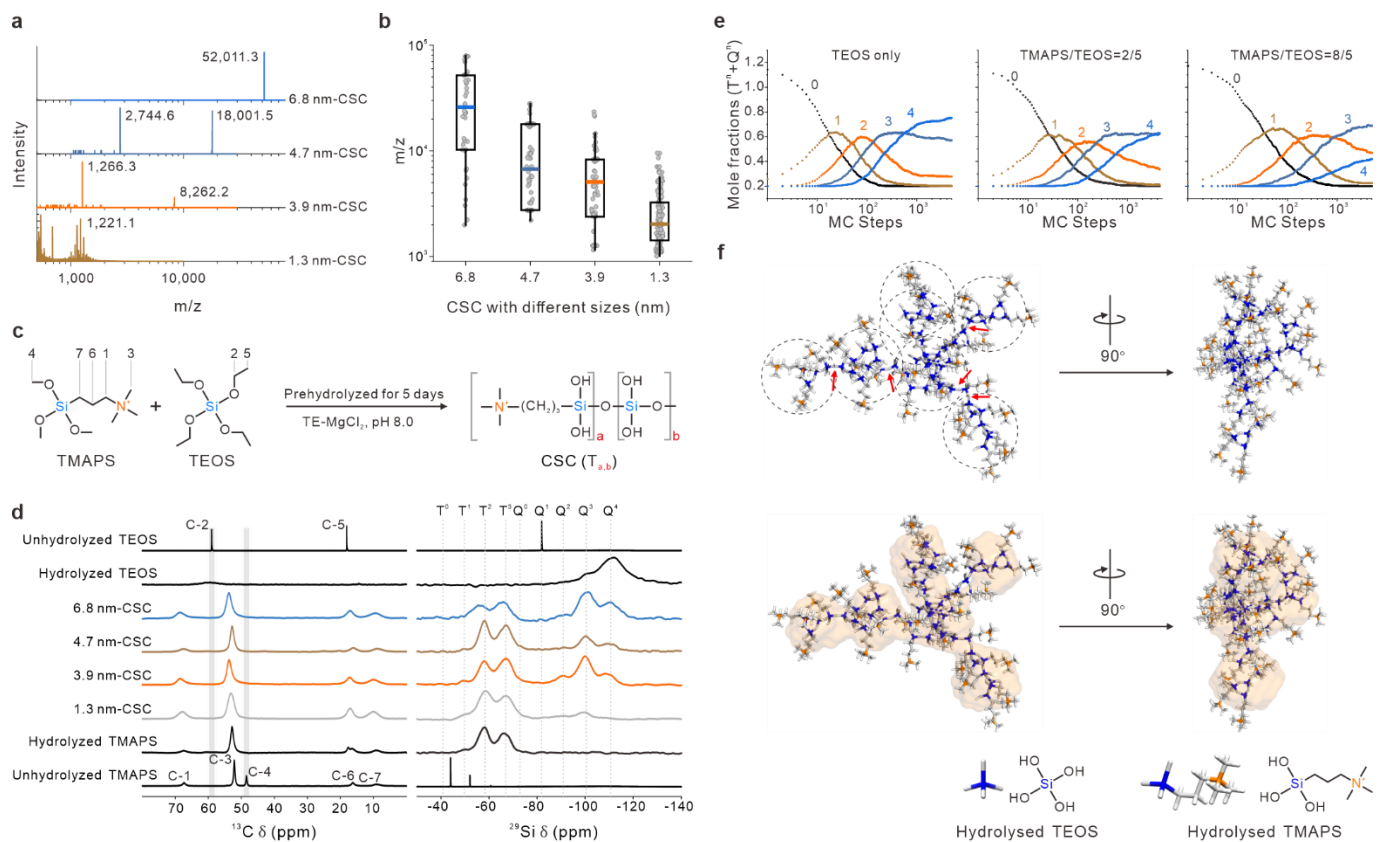


Fig. 3 | Molecular weight, NMR analysis and structural modelling of CSC. **a, b**, Mass spectra of CSC with different TMAPS: TEOS molar ratios (**a**) and scatter plot of m/z values for typical CSC (**b**); from left, $N = 40, 120, 90$ and 173 . **c**, Labelling of C atoms in TMAPS and TEOS used to assign ^{13}C NMR spectra chemical shifts. $T_{a,b}$ labels represent the number of TMAPS and TEOS units present in the CSC. **d**, ^{13}C (left) and ^{29}Si MAS (right) NMR spectra of various freeze-dried CSC and single-component samples of unhydrolyzed and hydrolyzed TMAPS or TEOS. Chemical shifts labelled with T^n or Q^n ($n = 0, 1, 2, 3$ or 4) represent Si atoms either from TMAPS or TEOS with different crosslinking degrees, respectively. **e**, Simulated evolutions of $T^n + Q^n$ distributions for three typical reaction conditions undertaken with increasing TMAPS/TEOS molar ratios. **f**, Representative atomic structure models of a 3.9 nm-CSC ($T_{32,29}$) based on siloxane-linked tetrahedra. Top image; front and side views showing 7 subunits (dashed circles) and Si-O-Si linkages between adjacent subunits (red arrows). Bottom image displays the overlapping of the atomic structure and coarse grained SAXS model of the 3.9 nm-CSC.

Solid-state ^{13}C and ^{29}Si MAS NMR spectroscopies were used to determine the molecular structure of the CSC produced by co-condensation (**Fig. 3c**). In general, the smallest CSC (1.3 nm-CSC) had a calculated molecular form of $T_{5,3}$, where a and b represent the number of TMAPS and TEOS units in the general form $T_{a,b}$. This was equivalent to the protonated and chlorinated cluster, $\text{C}_{30}\text{H}_{86}\text{Cl}_5\text{N}_5\text{O}_{19}\text{Si}_8^+$ produced by the loss of 8 water molecules via dehydration during formation of siloxane linkages. In contrast, the 3.9 nm-CSC showed two characteristic m/z peaks of 1,266.3 and 8,262.2, which corresponded to $T_{5,5}$ and $T_{32,29}$ structures with the loss of 12 and 78 water molecules, respectively. Specifically, ^{13}C MAS NMR spectra of freeze-dried CSC were consistent with complete hydrolysis of the TEOS and TMAPS alkoxide groups, as evidenced by the disappearance of both C2 (59 ppm) and C4 (48 ppm) peaks that were present in the spectra of pure TEOS and TMAPS molecules (**Fig. 3d**, left panel). Notably, four ^{13}C peaks from TMAPS (C1, 67 ppm; C3, 53 ppm; C6, 17 ppm; C7, 9 ppm) were retained in all the samples without significant changes in intensity ratios, suggesting that hydrolyzed TMAPS groups were incorporated into the CSC. The presence of significant proportions of T^2 and T^3 peaks in the ^{29}Si MAS NMR spectra confirmed co-polymerization of TMAPS and TEOS in the CSC as well as localization of TMAP side chains

at the cluster surface (**Fig. 3d**, right panel, **Supplementary Table 4**), where T^n ($n = 0, 1, 2$ or 3) represents Si atoms in the TMAPS molecules with different degrees of crosslinking. Moreover, the ^{29}Si MAS NMR spectra indicated a relatively low degree of crosslinking in the CSC, with an apparent increase in peak intensities from Q^4 to Q^3 to Q^2 as the size of CSC decreased, where Q^n ($n = 0, 1, 2, 3$ or 4)³⁹ represent Si atoms in TEOS molecules with different degrees of crosslinking. This agreed well with the calculated distribution of Q^n from MC/MD simulations (**Fig. 3e**). Specifically, the $Q^4/Q^3/Q^2$ percentages for the 3.9 nm-CSC and 1.3 nm-CSC were 12.0/80.7/7.2 and 0.0/70.9/29.1, respectively, suggesting the presence of linear or cyclic structures in both cases⁴⁰, in agreement with the cryo-EM images of the corresponding CSC (**Supplementary Fig. 7**).

Taken together, the SAXS *Kratky* plots, NMR spectra and MALDI MS data indicate a progressive process of condensation and densification as the CSC increase in size to produce ultrastable clusters. The growth of pre-nucleation silica clusters with molecular masses of ~1.2 kDa is constrained by segregation of TMAPS side chains at the cluster/water interface such that polycondensation becomes self-limited. This was consistent with the atomic structure model for the 3.9 nm-CSC ($T_{32,29}$), which showed a branched chain of corner-shared siloxane tetrahedra comprising seven subunits with TMAP moieties distributed preferentially along the periphery (**Fig. 3f**).

Importantly, analyses on the early stages of silicification revealed the presence of metastable intermediate silica building blocks, which resembled those proposed in the particle attachment mechanism of nonclassical bio-crystallization⁴. As previous studies on the hexactinellid sponge *Euplectella* sp⁴¹ and diatom shells⁴² indicate that discrete silica nanoparticles are closely associated with the microscopic biomineralized architectures, our results provide further support that the production and assembly of stabilized CSC could play a key role in biosilicification.

CSC-directed silicification of programmable DNA frameworks

Having substantiated the existence of ultrastable CSC, we were motivated to investigate the dynamic interactions between the silica clusters and biomacromolecules, e.g., double-stranded DNA (dsDNA) frameworks using HS-AFM (**Fig. 4 and Extended Data Fig. 4**). An aqueous suspension of 3.9 nm-CSC at a concentration of 0.8 mg/L was injected into the liquid HS-AFM sample pool containing two-dimensional (2D) square-latticed triangular DNA origami frameworks. HS-AFM images revealed cluster-by-cluster attachment feature of CSC onto the DNA framework. We observed that freely diffusing CSC located within ~10 nm of the DNA framework were attracted onto the template surface typically within 5-15 seconds (**Fig. 4a**). The attachment appeared to be irreversible with no apparent disassociation back into the external solution over 180 s of consecutive imaging (**Fig. 4a, Supplementary Video 1**). Continuous imaging of the samples over *ca.* 400 s indicated that the CSC were randomly attached onto the DNA framework, suggesting that appropriate inter-DNA helix distances were required for ordered assembly. To test this, we employed two-layer honeycomb-latticed

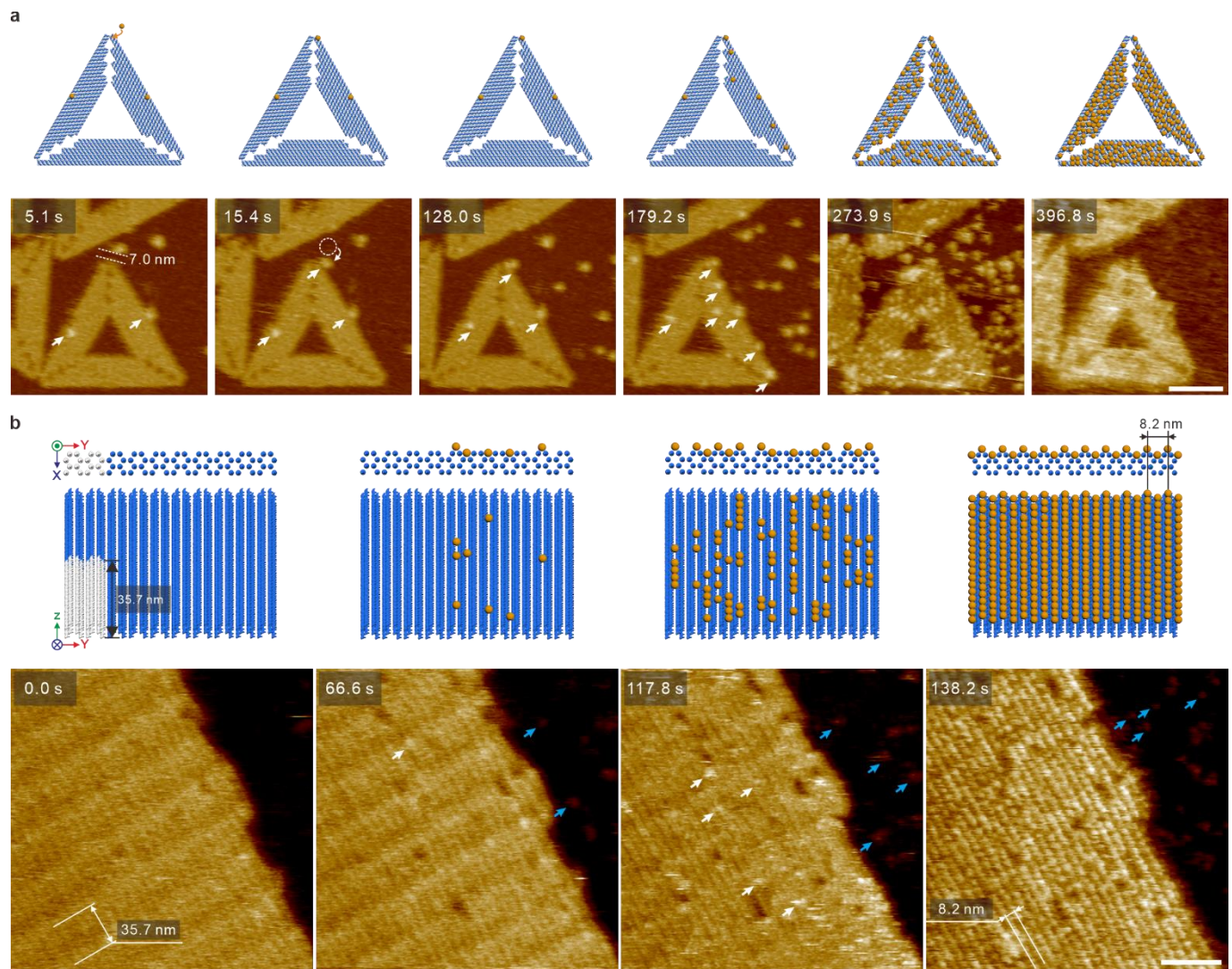


Fig. 4 | In-situ HS-AFM imaging of DNA framework-programmed silicification by CSC attachment. **a**, Schematics and HS-AFM images of single cluster attachment behavior of 3.9 nm-CSC observed on a triangular DNA origami framework. CSC attached to the DNA template are highlighted with white arrows. **b**, Schematics and HS-AFM images of collective assembly behavior of 3.9 nm-CSC observed on a two-layer honeycomb structured Y-Z DNA lattice. Free CSC are highlighted with blue arrows; assembled CSC are highlighted with white arrows. Scale bars, 50 nm.

Y-Z DNA frameworks and observed periodic ordering of the CSC specifically along the Z-axis of the Y-Z DNA lattice, with a center-to-center Y-axis distance of 8.2 nm (**Fig. 4b**). Ordered attachment of the CSC to the DNA nanostructures was accomplished within 5 min even when highly dilute CSC dispersions were used. This resulted in loss of the native framework Z-axis periodicity (35.7 nm), which was readily resolved in the HS-AFM images of the undecorated samples (**Supplementary Video 2**).

Cryo-EM studies further confirmed that the fidelity of template replication was increased by commensurate matching of cluster size and framework architecture. For example, attachment of 3.9 nm-CSC to a 24-helix DNA framework resulted in specific ordering of the clusters onto adjacent DNA helices in the honeycomb lattice (**Fig. 5a**). Interestingly, attachment of the CSC gave rise to uniform expansion of the DNA lattice with the inner pore size increasing from ~2.6 nm to a cluster matching size of ~3.1 nm. In contrast, larger CSC exhibited random attachment along the z-axis, indicating that the DNA framework was not sufficiently flexible to adapt to CSC larger than 3.9 nm (**Fig. 5b to 5d**).

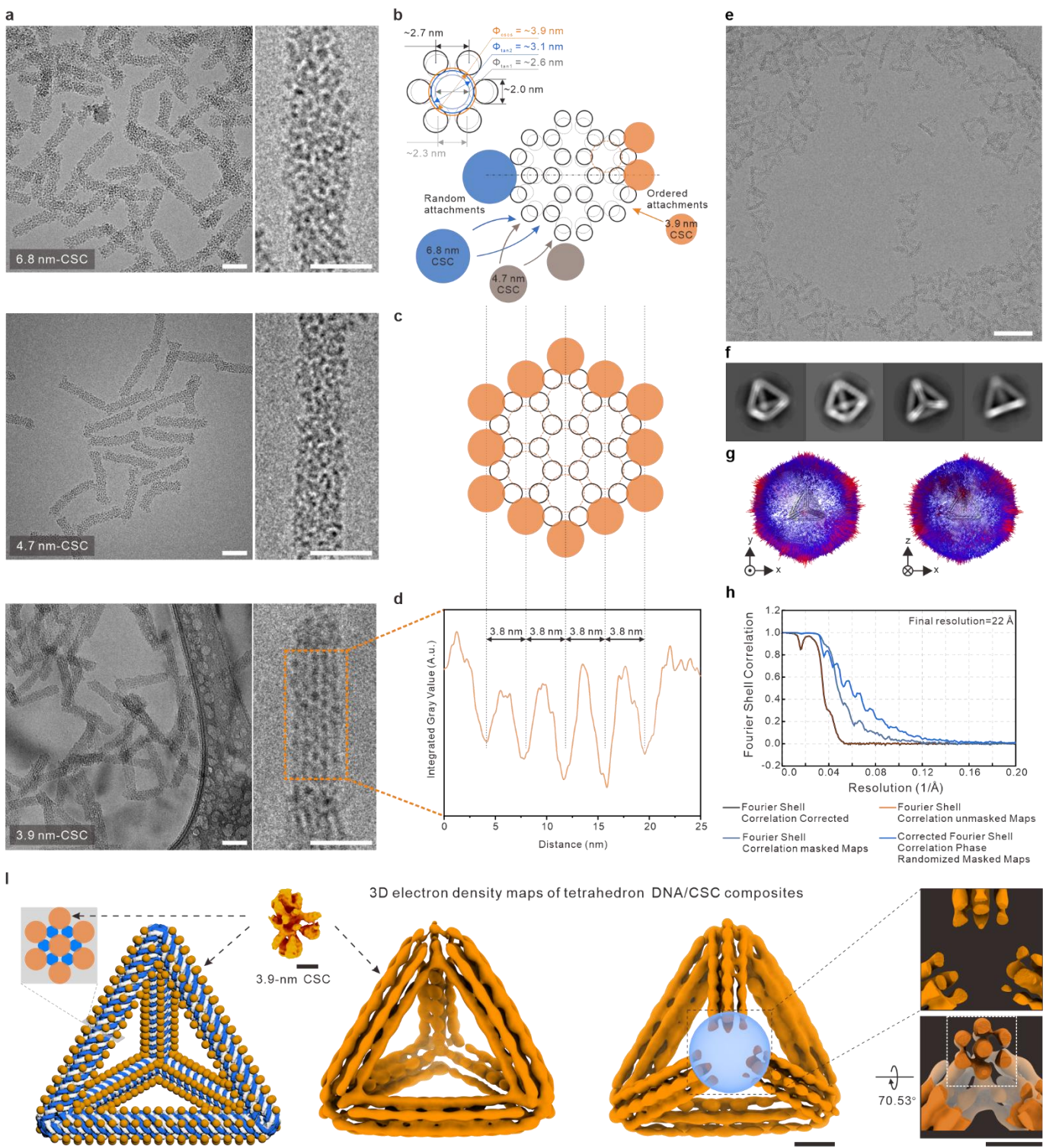


Fig. 5 | Size dependency of CSC during silicification by cluster attachment. **a**, Exemplary cryo-EM images for typical CSC (6.8 nm, 4.7 nm and 3.9 nm) assembled onto a honeycomb latticed 24-helix DNA framework. Of which, only 3.9 nm-CSC showed ordered attachment. Scale bars, 50 nm (left images), 25 nm (right images). **b**, Schematic of the attachment behavior of CSC with different sizes (drawn to scale). Top left inset; lattice expansion of the DNA framework after CSC attachment was illustrated. Where the theoretical diameter of dsDNA is ~2.0 nm and the diameter of internal tangent circle Φ_{tan1} (gray line) for ideal honeycomb structured DNA origami (dotted gray lines) is ~2.6 nm. However, the measured diameter of internal tangent circle Φ_{tan2} (blue line) is ~3.1 nm. Accordingly, the center-to-center distance of adjacent dsDNA strands increases from ~2.3 nm to ~2.7 nm to accommodate 3.9 nm-CSC. Orange circles ($\Phi_{CSC} = \sim 3.9\text{ nm}$) show the relationship between 3.9 nm-CSC and the DNA framework. **c**, Schematic of a section of the CSC/24-helix DNA framework composite. **d**, Line profile of integrated gray value analysis across the CSC/24-helix DNA framework shown in **(a)** (lower right panel, orange box) showed a ~3.8 nm interplanar spacing of the CSC. **e**, Exemplary micrograph of 3.9 nm-CSC-bound tetrahedron DNA framework. Scale bar, 100 nm. **f**, Representative 2D class averages. **g**, Histogram representing the orientational distribution of particles. **h**, Fourier shell correlation plots. **i**, Left, schematics of a 3.9 nm-CSC-bound tetrahedron DNA framework. Middle, 3D electron density maps of the DNA/3.9 nm-CSC nanocomposite determined by means of single-particle reconstruction from cryo-EM data. Right, interceptions generated by the blue sphere highlight the sections that are perpendicular to the long axis of the tetrahedron edges. Scale bars, 10 nm; for 3.9 nm-CSC, 2 nm.

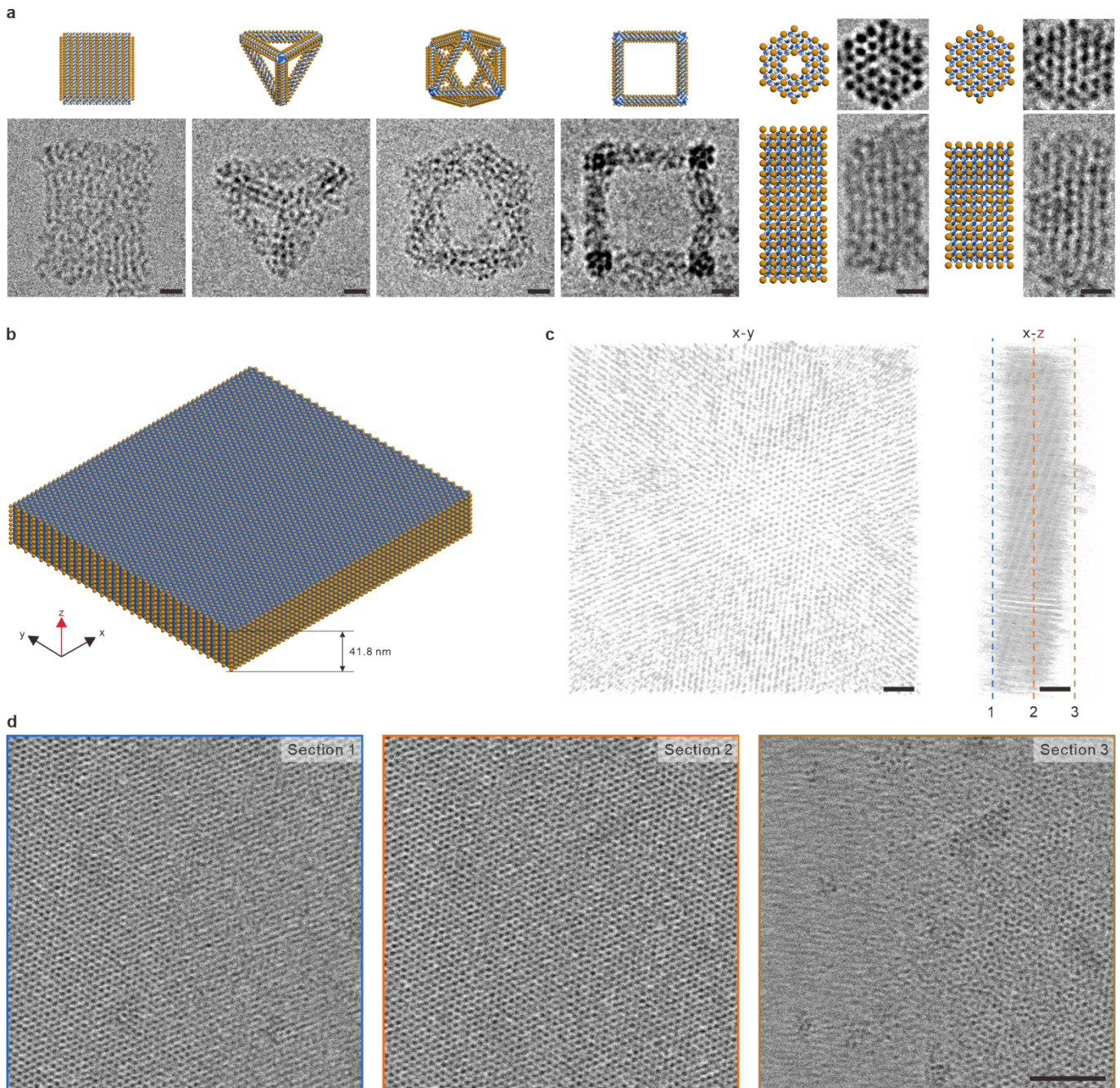


Fig. 6 | DNA framework-programmed CSC attachments. **a**, Representative DNA/CSC composites, including 3.9 nm-CSC bound double-layer, tetrahedron, octahedron, cube, 48-helix and 54-helix DNA frameworks. Scale bars, 10 nm. **b-d**, Schematic illustration, Cryo-ET images and sections of *p6mm* DNA/CSC superstructure. Scale bars, **c** and **d**, 20 nm, **e**, 50 nm.

In other studies, single-particle reconstruction of the cryo-EM data of a CSC-decorated tetrahedron DNA framework at a resolution 2.2 nm revealed that the attached CSC were organized preferentially onto the grooves of adjacent DNA helices with an inter-cluster distance of ~4.1 nm, and also located within the nanopores surrounded by six DNA helices (**Fig. 5e to 5i, Supplementary Fig. 8 and Supplementary Video 3**). These data suggested that high fidelity CSC attachment onto programmable DNA nanostructures is achieved by precise dimensional matching and enhanced by adaptive changes in the template microstructure. Given the above observations, we propose that the self-adapting nature of the silicification mechanism arises from the flexibility and structural dynamics of both the programmable DNA lattice and ultrastable CSC. This cooperativity enables high fidelity

attachment and enables limited levels of mismatch between the cluster and DNA nanopore sizes to be tolerated during the assembly process.

Lastly, we explored the generality of our approach by using a diversity of DNA origami nanostructures such as multihelix-rods, planar frameworks, and 3D architectures. In each case, ordered attachment of the CSC was observed giving rise to a series of organized silicified DNA superstructures (**Fig. 6a** **Supplementary Fig. 9 to 16**). Similar results were also observed for micrometer-scale DNA frameworks. For example, a modified single-stranded tile assembly technique was used to construct a *p6mm* DNA 2D lattice (**Fig. 6b**, **Supplementary Fig. 17 to 20**). High-resolution cryo-EM images recorded perpendicular to the Z-axis of the undecorated DNA lattice or DNA/CSC superstructure, along with the reconstructed Cryo-ET data revealed a high precision silicification process (**Fig. 6c and 6d, Supplementary Video 4 and 5**). The fast Fourier transform (FFT) analyses (data not shown) corresponding to the d_{1000} ($= d_{0100} = d_{0010} = 4.0$ nm) spacing for the *p6mm* DNA lattice and the d_{C1000} ($= d_{C0100} = d_{C0010} = 4.1$ nm) spacing for the *p6mm* DNA/CSC superstructure were almost identical, indicating that the original spatial information encoded in the DNA lattice was inherited by the silicified replica.

Discussion

In conclusion, our results demonstrate a unified approach to DNA framework-programmed silicification by precise spatial attachment of positively charged silica nanoclusters with tailored molecular composition, charge, size, and stability (**Extended Data Fig. 5**). We employ a spontaneous self-capping mechanism of alkoxide co-condensation to arrest the growth of pre-nucleation silica clusters to generate discrete nanoscale building blocks (CSC) capable of high-fidelity DNA framework silicification at single-cluster resolution. Significantly, growth of the CSC is inhibited due to spontaneous surface segregation of the positively charged side chains of TMAPS that increases interfacial hydrophilicity and attenuates polycondensation. Based on this mechanism, molecular tuning of the CSC is achieved by systematic changes in the TMAPS/TEOS molar ratio, leading to a range of clusters with different morphological, structural and physiochemical properties.

Having established a systematic approach to silica cluster stabilization, we use a range of complex DNA nanostructures as programmable attachment templates to probe the assembly dynamics of the CSC. Silica cluster attachment is facilitated by electrostatic interactions with the DNA templates and leads to silicified superstructures that can exhibit superlattice ordering under conditions of size matching and structural adaptation. The latter mechanism involves cooperative adjustments of both the DNA framework and cluster morphology, for example via stretching or compression of DNA crossovers and reconfiguration of the siloxane network, thereby minimizing the total energy of the silicified DNA superlattices.

Our results have direct implications for the programmed construction of new-generation hybrid materials through the systematic integration of sol-gel chemistry and DNA nanotechnology. In particular, the ability to generate silica/DNA superstructures with controllable surface-to-surface distances less than 1.0 nm surpasses the precision of previously

reported DNA nanotechnology-enabled strategies⁴³⁻⁴⁶. More indirectly, our work could offer insights into the mechanisms of biological silicification. For example, we observed that the properties of the CSC facilitate attachment with high specificity both at the surface and inside of the DNA frameworks, suggesting that similarly constructed silica-based building blocks could be responsible for the fine-scale elaboration of organic matrices involved in biosilicification⁴⁷⁻⁵⁰. In this regard, we note that our simple *p6mm* DNA/CSC superstructure highly resembles the natural hybrid silica/protein superstructure of the demosponge *T. aurantium*, both from the perpendicular and longitude cut of the structure⁵. Despite the fact that these two hybrid superstructures comprise different constituents - a cationic silicatein framework and anionic silicic acid precursors in the demosponge, and anionic DNA framework and cationic silica clusters in the DNA/CSC superstructure - they demonstrate identical hexagonal patterning of the silica building blocks and similar superlattice parameters ($d = 5.95$ nm and 4.1 nm, respectively)^{5,28}. Thus, it seems feasible that molecular tuning of organic framework-programmed silicification by silica cluster attachment is a potentially generic pathway in the formation of ordered amorphous silica minerals²⁴⁻²⁷. In conclusion, our studies provide new research directions for biomineralization, biomimetic materials chemistry and DNA nanotechnology.

References

- 1 Lowenstam, H. A. W., S. On biomineralization. *Paleobiology* **16**, 521-526 (1989).
- 2 Gong, Y. U. T. *et al.* Phase transitions in biogenic amorphous calcium carbonate. *Proceedings of the National Academy of Sciences* **109**, 6088-6093 (2012).
- 3 Lupulescu, A. I. & Rimer, J. D. In situ imaging of silicalite-1 surface growth reveals the mechanism of crystallization. *Science* **344**, 729-732 (2014).
- 4 James, J. D. Y. *et al.* Crystallization by particle attachment in synthetic, biogenic, and geologic environments. *Science* **349**, 6760-6769 (2015).
- 5 Görlich, S. *et al.* Natural hybrid silica/protein superstructure at atomic resolution. *Proceedings of the National Academy of Sciences of the United States of America* **117**, 31088-31093 (2020).
- 6 Wegst, U. G. K., Bai, H., Saiz, E., Tomsia, A. P. & Ritchie, R. O. Bioinspired structural materials. *Nature Materials* **14**, 23-36 (2015).
- 7 Meyers, M. A., McKittrick, J. & Chen, P. Y. Structural biological materials: critical mechanics-materials connections. *Science* **339**, 773-779 (2013).
- 8 Lakes, R. Materials with structural hierarchy. *Nature* **361**, 511-515 (1993).
- 9 Meldrum, F. C. & Colfen, H. Controlling mineral morphologies and structures in biological and synthetic systems. *Chemical Reviews* **108**, 4332-4432 (2008).
- 10 Reznikov, N., Bilton, M., Lari, L., Stevens, M. M. & Kröger, R. Fractal-like hierarchical organization of bone begins at the nanoscale. *Science* **360**, 507-517 (2018).
- 11 Gordon, L. M. *et al.* Amorphous intergranular phases control the properties of rodent tooth enamel. *Science* **347**, 746-750 (2015).
- 12 Li, X., Xu, Z.-H. & Wang, R. In situ observation of nanograin rotation and deformation in nacre. *Nano Letters* **6**, 2301-2304 (2006).
- 13 Yong, L. *et al.* Radially oriented mesoporous TiO₂ microspheres with single-crystal-like anatase walls for high-efficiency optoelectronic devices. *Science Advances* **1**, e1500166 (2015).
- 14 Sommerdijk, N. A. J. M. & de With, G. Biomimetic CaCO₃ Mineralization using Designer Molecules and Interfaces. *Chemical Reviews* **108**, 4499-4550 (2008).
- 15 Liu, Z. M. *et al.* Crosslinking ionic oligomers as conformable precursors to calcium carbonate. *Nature* **574**, 394-398 (2019).
- 16 Zhao, M. *et al.* Pressure-driven fusion of amorphous particles into integrated monoliths. *Science* **372**, 1466-1470 (2021).
- 17 Mao, L. B. *et al.* Synthetic nacre by predesigned matrix-directed mineralization. *Science* **354**, 107-110 (2016).
- 18 Palmer, L. C., Newcomb, C. J., Kaltz, S. R., Spoerke, E. D. & Stupp, S. I. Biomimetic systems for hydroxyapatite mineralization inspired by bone and enamel. *Chemical Reviews* **108**, 4754-4783 (2008).
- 19 Changyu, S. *et al.* Repair of tooth enamel by a biomimetic mineralization frontier ensuring epitaxial growth. *Science Advances* **5**, eaaw9569 (2019).
- 20 Cho, K.-S., Talapin, D. V., Gaschler, W. & Murray, C. B. Designing PbSe nanowires and nanorings through oriented attachment of nanoparticles. *Journal of the American Chemical Society* **127**, 7140-7147 (2005).
- 21 Jawaid, A. M., Asunskis, D. J. & Snee, P. T. Shape-controlled colloidal synthesis of rock-salt lead selenide nanocrystals. *ACS Nano* **5**, 6465-6471 (2011).
- 22 Mirabello, G., Lenders, J. J. M. & Sommerdijk, N. A. J. M. Bioinspired synthesis of magnetite nanoparticles. *Chemical Society Reviews* **45**, 5085-5106 (2016).
- 23 Guomin, Z. *et al.* Self-similar mesocrystals form via interface-driven nucleation and assembly. *Nature* **590**, 416-422 (2021).
- 24 Hildebrand, M. Diatoms, biomineralization processes, and genomics. *Chemical Reviews* **108**, 4855-4874 (2008).
- 25 Van Soest, R. W. M. *et al.* Global diversity of sponges (Porifera). *PLOS ONE* **7**, e35105 (2012).
- 26 Takahashi, K., Hurd, D. C. & Honjo, S. Phaeodarian skeletons: their role in silica transport to the deep sea. *Science* **222**, 616-618 (1983).
- 27 Guerrero, G., Stokes, I., Valle, N., Hausman, J.-F. & Exley, C. Visualising silicon in plants: histochemistry, silica sculptures and elemental imaging. *Cells* **9**, 1066-1085 (2020).
- 28 Werner, P., Blumtritt, H. & Natalio, F. Organic crystal lattices in the axial filament of silica spicules of Demospongiae. *Journal of Structural Biology* **198**, 186-195 (2017).
- 29 Tiancong, Z., Ahmed, E., Xiaomin, L. & Dongyuan, Z. Single-micelle-directed synthesis of mesoporous materials. *Nature Reviews Materials* **4**, 775-791 (2019).
- 30 Ma, K. *et al.* Self-assembly of highly symmetrical, ultrasmall inorganic cages directed by surfactant micelles. *Nature* **558**, 577-580 (2018).
- 31 Sumper, M. Biomimetic patterning of silica by long-chain polyamines. *Angew. Chem. Int. Ed.* **43**, 2251-2254 (2004).
- 32 Liu, X. G. *et al.* Complex silica composite nanomaterials templated with DNA origami. *Nature* **559**, 593-598 (2018).
- 33 Liu, B., Cao, Y. Y., Huang, Z. H., Duan, Y. Y. & Che, S. N. Silica biominerization via the self-assembly of helical biomolecules. *Advanced Materials* **27**, 479-497 (2015).
- 34 Hench, L. L. & West, J. K. The sol-gel process. *Chemical Reviews* **90**, 33-72 (1990).
- 35 Carcouet, C. C. M. C. *et al.* Nucleation and growth of monodisperse silica nanoparticles. *Nano Letters* **14**, 1433-1438 (2014).
- 36 Gebauer, D., Kellermeier, M., Gale, J. D., Bergstrom, L. & Colfen, H. Pre-nucleation clusters as solute precursors in crystallisation. *Chemical Society Reviews* **43**, 2348-2371 (2014).
- 37 Robert, P. R. & John, A. T. Accurate assessment of mass, models and resolution by small-angle scattering. *Nature* **496**, 477-481 (2013).

- 38 Rambo, R. P. & Tainer, J. A. Characterizing flexible and intrinsically unstructured biological macromolecules by SAS using
the Porod-Debye law. *Biopolymers* **95**, 559-571 (2011).
- 39 Protsak, I. S. et al. A ²⁹Si, 1H, and ¹³C solid-state NMR study on the surface species of various depolymerized
organosiloxanes at silica surface. *Nanoscale Research Letters* **14**, 160 (2019).
- 40 Herman, C. et al. Solution state structure determination of silicate oligomers by ²⁹Si NMR spectroscopy and molecular
modeling. *Journal of the American Chemical Society* **128**, 2324-2335 (2006).
- 41 Aizenberg, J. et al. Skeleton of Euplectella sp.: Structural hierarchy from the nanoscale to the macroscale. *Science* **309**,
275-278 (2005).
- 42 Sumper, M. A phase separation model for the nanopatterning of diatom biosilica. *Science* **295**, 2430-2433 (2002).
- 43 Park, S. Y. et al. DNA-programmable nanoparticle crystallization. *Nature* **451**, 553-556 (2008).
- 44 Macfarlane, R. J. et al. Nanoparticle superlattice engineering with DNA. *Science* **334**, 204-208 (2011).
- 45 Liu, W. et al. Diamond family of nanoparticle superlattices. *Science* **351**, 582-586 (2016).
- 46 Wang, S. et al. The emergence of valency in colloidal crystals through electron equivalents. *Nature Materials* **21**, 580-587
(2022).
- 47 Kroger, N., Deutzmann, R. & Sumper, M. Polycationic peptides from diatom biosilica that direct silica nanosphere
formation. *Science* **286**, 1129-1132 (1999).
- 48 Yang, S. H., Park, J. H., Cho, W. K., Lee, H. S. & Choi, I. S. Counteranion - Directed, Biomimetic Control of Silica
Nanostructures on Surfaces Inspired by Biosilicification Found in Diatoms. *Small* **5**, 1947-1951 (2009).
- 49 Ehrlich, H. et al. Mineralization of the metre-long biosilica structures of glass sponges is templated on hydroxylated
collagen. *Nature chemistry* **2**, 1084-1088 (2010).
- 50 Maldonado, M. et al. Cooperation between passive and active silicon transporters clarifies the ecophysiology and
evolution of biosilicification in sponges. *Science advances* **6**, eaba9322 (2020).

Supplementary Information is available in the online version of the paper.

Acknowledgements We thank Huan Wang, Kevin Chan, Zhi He, Yichong Lao and Dong Zhang for helpful discussions. This work was partially supported by the National Key R&D Program of China (2021YFA1201200, 2021YFF1200404), the National Natural Science Foundation of China (22322205, 92056117, U1967217), the National Center of Technology Innovation for Biopharmaceuticals (NCTIB2022HS02010), the National Independent Innovation Demonstration Zone Shanghai Zhangjiang Major Projects (ZJZX2020014), Shanghai Artificial Intelligence Lab (P22KN00272), and the Starry Night Science Fund of Zhejiang University Shanghai Institute for Advanced Study (SN-ZJU-SIAS-003).

Author Contributions X.J., X.L. and C.F. conceived the research, designed the experiments. R.Z., J.H. designed the molecular simulations. R.Z., X.L. S.M. and C.F. supervised the research. X.J. performed the experiments, supported by H.W.. J.H., D.B., and M.L. performed the full-atomic MD and hybrid MC/MD simulations. J.H. carried out potential of mean force calculations. Z.L. developed the Python scripts for SST tile sequence generation and MS analysis. Y.L. and M.P. analyzed cryo-EM data. J.C. and Y.L. assisted with the analysis of MAS-NMR and MS data. Y.X. assisted with the analysis of SAXS data. L.L. performed the statistics of CSC. Q.X. assisted with the HS-AFM experiments. Y.W. assisted with design of DNA lattices. X.J., X.L., S.M. and C.F. interpreted the data. R.Z., X.L., S.M. and C.F. wrote the manuscript. All authors edited and commented on the manuscript.

Author Information

Materials and Methods

Materials. N-trimethoxysilylpropyl-N,N,N-trimethylammonium chloride (TMAPS) (50% in methanol, cat. no. T2796) and tetraethyl orthosilicate (TEOS) (cat. no. T0100) were purchased from TCI, Japan. Staple DNA strands were purchased from Sangon Biotech (Shanghai, China). Scaffold DNA strands (5,250 nt, 7,249 nt, 8,064 nt and 10,004 nt) were purchased from Bioruler (cat. no. B3009, B3007, B3005 and B3003). All DNA strands were stored at -20 °C after being dissolved in ultrapure water. Other chemicals were purchased from Sinopharm and Sigma-Aldrich. Carbon-coated TEM grids were purchased from Beijing Zhongjingkeyi Technology Co., Ltd (Beijing, China). Lacey grids were purchased from Ted Pella. C-Flat-1.2/1.3-4 C grids were purchased from Protochips. AFM tips were purchased from Bruker and Olympus. All the reagents were used as received without further purification.

Preparation of CSC. TMAPS were added dropwise into TE-MgCl₂ buffer (5 mM Tris, 1 mM EDTA, 12 mM MgCl₂, pH=8.0). The mixture was then shaken at 800 rpm for 10 min in an Eppendorf Thermomixer, after which TEOS was added, followed by shaking for another 5 days. The stoichiometric ratios of CSC were summarized in **Supplementary Table 2**. All CSC were stored at 25 °C before further use.

Preparation of DNA frameworks. All DNA structures were designed with the help of caDNAno software. To fold the DNA origami, staple strands were mixed with the scaffold strands in a molar ratio of 5:1 in TE-MgCl₂ buffer. The mixture was then annealed in a PCR thermocycler (Eppendorf) using the following cooling protocol, 65 °C 20 min; 60 to 40 °C at 1 °C per 50 min; 40 to 25 °C at 1 °C per 30 min. To remove excess staples, the annealed mixture was mixed with PEG buffer (5 mM Tris, 1 mM EDTA, 500 mM NaCl, 15% w/v PEG, M_w: 8,000 g/mol) in a 1:1 volumetric ratio and centrifuged at 10,000 rcf for 15 min. The DNA pellet was redissolved in TE-MgCl₂ buffer and shaken for 12 hours at 800 rpm, 37 °C. The purified DNA origami was diluted to 100 ng/μL with TE-MgCl₂ buffer and quantified by UV-visible spectroscopy. All purified DNA origami were stored at 4 °C before further use.

To assemble the 2D DNA lattices, unpurified ssDNA strands were mixed in an equimolar stoichiometric ratio from a 100 μM stock in TE buffer (5 mM Tris, pH=8.0, 1 mM EDTA) supplemented with 40 mM MgCl₂. The cooling protocol was as following, 70 °C 10 min, 50-25 °C, at 1 °C per 6 h.

For SST design, the sequences of DNA tiles should be orthogonal and satisfy the following rules. Each sequence should avoid continuous bases of more than 3 nt. E.g., ‘AAA’ is permitted, while ‘AAAA’, ‘AAAAA’ are prohibited. The GC content should range from 45% to 55% to ensure sequence stability. For different sequences in the same group of DNA tiles, every two sequences should avoid identical sub-sequence of bases more than 8 nt. A Python script that integrates the above rules was provided to automatically generate DNA tile sequences of given lengths (See code availability).

SCA process. A typical DNA framework solution (100 ng/μL) was quickly added into the CSC dispersion (6.8 nm-CSC, ~7.1 mg/mL; 4.7 nm-CSC, ~9.8 mg/mL; 3.9 nm-CSC, ~15.4 mg/mL; 1.3 nm-CSC, ~26.5 mg/mL) in a 1:1 volumetric ratio. The mixture was shaken at 800 rpm, 25 °C for 10 min. After that, the mixture was centrifuged at 10,000 rcf, 25 °C for 15 min. The supernatant was carefully removed with a pipet under UV lamps, and the sediments (DNA/CSC composites) were resuspended in water. At last, the DNA/CSC composites in pure water were shaken at 800 rpm, 25 °C for 10 min. The DNA/CSC composites should be characterized within 24 h after they are formed.

Further silicification. Additional 2.5 μL 5.6% ammonia (v/v, in water) and 2.0 μL 5.0% TEOS (v/v, in ethanol) were added into 100 μL DNA/CSC dispersion. The mixture was shaken at 800 rpm, 25 °C for 1 day. After that, the mixture was centrifuged at 10,000 rcf for 15 min, followed by washing with pure water and ethanol 3 times, respectively.

Agarose gel analysis. DNA origami and DNA/CSC assembly were electrophoresed on a 1.0 % agarose gel containing 0.2×GelRed in TAE-Mg²⁺ buffer (40 mM Tris, 2 mM EDTA, 12.5 mM MgAc₂, pH=8.0) for 1 h at 100 V bias in an ice-water-cooled gel box. The electrophoresed agarose gels were scanned using a G:BOX Chemi XL1.4 gel image-analysis system at a resolution of 300 DPI.

DLS and Zeta potential measurements. Dynamic light scattering experiments of CSC were conducted using Zetasizer Ultra (Malvern Instruments). 100 μL CSC (~2 mM) was pipetted into a disposable cuvette. The hydrodynamic size and ζ-potential value of one sample group were averaged over all parallel measurements (hydrodynamic size, N = 90; ζ-potential, N = 15) and were summarized in **Supplementary Table 2 and 3**.

HS-AFM characterization. HS-AFM experiments were conducted using tapping mode HS-AFM (RIBM, Japan) at 25 °C. A silicon nitride cantilever (9 μm long, 2 μm wide and 130 nm thick; BL-AC10DS, Olympus, Tokyo, Japan) with nominal spring constants of 0.1 N/m and a resonance frequency of 1,500 kHz was used.

To capture the dynamic assembly process of CSC, 5 μL of purified triangle DNA origami (5 ng/μL) or Y-Z DNA lattice (100 ng/μL) was incubated on freshly cleaved mica for 5 min. After successful visualization of DNA frameworks, 3.9 nm-CSC with a final diluted ratio of 1:20 (~0.8 mg/mL) in TE-MgCl₂ buffer was pumped into the liquid cell (0.5 mL/h for DNA origami, 1.0 mL/h for Y-Z DNA lattice). HS-AFM images were captured at a rate of 100 Hz (DNA origami, 2.56 s/frame) and 50 Hz (DNA lattice, 5.12 s/frame) with scan areas of 250 nm² and 300 nm².

Negative-staining TEM. For TEM imaging of DNA frameworks, 10 μL of purified DNA origami (5 ng/μL) or unpurified DNA lattice (100 ng/μL) was adsorbed onto glow discharged, carbon-film-coated copper grid for 10 min. The sample drop was wicked from the copper grid with filter paper and the grid was washed three times with pure water. Then the sample was stained for 30 s using a 0.75% aqueous uranyl formate solution. After this, the excess solution was removed with filter paper

and the grid was washed three times with pure water. The copper grid was dried at 25 °C. For TEM imaging of DNA/CSC composites, 10 µL of freshly prepared DNA/CSC composites dispersion was adsorbed onto glow discharged, carbon-film-coated copper grids for 10 min. The grid was then washed three times by pure water and dried at 25 °C. All images were acquired using a Talos L120C G2 operated at 120 kV.

Cryo-EM characterization. 3 µL of the sample (CSC, DNA origami, DNA lattice or DNA/CSC composites) was piped onto glow discharged lacey grid or C-Flat-1.2/1.3-4 C grid. Then the sample was plunge-frozen using a Vitrobot Mark IV with the temperature of 20 °C, the humidity of 90%, wait time of 60 s, blot time of 10 s, blot force of -1 and drain time of 0 s.

Images of 3.9 nm-CSC were collected using an FEI Titan Krios G3i TEM (Thermo Fisher Scientific) operated at 300 kV that equipped with a K2 direct electron detector (Gatan) with a pixel size of 0.822 Å. The CSC datasets have a defocus range from 0.8 to 2.5 µm. Each micrograph was dose-fractioned to 25 frames with 2.4 s exposure time for each frame. The total accumulated dose of each micrograph is 60.0 e-/Å². The images of DNA origami and DNA/CSC composites were collected using a Glacios TEM (Thermo Fisher Scientific) operated at 200 kV. The images were collected on a Falcon III detector, with defocus ranges from -1.0 to -2.0 µm or -0.8 to -2.6 µm, respectively. Each micrograph was dose-fractioned to 16 frames with 2.5 s exposure time for each frame. The total accumulated dose of each micrograph is 40.0 e-/Å².

A total of 2,236 cryo-EM images of 3.9 nm-CSC were collected on a K2 detector. Motion correction was performed on the dose-fractioned image stacks using RELION's own MotionCor2 with dose weighting⁵¹. The CTF parameters of each image were determined with CTFFIND-4.1⁵². Particle picking, 2D classification, 3D initial model, 3D classification, 3D auto-refine and PostProcess were performed with RELION-4.0⁵³. An overview of the data processing procedure is shown in **Supplementary Table 5**. After two rounds of 2D classification and two rounds of 3D classification with exhaustive angular searches, a total of 32,564 particles that belong to the CSC were processed with 3D auto-refine and solvent-masked post-processing. A cryo-EM map of the CSC was finally calculated from 32,564 particles at an overall resolution of 8.1 Å. The resolution estimation was based on the gold-standard Fourier shell correlation (FSC) 0.143 criterion⁵⁴. The cryo-EM datasets of the DNA origami and DNA/CSC composites were processed similarly to that of the CSC.

Single-particle style image processing of typical DNA lattices and their corresponding DNA/CSC composites (including contrast transfer function estimation, particle picking, particle extraction and 2D alignment and averaging) were also accomplished using the Relion software package.

Cryo-tomograms were acquired using a Glacios TEM (Thermo Fisher Scientific) operated at 200 kV. Images were collected with EPU tomography with a defocus range from -2 to -3 µm at a calibrated magnification of 120,000, corresponding to a magnified pixel size of 1.2 Å. Movies were comprised of 4 frames and 5 s exposure time. The session was set up as single directional tilting in increments of 2 - 3° up to 60° and the dose rate was set to ~1.03 e/pixel/s. Cryo-tomograms were processed with the IMOD 4.9 routine.

NMR analysis. For unhydrolyzed TEOS and TMAPS, 1 mL of TMAPS or TEOS solution was measured on a 700 MHz Bruker Advance NEO operating at 176 MHz for ¹³C and 139 MHz for ²⁹Si. For CSC, hydrolyzed TMAPS and TEOS, 1 mL of freshly prepared samples were desaltsed by using a NAP-10 column and redispersed into 1 mL pure water, followed by subsequent freeze-drying. The MAS NMR measurements were carried out using a 3.2 mm BL3.2 HXY MAS probe head with a sample rotation rate of 10 kHz, in a magnetic field of 14.09 Tesla on a 600 MHz Bruker Avance NEO operating at 150 MHz for ¹³C and 119 MHz for ²⁹Si. Q8M8 was used for ²⁹Si NMR shift calibration. The intensities of the spectral components T⁰, T¹, T², T³ and Q⁰, Q¹, Q², Q³, Q⁴ were obtained by deconvolution of the ²⁹Si MAS NMR spectra in terms of Gaussian line shapes using DMfit2011. The chemical shifts and corresponding intensities percentages of spectral components of CSC were summarized in **Supplementary Table 4**.

MS analysis. Freshly prepared CSC dispersions were directly used for analysis. For MALDI MS measurement, a Shimadzu MALDI-7090 was used with the following parameters, Tuning Linear, Power139, P. Ext at 3,000.00 (bin189), Ion Gate Blanking: 500.00, Laser Diameter 200.

MS spectra Analysis. For MALDI MS spectra analysis, the molecule fragment ions always have one positive charge. Therefore, the m/z peak value (*N*) equals the corresponding molecule fragment ion's total molecular weight (MW_{TOTAL}). Given that a single CSC is formed through condensation of the certain number of TMAPS (*a*) and TEOS (*b*) molecules, meanwhile losing *m* H₂O, the function of *N* can be described as follow,

$$N = MW_{TOTAL} = a * MW_{TMAPS} + b * MW_{TEOS} - m * MW_{H2O} \quad (1)$$

in which $(2a + 2b)/2 < m < (3a + 4b)/2$, according to the lowest crosslinking degree of 2 from NMR data. The exact mass values of these molecules are MW_{TMAPS} = 180.105, MW_{TEOS} = 95.988 and MW_{H2O} = 18.010, respectively. Based on the above restrictions, we wrote a script in Python (See Code availability) to screen out all possible combinations of *a*, *b* and *m*. Then, the final molecular formula of a typical CSC was figured out based on the comparative analysis of this value and the experimental *N* value.

Hybrid MC/MD simulations. We built the structures of TMAPS and TEOS using Avogadro software⁵⁵. The force field parameters involving silicone atoms used were as described previously⁵⁶. The molecular topology of TMAPS and TEOS were created using the antechamber tool⁵⁷. Specifically, the Antechamber tool⁵ was used to assign the atomic type of TMAPS and TEOS using the GAFF force field⁵⁸ and the partial charges on the atoms were assigned using the AM1-BCC method⁵⁹. Initially, three simulation systems were built and the first system consisted of 1,001 TEOS molecules. The second and third systems were composed of 1,001 TEOS and TMAPS molecules with ratios of 5:2 and 5:8, respectively. These ratios of the three simulated systems were in line with the experimental conditions. These molecules were randomly distributed in cubic simulation boxes of 10×10×10 nm³ and simulation boxes were solvated with the TIP3P explicit water model⁶⁰. All molecular

dynamic simulations were performed using the GROMACS 2020⁶¹ simulation package. The temperature ($T = 300$ K) and pressure ($P = 1$ atm) were maintained using a stochastic velocity rescaling thermostat⁶² and Parrinello–Rahman barostat⁶³, respectively. Periodic boundary conditions were applied to all systems in all directions, and using of the LINCS algorithm enabled a standard integration time step of 2 fs⁶⁴. All systems were simulated for 0.1 ns for each step. Short-range electrostatic and *van der Waals* interactions were calculated at a cut-off distance of 1.2 nm, while long-range electrostatic interactions were treated via the particle mesh Ewald (PME) method⁶⁵. All the simulation snapshots were rendered with VMD⁶⁶. In addition to the analysis tools of GROMACS, MDAnalysis⁶⁷ was also extensively used for the analysis of the simulated trajectories.

The hybrid MC/MD workflow was created and implemented using a Python pipeline. After the initial energy minimization and MD simulation, the distances among silicon atoms of TEOS and TMAPS were calculated. Molecule pairs with silicon atoms within 6 angstroms were counted and a *Monte Carlo* step using metropolis algorithm was used to determine whether the dehydration reaction was accepted for the counted molecule pairs. Specifically, a random number was generated and if the random number was smaller than the reaction probability, the dehydration reaction of the closest hydroxyl groups was accepted. The reaction probability was determined by the specific molecules (i.e., TEOS and TMAPS) and described in detail below.

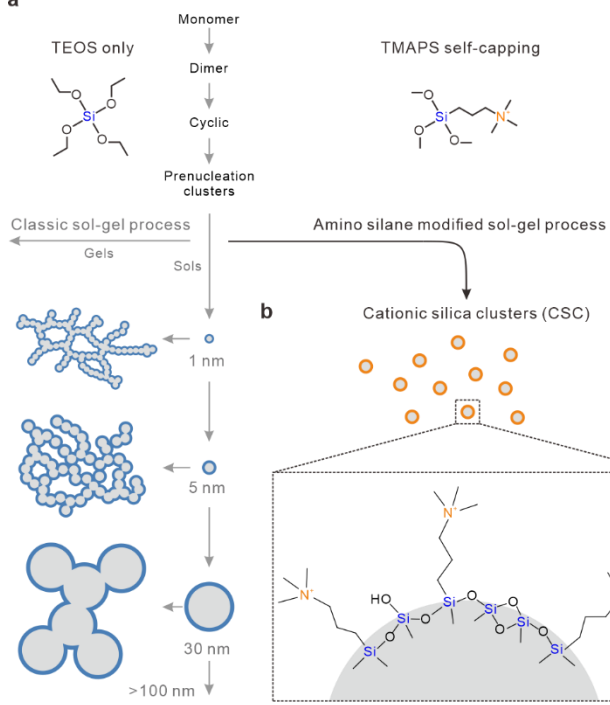
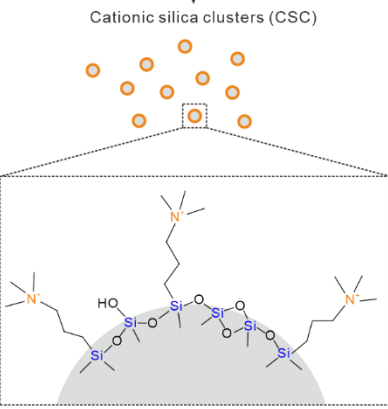
From the NMR experiments, a silica unit with n Si-O-Si bonds can be inferred, denoted here as Q^n . As a result, Q^0 stands for a monomer with no bonds, while Q^4 symbolizes a silica unit with bonds at all four of its vertices with four other silica units. While TEOS is viewed as Q^0 , TMAPS is treated as T^0 due to its propyl-N, N, N-trimethylammonium moiety. We have set different reaction probabilities ($P(T^m Q^n)$) based on the T^m of TMAPS and Q^n of TEOS molecules. The reaction probability of T^m and Q^n is similar to the previous kinetic *Monte Carlo* algorithm by Malani et al.⁶⁸,

$$P(T^m Q^n) = \frac{1}{1+(m+2)} \cdot \frac{1}{1+(n+1)} \cdot S \quad (2)$$

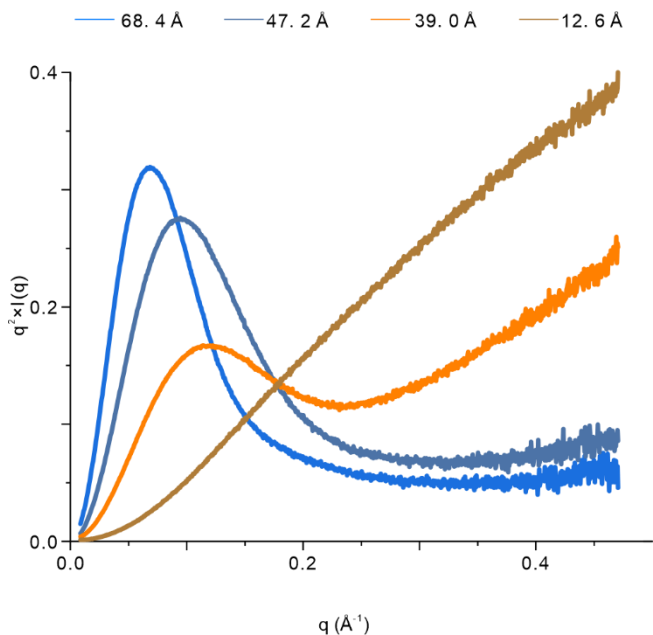
where S is the scaling factor and in this study $S=0.1$ was used. After the *Monte Carlo* step, the system topology was modified accordingly using the automatic Python code. The next round of MD simulations was then conducted until the specified 1,000 of runs were reached.

Code availability. The Python scripts for SST tile sequence generation and MS analysis can be downloaded from <https://github.com/zimu-liii/SST-sequence-generator.git> and <https://github.com/zimu-liii/MS-analysis.git>.

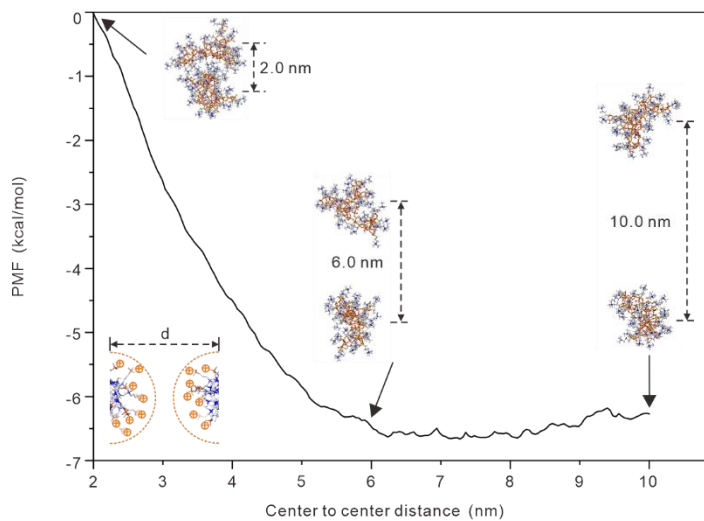
- 51 Zheng, S. Q. *et al.* MotionCor2: anisotropic correction of beam-induced motion for improved cryo-electron microscopy. *Nature Methods* **14**, 331-332 (2017).
- 52 Rohou, A. & Grigorieff, N. CTFFIND4: Fast and accurate defocus estimation from electron micrographs. *Journal of Structural Biology* **192**, 216-221 (2015).
- 53 Kimanis, D., Dong, L., Sharov, G., Nakane, T. & Scheres, S. H. W. New tools for automated cryo-EM single-particle analysis in RELION-4.0. *Biochemical Journal* **478**, 4169-4185 (2021).
- 54 Scheres, S. H. W. & Chen, S. Prevention of overfitting in cryo-EM structure determination. *Nature Methods* **9**, 853-854 (2012).
- 55 Hanwell, M. D. *et al.* Avogadro: an advanced semantic chemical editor, visualization, and analysis platform. *Journal of Cheminformatics* **4**, 17 (2012).
- 56 Lin, P.-H. & Khare, R. Molecular simulation of cross-linked epoxy and epoxy-POSS nanocomposite. *Macromolecules* **42**, 4319-4327 (2009).
- 57 Wang, J. M., Wang, W., Kollman, P. A. & Case, D. A. Automatic atom type and bond type perception in molecular mechanical calculations. *J Mol Graph Model* **25**, 247-260 (2006).
- 58 Wang, J., Wolf, R. M., Caldwell, J. W., Kollman, P. A. & Case, D. A. Development and testing of a general amber force field. *Journal of Computational Chemistry* **25**, 1157-1174 (2004).
- 59 Jakalian, A., Jack, D. B. & Bayly, C. I. Fast, efficient generation of high-quality atomic charges. AM1-BCC model: II. Parameterization and validation. *Journal of Computational Chemistry* **23**, 1623-1641 (2002).
- 60 Jorgensen, W. L., Chandrasekhar, J., Madura, J. D., Impey, R. W. & Klein, M. L. Comparison of simple potential functions for simulating liquid water. *Journal of Chemical Physics* **79**, 926-935 (1983).
- 61 Abraham, M. J. *et al.* GROMACS: High performance molecular simulations through multi-level parallelism from laptops to supercomputers. *Softwarex* **1**, 19-25 (2015).
- 62 Bussi, G., Donadio, D. & Parrinello, M. Canonical sampling through velocity rescaling. *Journal of Chemical Physics* **126** (2007).
- 63 Parrinello, M. & Rahman, A. Polymorphic transitions in single crystals: A new molecular-dynamics method. *Journal of Applied Physics* **52**, 7182-7190 (1981).
- 64 Hess, B., Bekker, H., Berendsen, H. J. & Fraaije, J. G. LINCS: a linear constraint solver for molecular simulations. *Journal of Computational Chemistry* **18**, 1463-1472 (1997).
- 65 Darden, T., York, D. & Pedersen, L. Particle mesh Ewald: An $N \cdot \log(N)$ method for Ewald sums in large systems. *Journal of Chemical Physics* **98**, 10089-10092 (1993).
- 66 Humphrey, W., Dalke, A. & Schulten, K. VMD: visual molecular dynamics. *Journal of Molecular Graphics* **14**, 33-38 (1996).
- 67 Michaud-Agrawal, N., Denning, E. J., Woolf, T. B. & Beckstein, O. MDAnalysis: a toolkit for the analysis of molecular dynamics simulations. *Journal of Computational Chemistry* **32**, 2319-2327 (2011).
- 68 Shere, I. & Malani, A. Polymerization kinetics of a multi-functional silica precursor studied using a novel Monte Carlo simulation technique. *Physical Chemistry Chemical Physics* **20**, 3554-3570 (2018).

a**b**

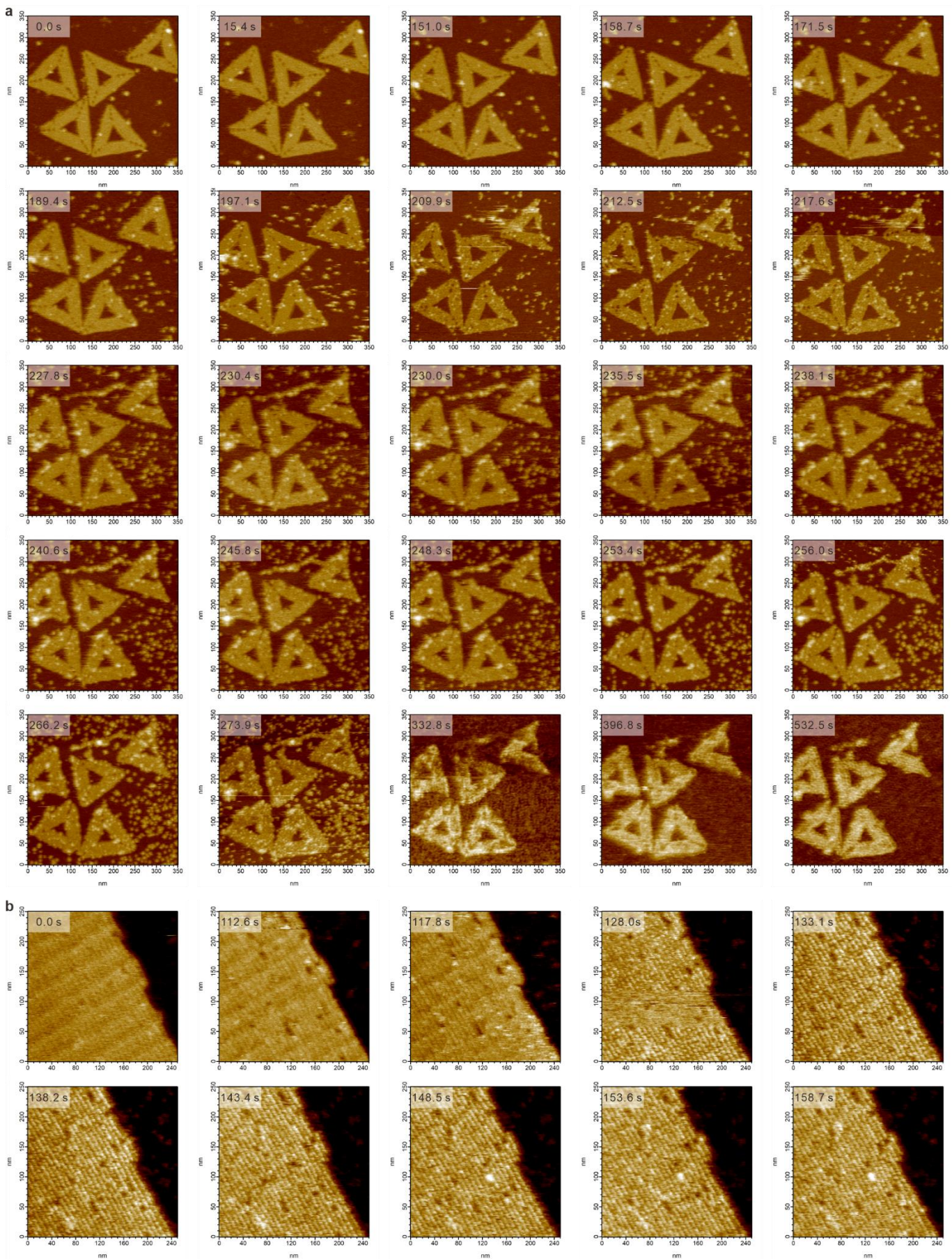
Extended Data Fig.1 | Comparison between amino silane modified sol-gel process and classic sol-gel process. **a**, Scheme showing classical silica sol-gel process (left) and arrested growth of silica pre-nucleation clusters by self-capping to produce ultrastable CSC (right). **b**, Schematic illustration of the self-capped CSC showing spontaneous surface segregation of the positively charged side chains of TMAPS that increases interfacial hydrophilicity and attenuates polycondensation.



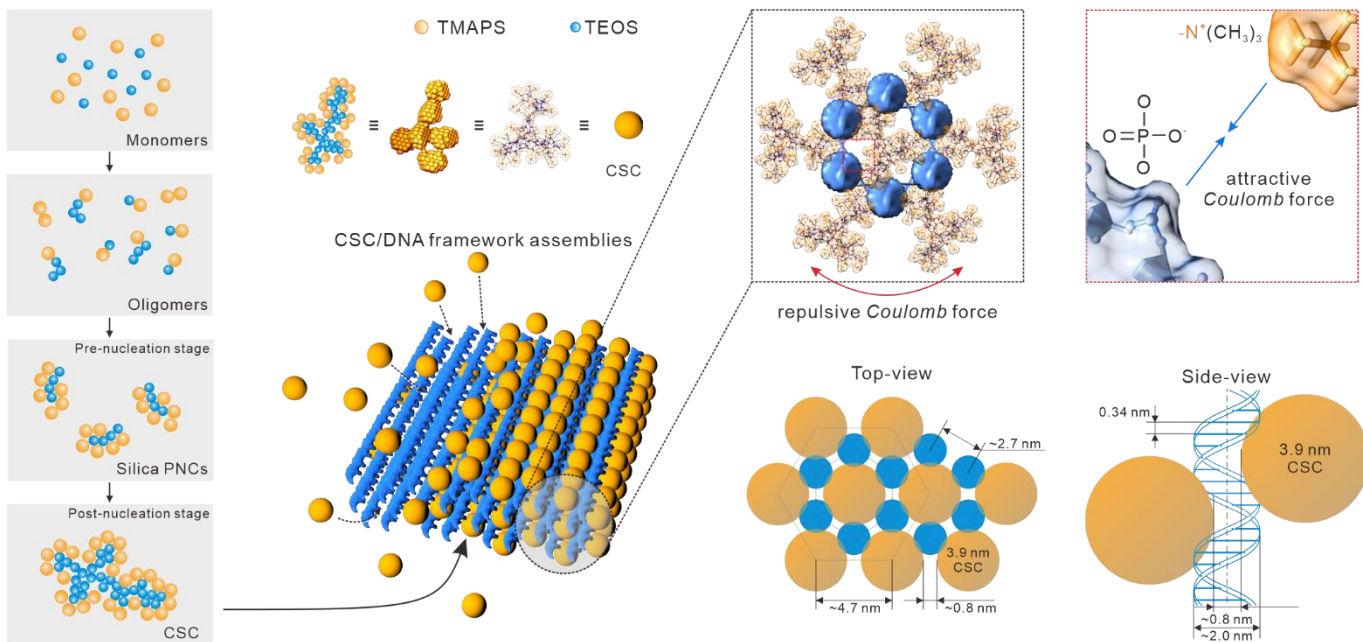
Extended Data Fig.2 | Kratky plots derived from SAXS profiles. 3.9 nm-CSC showed characteristic partial parabolic convergence curve.



Extended Data Fig.3 | Potential Mean Force (PMF) analysis of a two-cluster system. The PMF plot revealed that a ~6.0 nm center-to-center distance was critical for 3.9 nm-CSC stabilization in solution.



Extended Data Fig.4 | Sequential in-situ HS-AFM images from Supplementary Videos 1 (a) and 2 (b).



Extended Data Fig.5 | Schematic illustration summarizing the CSC-directed silicification of programmable DNA frameworks. We proposed a picture of organic template-directed precise amorphous silica mineralization, which starts with the formation of silica PNCs with molecular weight of ~1.2 kDa and size of ~1.3 nm. Their self-limited aggregation leads to the formation of size-controlled CSCs with typical molecular weight of ~8.2 kDa and size of ~3.9 nm. Further, these CSCs are orderly arranged by Coulomb forces on substrate frameworks.

Supplementary Information for
Molecular tuning of DNA framework-programmed silicification
by cationic silica cluster attachment

Xinxin Jing^{1,2,8}, Haozhi Wang^{1,8}, Jianxiang Huang^{3,4,8}, Yingying Liu^{1,8}, Zimu Li¹, Jielin Chen¹, Yiqun Xu¹, Lingyun Li¹, Yunxiao Lin¹, Qinglin Xia⁵, Muchen Pan⁵, Yue Wang⁵, Mingqiang Li¹, Ruhong Zhou^{3,4,*}, Xiaoguo Liu^{1,*}, Stephen Mann^{6,7,*} and Chunhai Fan^{1,*}

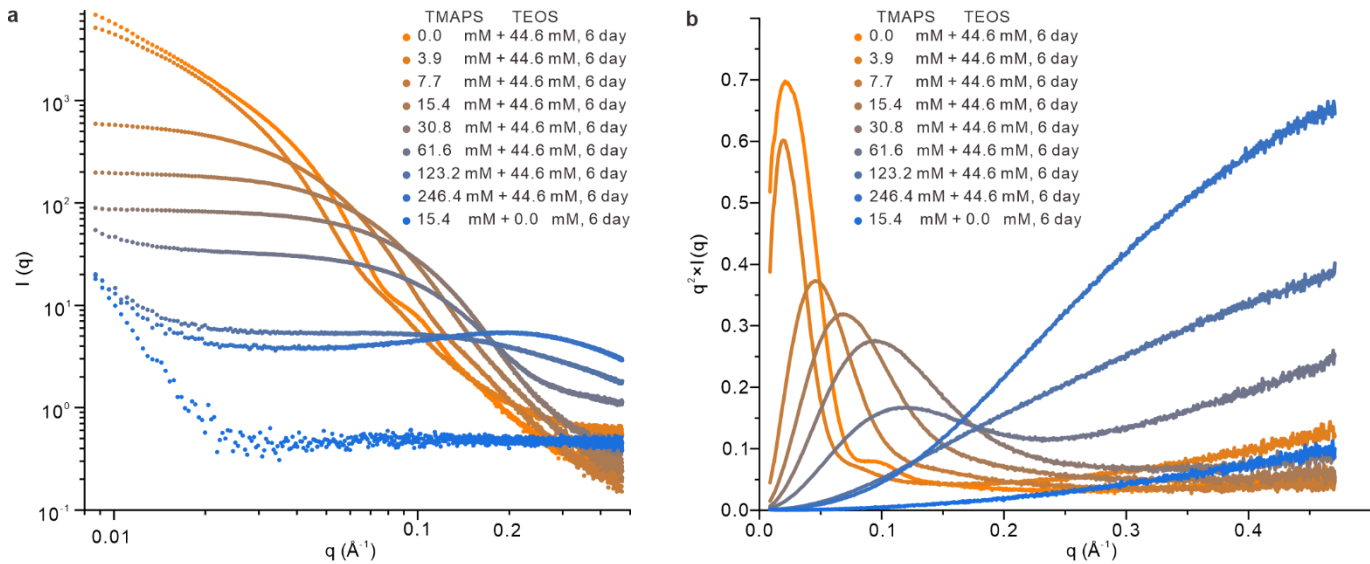
1. School of Chemistry and Chemical Engineering, New Cornerstone Science Laboratory, Frontiers Science Center for Transformative Molecules, Zhangjiang Institute for Advanced Study and National Center for Translational Medicine, Shanghai Jiao Tong University, Shanghai 200240, China.
2. Institute of Molecular Medicine, Shanghai Key Laboratory for Nucleic Acid Chemistry and Nanomedicine, Renji Hospital, School of Medicine, Shanghai Jiao Tong University, Shanghai, China.
3. Institute of Quantitative Biology, College of Life Sciences, and Department of Physics, Zhejiang University, Hangzhou, China.
4. Shanghai Institute for Advanced Study, Zhejiang University, Shanghai, China.
5. Division of Physical Biology, CAS Key Laboratory of Interfacial Physics and Technology, Shanghai Institute of Applied Physics, Chinese Academy of Sciences, Shanghai 201800, China.
6. School of Materials Science and Engineering, Shanghai Jiao Tong University, Shanghai 200240, China.
7. Max Planck-Bristol Centre for Minimal Biology, School of Chemistry, University of Bristol, Bristol BS8 1TS, United Kingdom.
8. These authors contribute equally, Xinxin Jing, Haozhi Wang, Jianxiang Huang and Yingying Liu.

*e-mails: rz24@columbia.edu, liuxiaoguo@sjtu.edu.cn, s.mann@bristol.ac.uk, and fanchunhai@sjtu.edu.cn

Contents

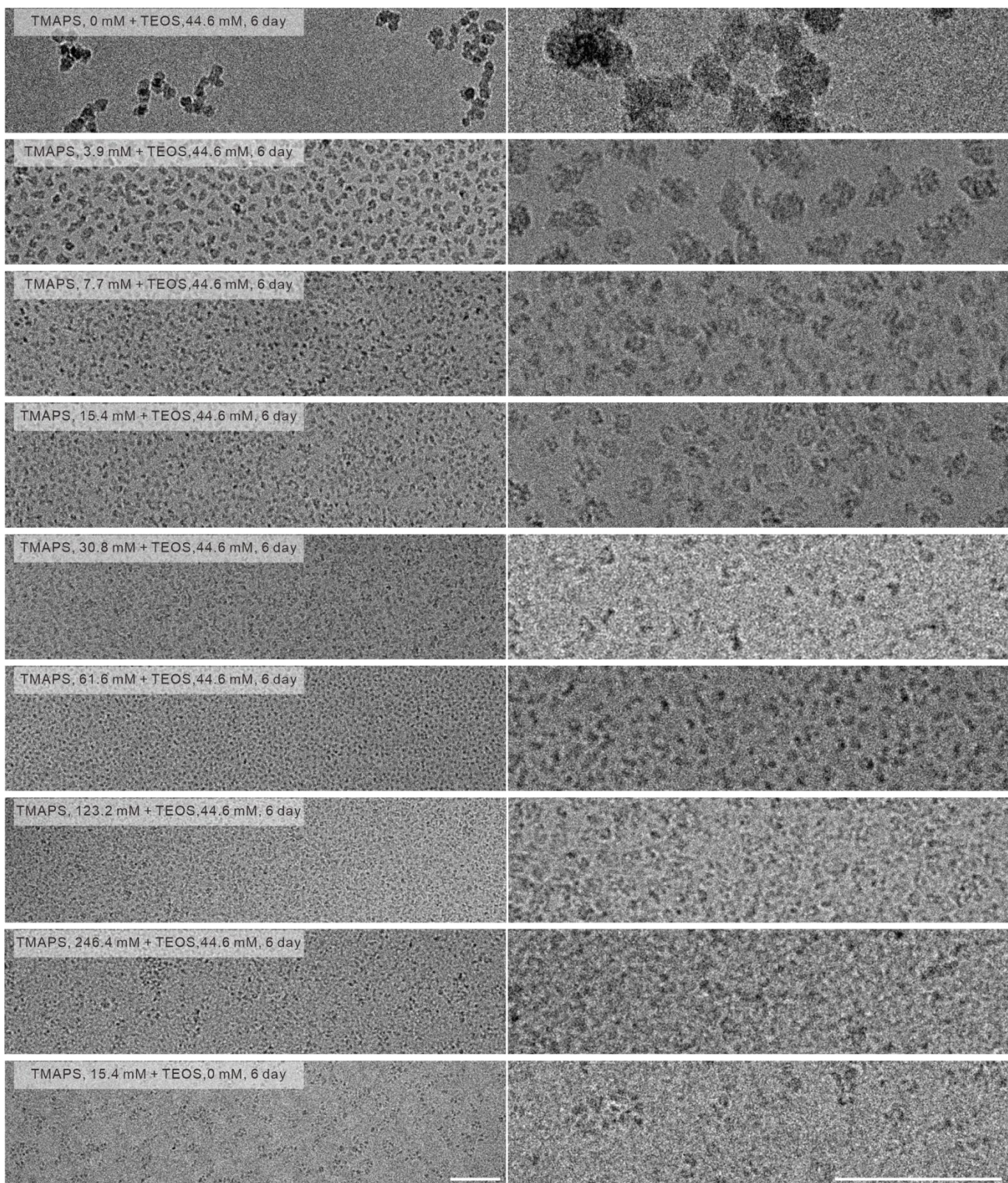
S1. Supplementary data for CSC	3
Supplementary Fig.1 SAXS analysis of CSC prepared with different TMAPS/TEOS ratios.....	3
Supplementary Fig.2 Cryo-EM images of CSC prepared with different TMAPS/TEOS ratios.....	4
Supplementary Fig.3 Cryo-EM images of CSC prepared with different TMAPS/TEOS ratios.....	5
Supplementary Fig.4 ζ -potential phase diagram of CSC.	6
Supplementary Fig.5 pH binary phase diagram of CSC.	7
Supplementary Fig.6 CSC formation under different pH conditions.	8
Supplementary Fig.7 Cryo-EM images of silica prenucleation clusters (PNCs) and CSC.	9
Supplementary Table 1 Averaged sizes of CSC using different characterization methods.	10
Supplementary Table 2 DLS diameters (nm) of CSC prepared with different stoichiometric ratios.....	11
Supplementary Table 3 ζ -potential (mV) of CSC prepared with different stoichiometric ratios.....	12
Supplementary Table 4 Integrated intensity ratios of ^{29}Si NMR peaks in different-size CSC.	13
S2. Supplementary data for CSC-directed silicification of programmable DNA frameworks.....	14
Supplementary Fig.8 Cryo-EM single-particle analysis of native tetrahedron DNA origami.....	14
Supplementary Fig.9 TEM and cryo-EM images of triangle DNA origami sample group.....	15
Supplementary Fig.10 TEM and cryo-EM images of rectangle DNA origami sample group.	16
Supplementary Fig.11 TEM and cryo-EM images of double-layer DNA origami sample group.....	17
Supplementary Fig.12 TEM and cryo-EM images of 14-helix DNA origami sample group.....	18
Supplementary Fig.13 TEM and cryo-EM images of 24-helix DNA origami sample group.....	19
Supplementary Fig.14 Cryo-EM images of tetrahedral DNA origami sample group.	20
Supplementary Fig.15 Cryo-EM images of octahedral DNA origami sample group.....	21
Supplementary Fig.16 Cryo-EM images of cubic DNA origami sample group.....	22
Supplementary Fig.17 TEM/SEM/cryo-EM images of <i>p6mm</i> 2D DNA and DNA/CSC superstructure.	23
Supplementary Fig.18 EDS mapping of <i>p6mm</i> 2D DNA/CSC superstructure.	24
Supplementary Fig.19 Detailed characterization of <i>p6mm</i> 2D DNA lattice.	25
Supplementary Fig.20 Detailed characterization of <i>p6mm</i> 2D DNA/CSC superstructure.	26
Supplementary Table 5 Cryo-EM Data Collection and Refinement Statistics.	27
S3. Design of DNA frameworks	28
Supplementary Fig.21 Strand diagram of tetrahedral DNA origami.....	28
Supplementary Fig.22 Strand diagram of octahedral DNA origami.	29
Supplementary Fig.23 Strand diagram of cubic DNA origami.	30
Supplementary Fig.24 Strand diagram of 48-helix DNA origami.	31
Supplementary Fig.25 Strand diagram of 54-helix DNA origami.	32
Supplementary Fig.26 Strand diagram of 2-layer DNA origami.	33
Supplementary Fig.27 Strand diagram of 24-helix DNA origami.	34
Supplementary Fig.28 Strand diagram of <i>p6mm</i> 2D DNA lattice.	35
S4. DNA sequences.....	36
Supplementary Table 8 DNA sequences of tetrahedron DNA origami (Scaffold 5250).	36
Supplementary Table 9 DNA sequences of octahedron DNA origami (Scaffold 10004).	39
Supplementary Table 10 DNA sequences of cube DNA origami (Scaffold 10004).....	44
Supplementary Table 11 DNA sequences of 48helix DNA origami (Scaffold 7249).	49
Supplementary Table 12 DNA sequences of 54helix DNA origami (Scaffold 8064).	54
Supplementary Table 13 DNA sequences of 2-layer DNA origami (Scaffold 8064)	58
Supplementary Table 14 DNA sequences of 24helix DNA origami (Scaffold 8064).	63
Supplementary Table 15 DNA sequences of <i>p6mm</i> DNA lattice.....	67

S1. Supplementary data for CSC



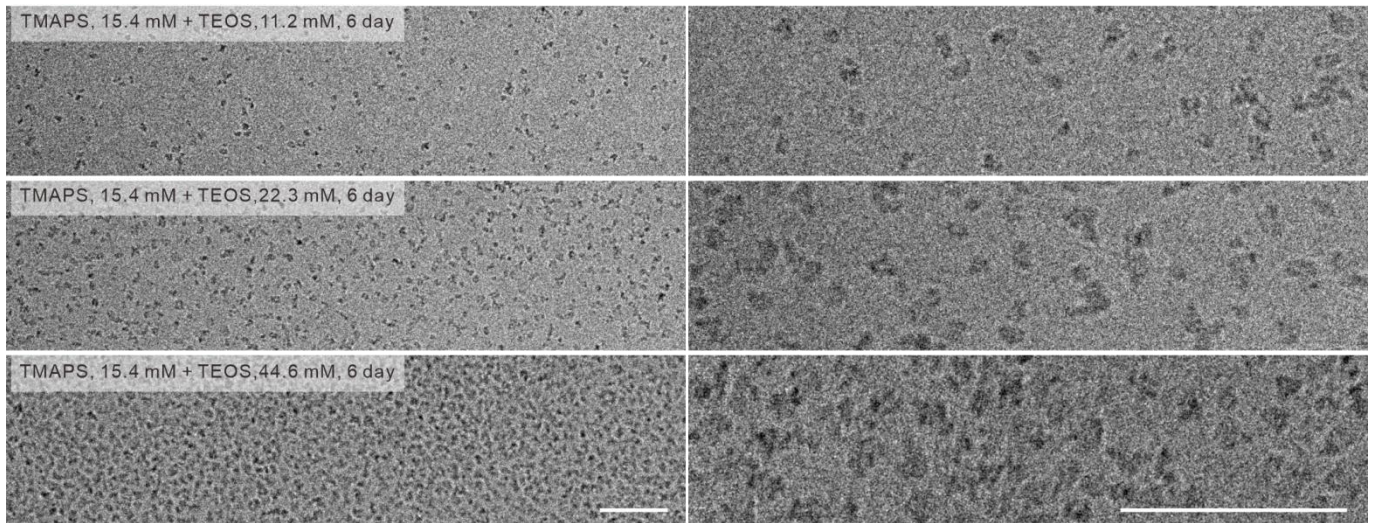
Supplementary Fig.1 | SAXS analysis of CSC prepared with different TMAPS/TEOS ratios.

a. The slope of the SAXS profiles in the low- q region decreased as the TMAPS concentrations increased, indicating a negative correlation between CSC size and TMAPS concentration. **b.** Kratky plots showed continuous changes of curve shapes from parabolic convergence, partial parabolic convergence to linear divergence, revealing a decrease in the compactness of CSC with increasing TMAPS concentration. The Kratky plot of 15.4 mM TMAPS + 0.0 mM TEOS exhibited a linear divergence feature, suggesting that CSC formation was inhibited in the absence of TEOS.



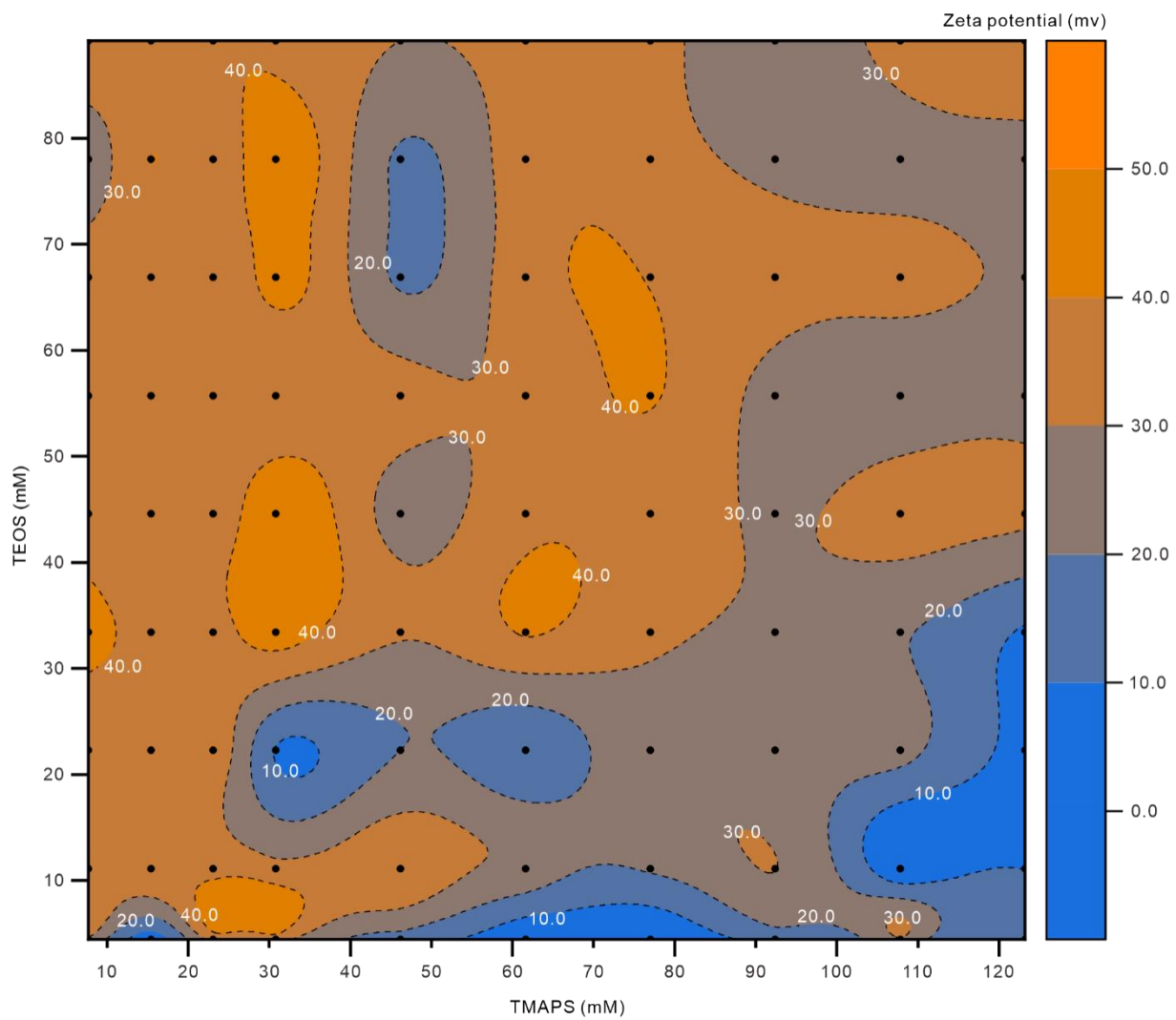
Supplementary Fig.2 | Cryo-EM images of CSC prepared with different TMAPS/TEOS ratios.

Corresponding cryo-EM images of samples characterized by SAXS in Fig. S1. The images showed that the sizes of the CSC decrease as the concentration of TMAPS increases (TEOS = 44.6 mM). Inhomogeneous silica clusters occurred when the TMAPS concentration was higher than 123.2 mM, or in the absence of TEOS. Scale bars, 50 nm. See also Supplementary Figure 3.



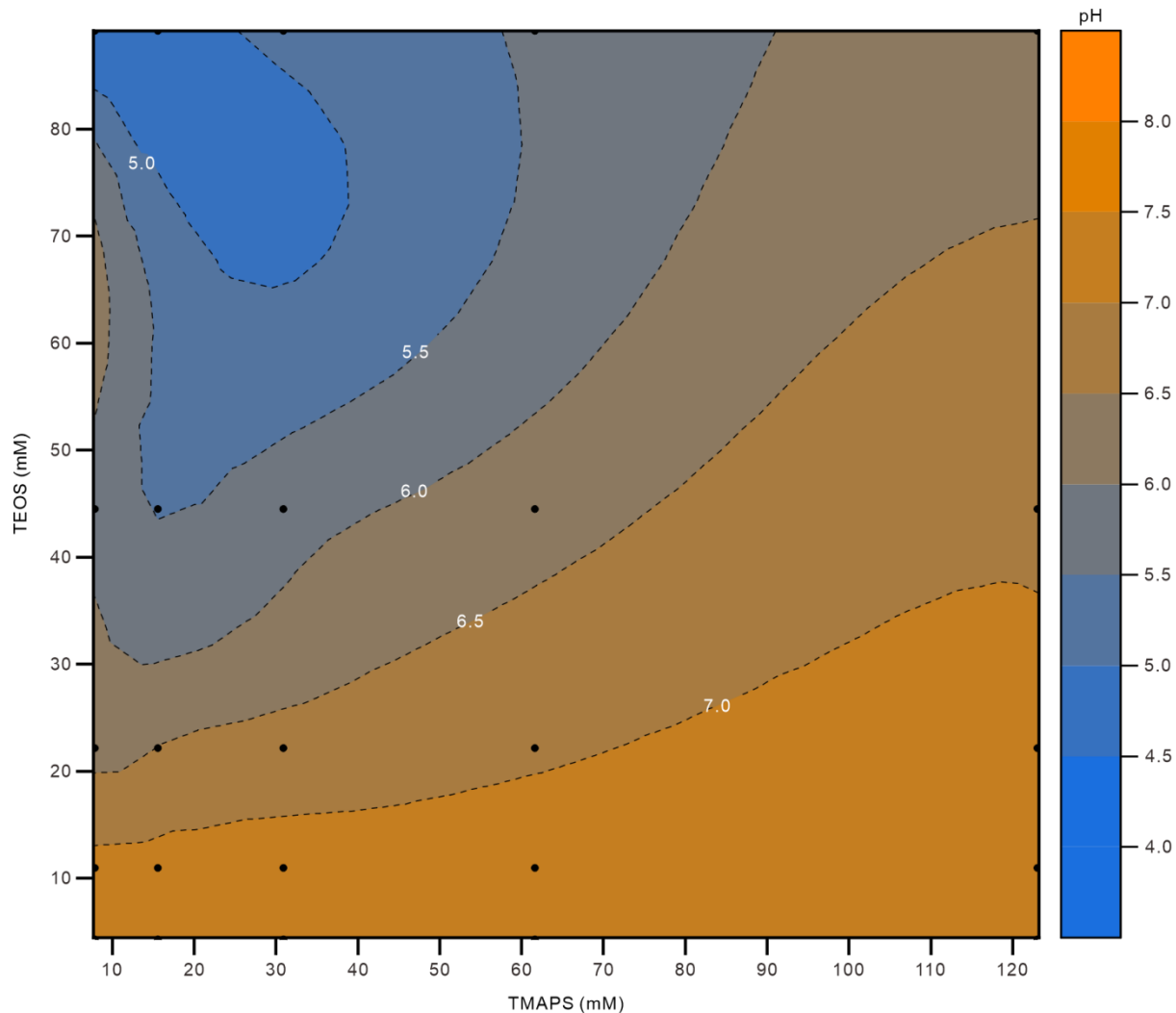
Supplementary Fig.3 | Cryo-EM images of CSC prepared with different TMAPS/TEOS ratios.

The results revealed that the sizes of CSC mainly depended on the concentrations of TMAPS rather than TEOS. As TEOS concentration increased from 11.2 mM to 22.3 mM and 44.6 mM, there was no significant change in the sizes of the CSC. An increase in the particle number was observed as the TEOS concentrated increased. Scale bars, 50 nm.



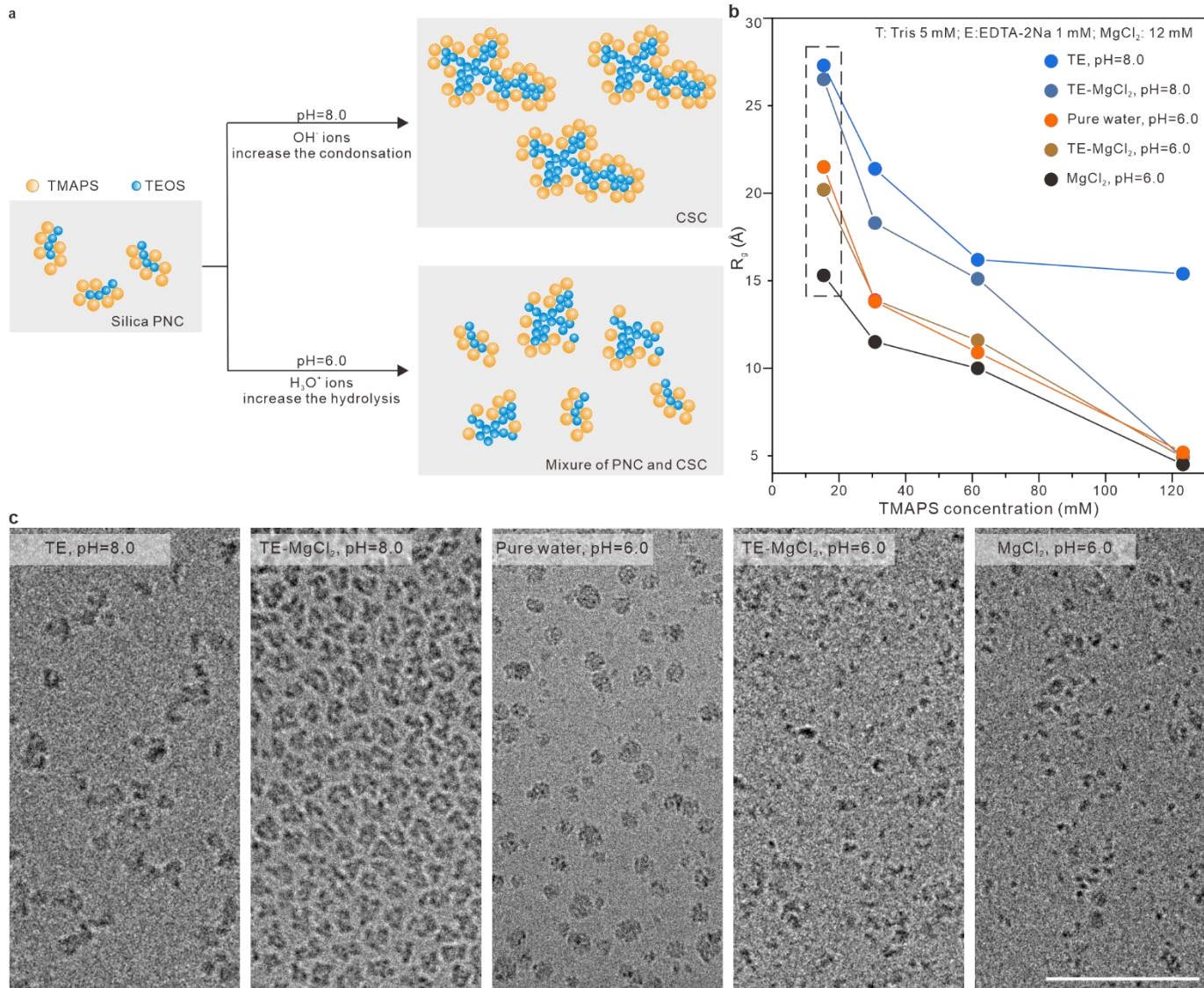
Supplementary Fig.4 | ζ -potential phase diagram of CSC.

Most CSC exhibited positive ζ -potentials in the range of 30 mV to 40 mV, owing to the pendent trimethylammonium side chain ($-N^+(CH_3)_3$) of TMAPS. The ζ -potentials below 10 mV occurred frequently when the concentration of TMAPS was extremely high (123.2 mM or 246.2 mM). This result mainly derived from the inhibitory effect of high concentrations of TMAPS on the formation of silica pre-nucleation clusters. The black dots are recorded experimental data. Dotted contour lines indicate the boundaries of different ζ -potentials, as marked by white letters.



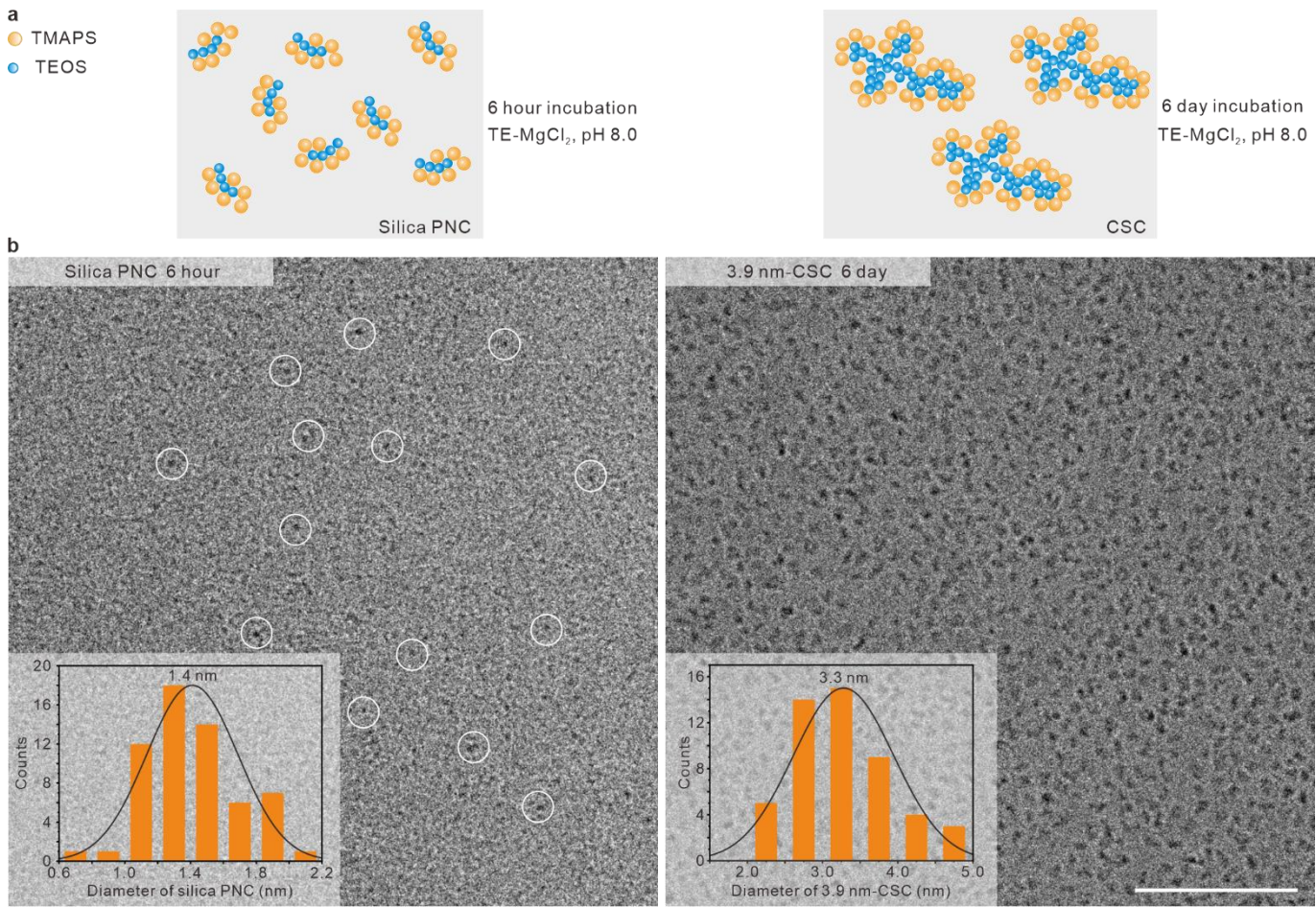
Supplementary Fig.5 | pH binary phase diagram of CSC.

A gradual decrease of pH was observed as the concentration of TMAPS decreased or the concentration of TEOS increased due to consumption of hydroxide ions during the sol-gel process. The initial mixtures of TMAPS+TEOS in TE-MgCl₂ buffer all have a pH of 8.0. The black dots are recorded experimental data. Dotted contour lines indicated the boundaries of different pH, as marked by white letters.



Supplementary Fig.6 | CSC formation under different pH conditions.

a, b. Schematics and corresponding SAXS R_g data of CSC formation under different pH conditions. Previous studies indicated that H_3O^+ ions in the solution increase the hydrolysis rate, whereas OH^- ions increase the condensation rate³³. Homogeneous CSC are produced only when the pH of solution is ~8.0. In contrast, at pH ~6.0, a mixture of silica pre-nucleation cluster (PNC) and CSC are produced due to the hydrolysis rate being higher than the condensation rate. **c.** Five typical samples (dashed box in **b**) were imaged by cryo-EM. In general, CSC were only produced in TE- $MgCl_2$ buffer (pH=8.0). TE buffer (pH=8.0) without $MgCl_2$ induced further aggregation of the CSC, while buffers at pH 6.0 resulted in inhomogeneous clusters with reduced dimensions compared with the CSC. Scale bar, 50 nm.



Supplementary Fig.7 | Cryo-EM images of silica prenucleation clusters (PNCs) and CSC.

a. Schematics of the formation of silica PNCs after 6-hour incubation and CSC after 6-day incubation. **b.** Cryo-EM images of silica PNCs and CSC. Small silica PNCs can be clearly observed in the early growth stage of CSC (left panel). Representative silica PNCs were marked by white circles. The bottom left insets showed the statistics of the silica PNCs and CSC sizes; ~1.4 nm for silica PNCs and ~3.3 nm for CSC. Scale bar, 50 nm.

Supplementary Table 1 | Averaged sizes of CSC using different characterization methods.

Characterization method	Diameter (Å)			
	15.4 mM TMAPS +44.6 mM TEOS	30.8 mM TMAPS +44.6 mM TEOS	61.6 mM TMAPS +44.6 mM TEOS	123.2 mM TMAPS +44.6 mM TEOS
	72.3	45.0	36.0	14.2
Cryo-EM	60.2	50.0	32.8	27.3
SAXS ($2 \times (5/3)^{0.5} \times R_g$)	68.4	47.2	39.0	12.6
Name of CSC	6.8 nm-CSC	4.7 nm-CSC	3.9 nm-CSC	1.3 nm-CSC

Supplementary Table 2 | DLS diameters (nm) of CSC prepared with different stoichiometric ratios.

TMAPS(mM)\TEOS(mM)	0.0	3.9	7.7	15.4	23.1	30.8	46.2	61.6	77.0	92.4	107.8	123.2
0.0	0.0	0.8	0.7	0.8	\	0.7	\	0.8	\	\	\	0.8
2.2	0.7	0.7	0.7	0.7	\	0.7	\	0.7	\	\	\	0.8
4.5	60.7	16.7	7.8	5.7	4.3	4.7	0.7	0.7	0.8	0.8	0.7	0.8
11.2	18.0	11.9	6.7	5.6	4.8	4.8	4.7	3.9	0.7	0.9	0.7	0.7
22.3	22.2	14.3	7.9	5.6	4.8	4.8	3.8	4.2	3.4	0.8	0.7	0.7
33.5	\	\	6.6	5.3	5.0	4.7	3.0	4.5	4.4	5.3	0.8	0.8
44.6	34.1	23.4	7.6	5.5	4.4	5.7	3.3	4.6	4.8	4.3	0.6	0.8
55.8	\	\	8.9	6.0	4.6	4.9	3.7	3.1	4.5	4.3	0.8	1.0
66.9	\	\	6.8	6.1	5.1	5.9	4.0	4.1	4.2	4.5	0.9	0.8
78.1	\	\	9.3	6.4	5.2	5.8	4.0	4.5	4.4	3.8	3.7	4.5
89.2	31.3	16.3	9.3	6.4	6.6	6.1	4.0	4.5	3.2	3.8	3.9	4.4

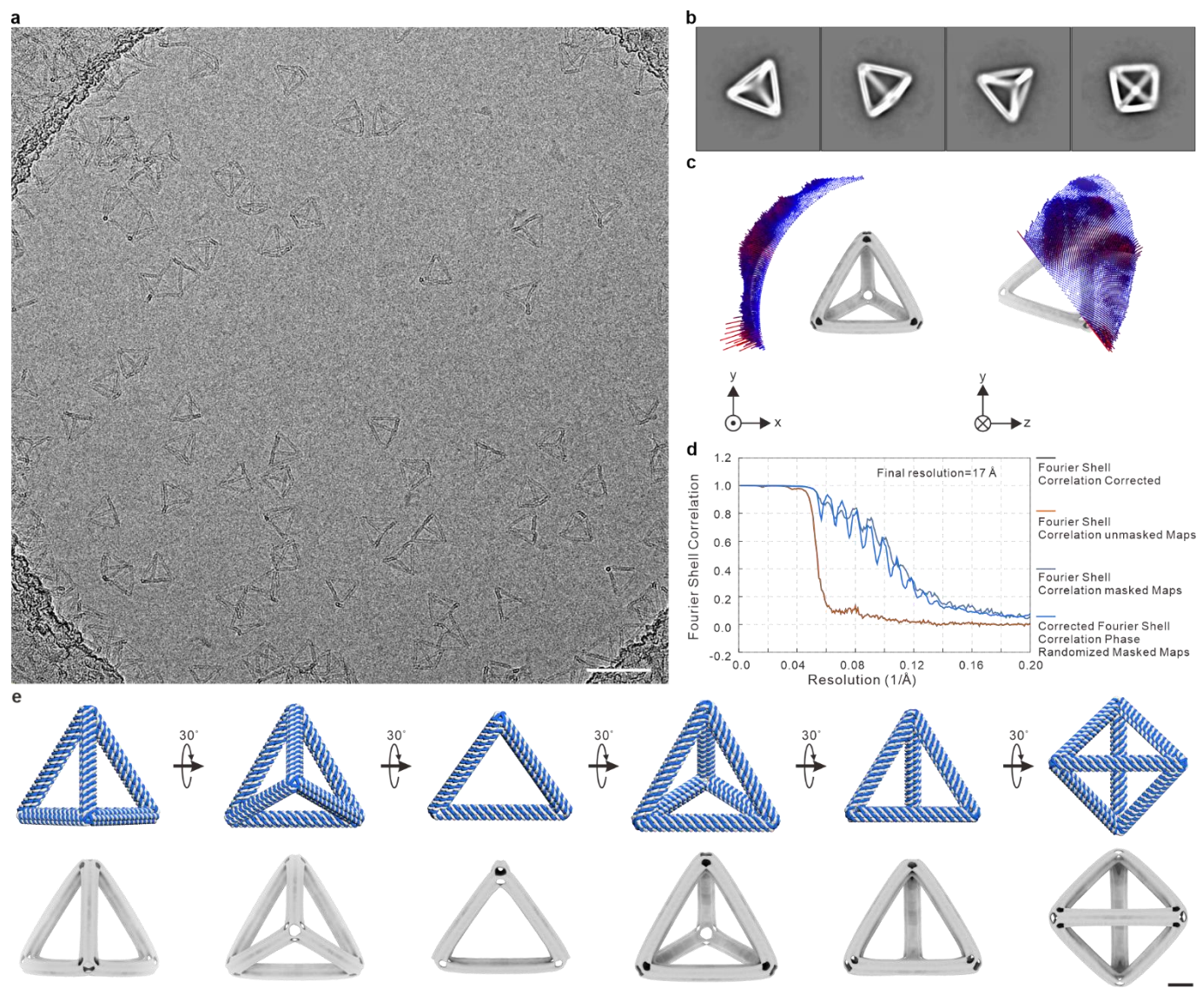
Supplementary Table 3 | ζ -potential (mV) of CSC prepared with different stoichiometric ratios.

TMAPS(mM)\TEOS(mM)	7.7	15.4	23.1	30.8	46.2	61.6	77.0	92.4	107.8	123.2
4.5	28.1	4.9	33.8	35.2	15.0	1.8	0.3	14.3	29.1	11.5
11.2	32.4	37.6	37.0	33.2	38.5	27.2	21.1	30.1	1.9	9.9
22.3	35.1	34.6	37.8	9.5	20.0	11.3	26.9	25.1	23.5	7.6
33.5	41.7	37.7	36.6	44.7	30.9	40.8	31.6	28.8	21.0	9.0
44.6	37.2	32.7	33.0	47.7	25.5	37.2	34.7	29.1	34.5	31.9
55.8	32.6	37.9	34.8	34.5	33.6	32.0	40.7	26.6	24.4	26.8
66.9	35.1	37.8	30.7	43.5	18.4	36.3	39.7	33.9	32.9	29.2
78.1	23.0	40.1	33.2	47.1	18.4	36.1	35.0	27.2	26.8	27.4
89.2	40.0	36.0	39.7	38.7	30.0	34.8	34.0	20.9	34.4	38.1

Supplementary Table 4 | Integrated intensity ratios of ^{29}Si NMR peaks in different-size CSC.

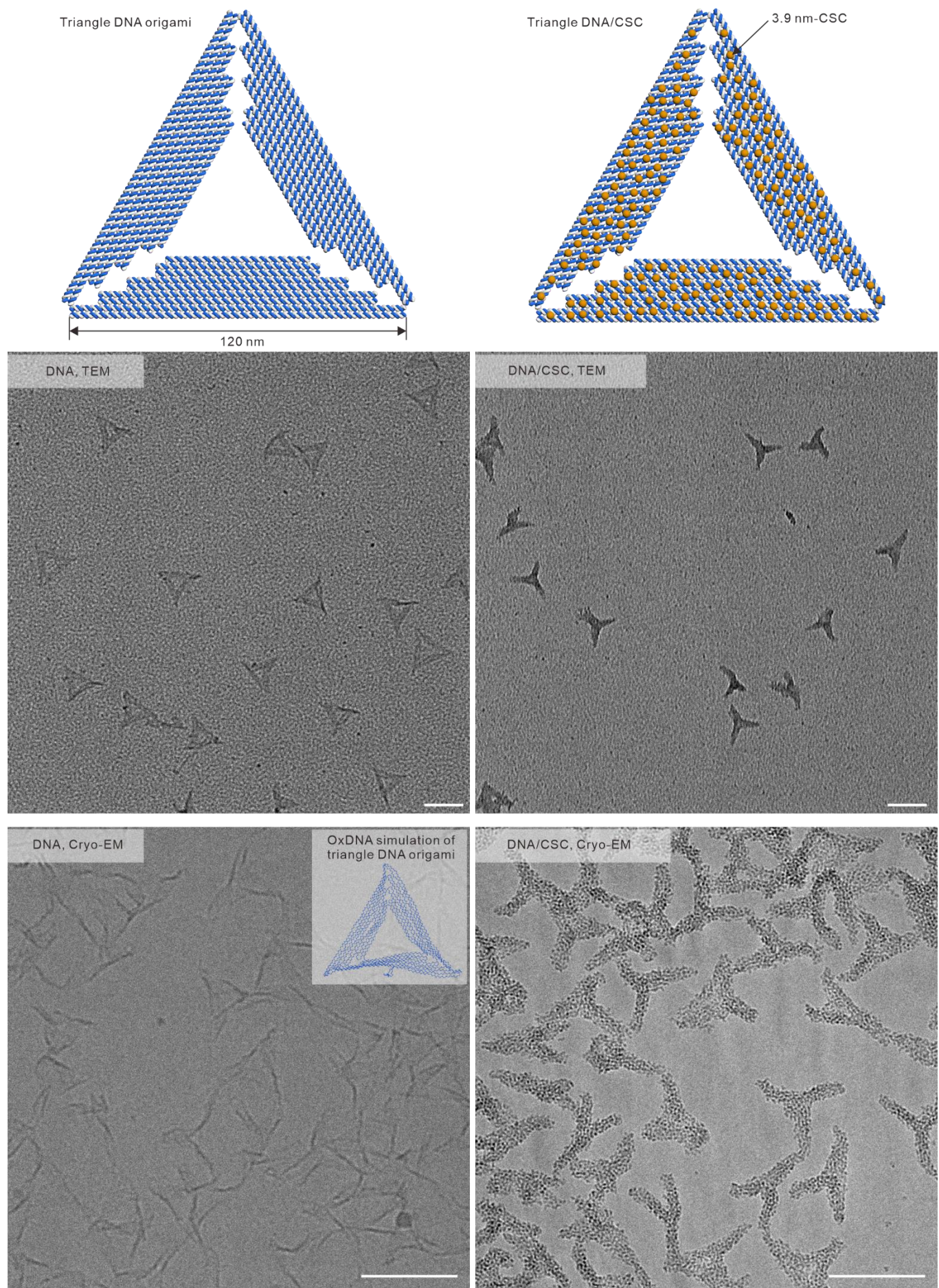
^{29}Si NMR peak	Chemical shift (ppm)	Integrated intensity ratios (%)						
		TEOS only	11.9-nm CSC	6.8-nm CSC	4.7-nm CSC	3.9-nm CSC	1.3-nm CSC	TMAPS only
T ⁰	-41	\	\	\	\	\	\	\
T ¹	-50	\	\	\	\	0.4	\	0.2
T ²	-59	\	15.0	6.8	36.0	22.7	57.9	59.5
T ³	-68	\	27.1	27.6	34.1	31.5	30.7	40.3
Q ⁰	-73	\	\	\	\	\	\	\
Q ¹	-82	\	\	\	\	\	\	\
Q ²	-91	\	0.5	2.3	\	2.2	\	\
Q ³	-100	20.5	43.4	45.9	22.7	34.0	11.4	\
Q ⁴	-109	79.5	14.0	17.4	7.2	9.2	\	\

S2. Supplementary data for CSC-directed silicification of programmable DNA frameworks



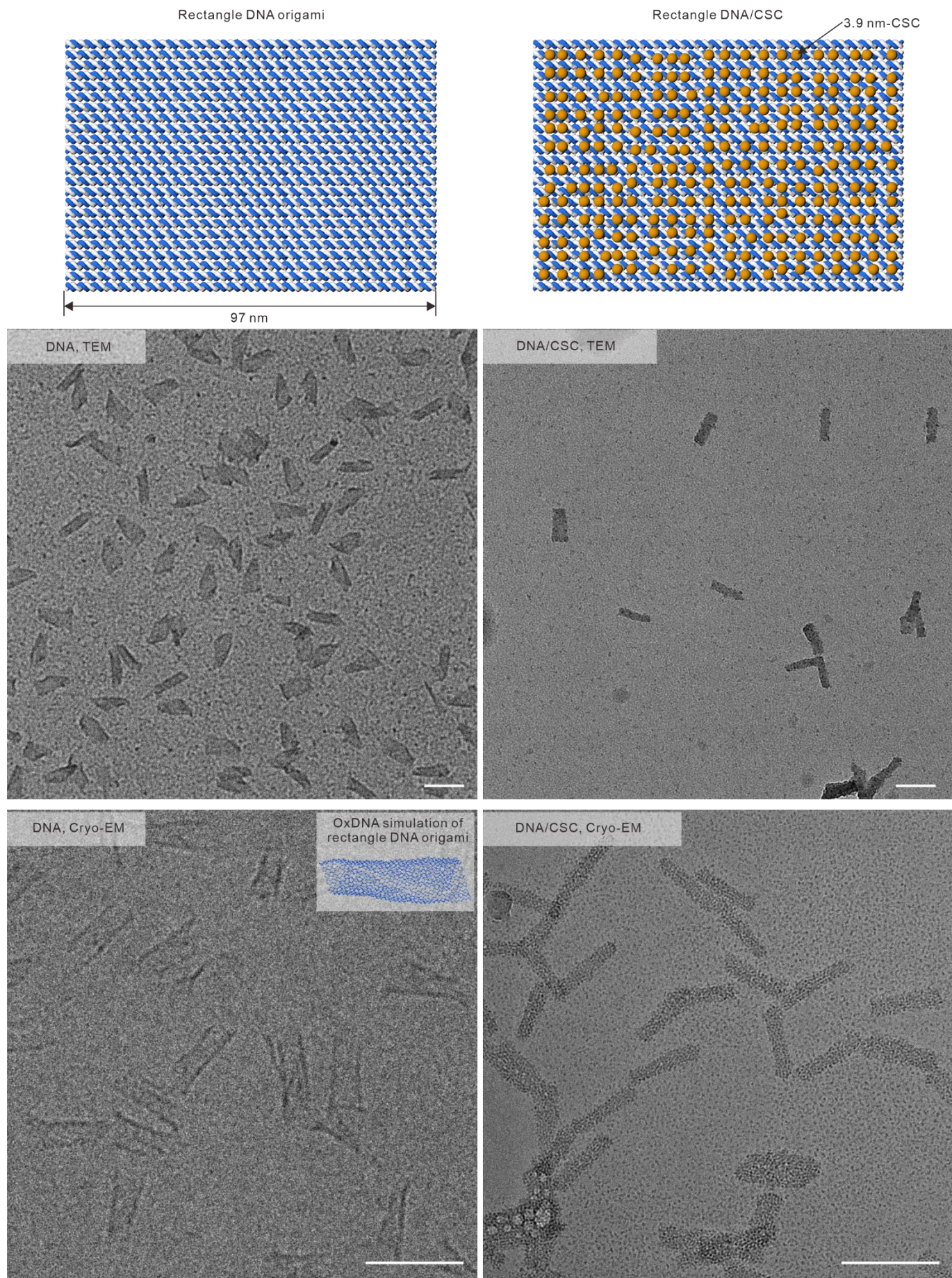
Supplementary Fig.8 | Cryo-EM single-particle analysis of native tetrahedron DNA origami.

a. Exemplary micrograph. Scale bar, 100 nm. **b.** Representative 2D class averages. **c.** Histogram representing the orientational distribution of particles. To reduce computational complexity, T symmetry was used in the 3D classifications and refinements. **d.** Fourier shell correlation plot. **e.** Six different views of the electron density map. Scale bar, 10 nm.



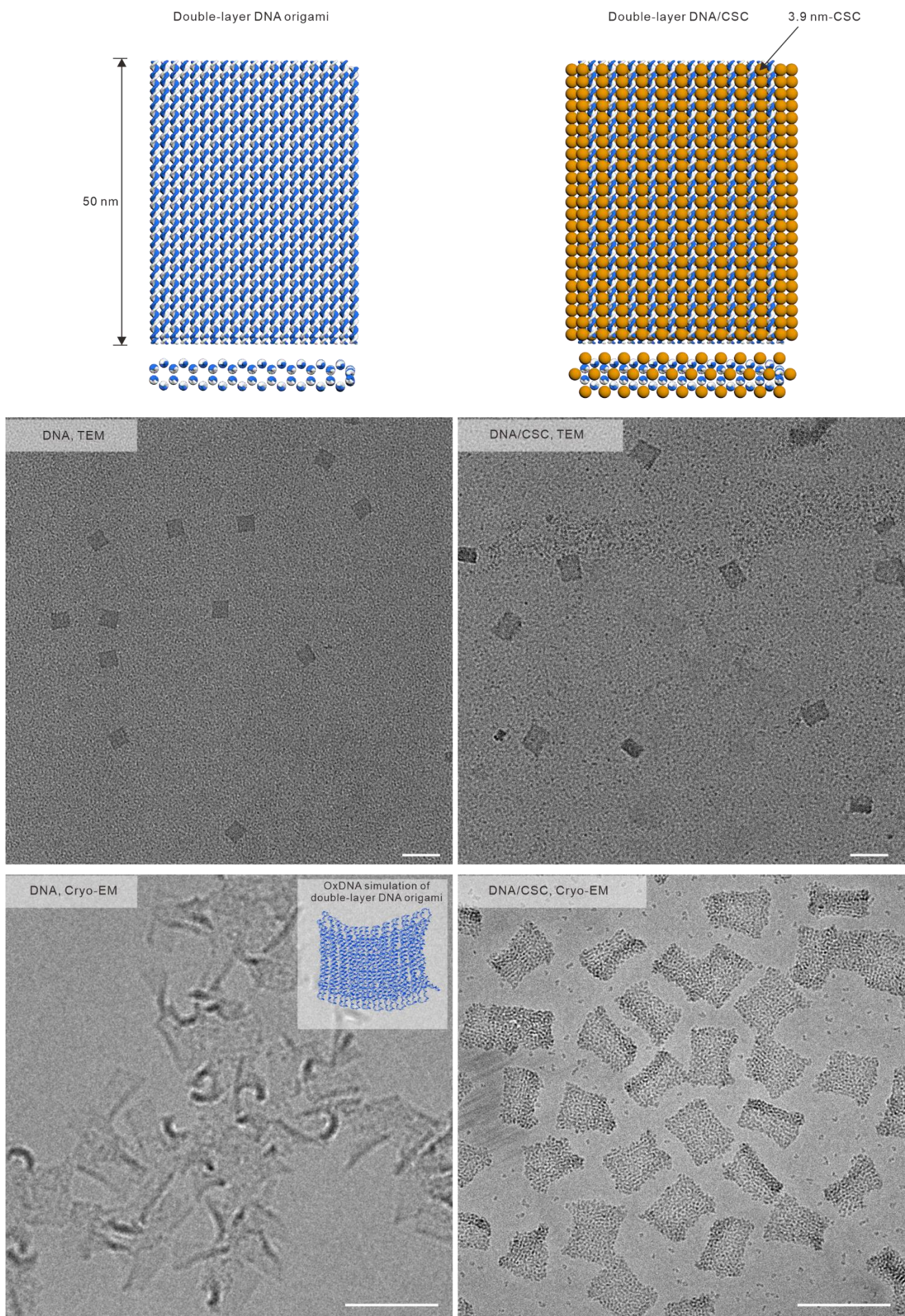
Supplementary Fig.9 | TEM and cryo-EM images of triangle DNA origami sample group.

The inset in the cryo-EM image is the OxDNA simulation of triangle DNA origami, illustrating the twisted conformation of the initially planar triangle DNA origami, consistent with the cryo-EM images. Scale bars, 100 nm.



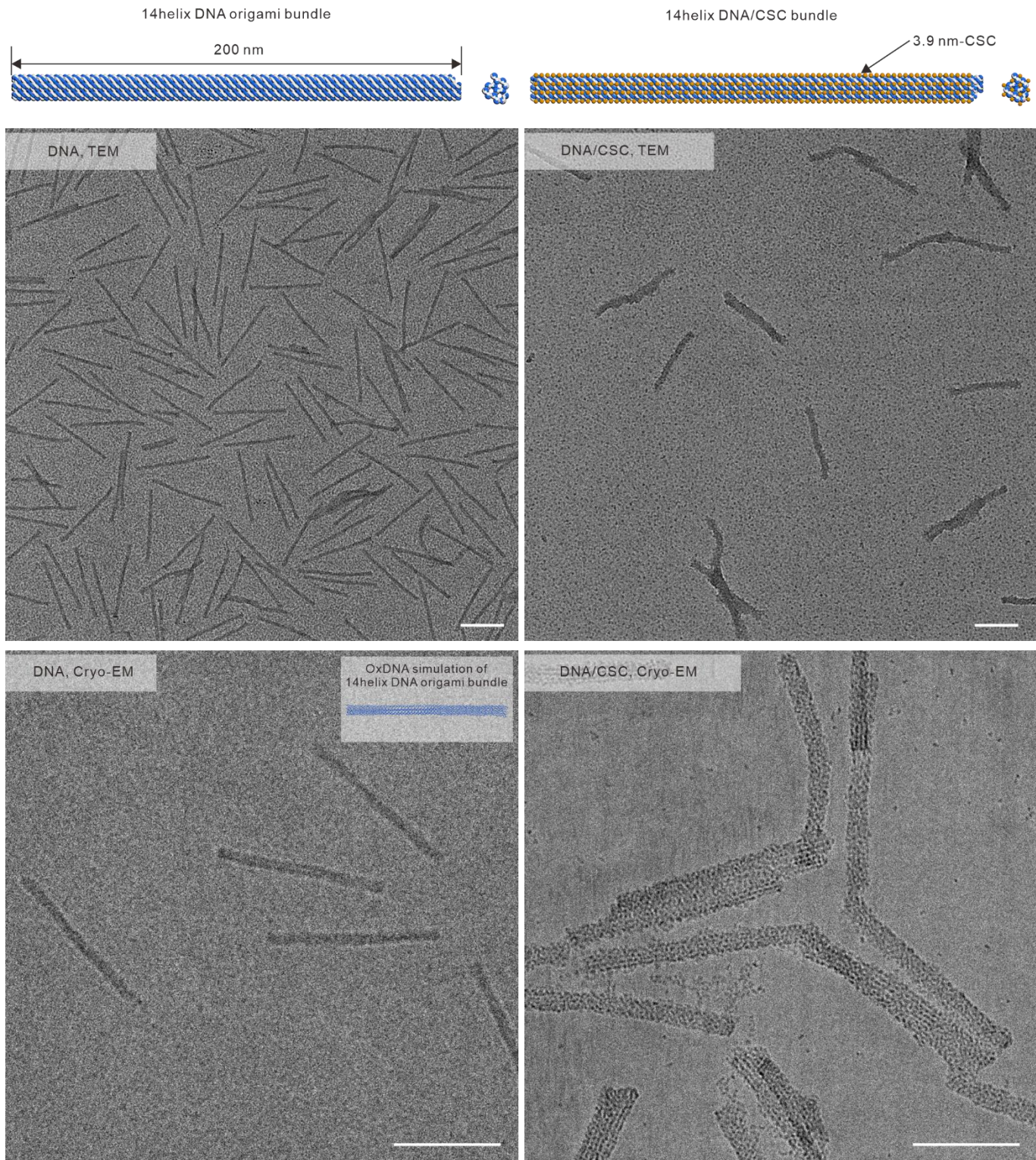
Supplementary Fig.10 | TEM and cryo-EM images of rectangle DNA origami sample group.

Rectangle DNA origami and DNA/CSC superstructure have a twisted conformation. Inset showed a barrel-shaped conformation of rectangle DNA origami by OxDNA simulation that was consistent with the cryo-EM images. Scale bars, 100 nm.



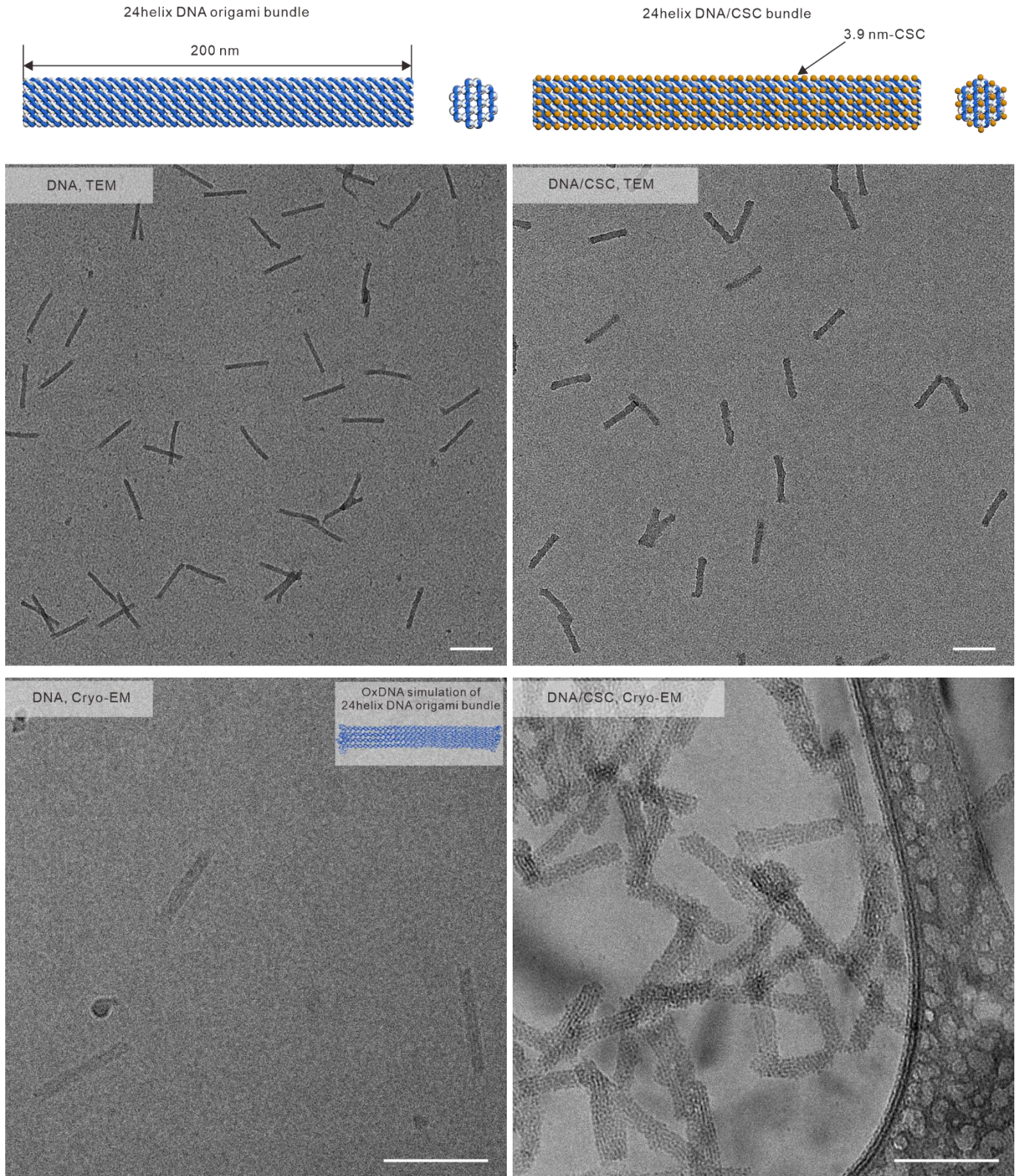
Supplementary Fig.11 | TEM and cryo-EM images of double-layer DNA origami sample group.

Inset showed a twisted conformation of double-layer DNA origami by OxDNA simulation, consistent with the cryo-EM images.
Scale bars, 100 nm.



Supplementary Fig.12 | TEM and cryo-EM images of 14-helix DNA origami sample group.

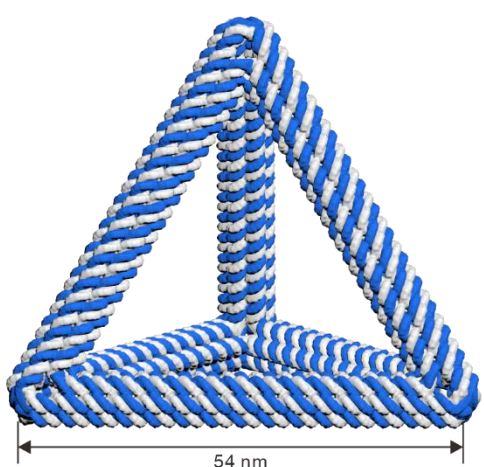
Inset showed rigid conformation of 14helix DNA origami bundle by OxDNA simulation, consistent with the cryo-EM images. Scale bars, 100 nm.



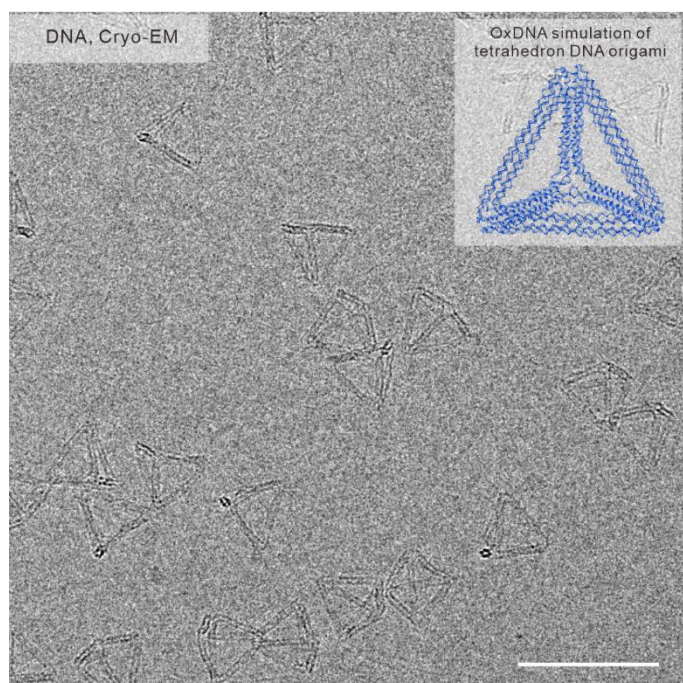
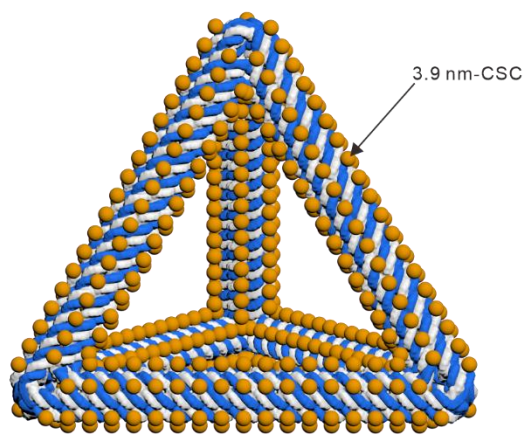
Supplementary Fig.13 | TEM and cryo-EM images of 24-helix DNA origami sample group.

Inset showed rigid conformation of 24helix DNA origami bundle by OxDNA simulation, consistent with the cryo-EM images. Scale bars, 100 nm.

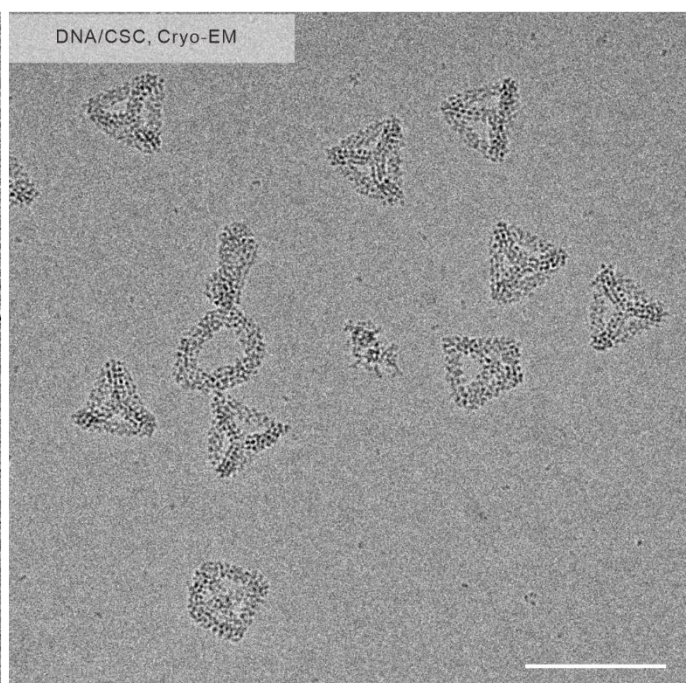
Tetrahedron DNA origami



Tetrahedron DNA/CSC

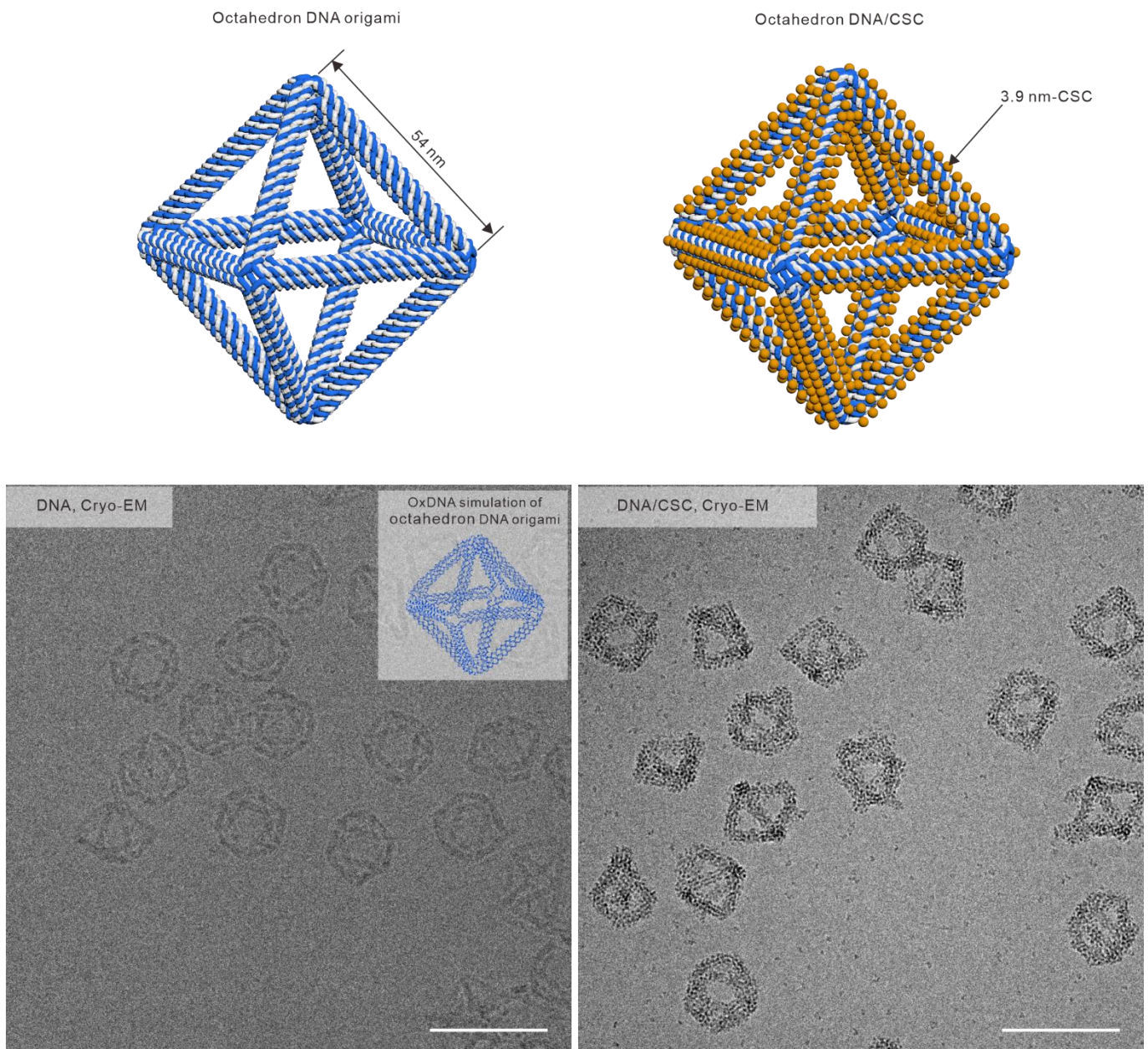


OxDNA simulation of tetrahedron DNA origami



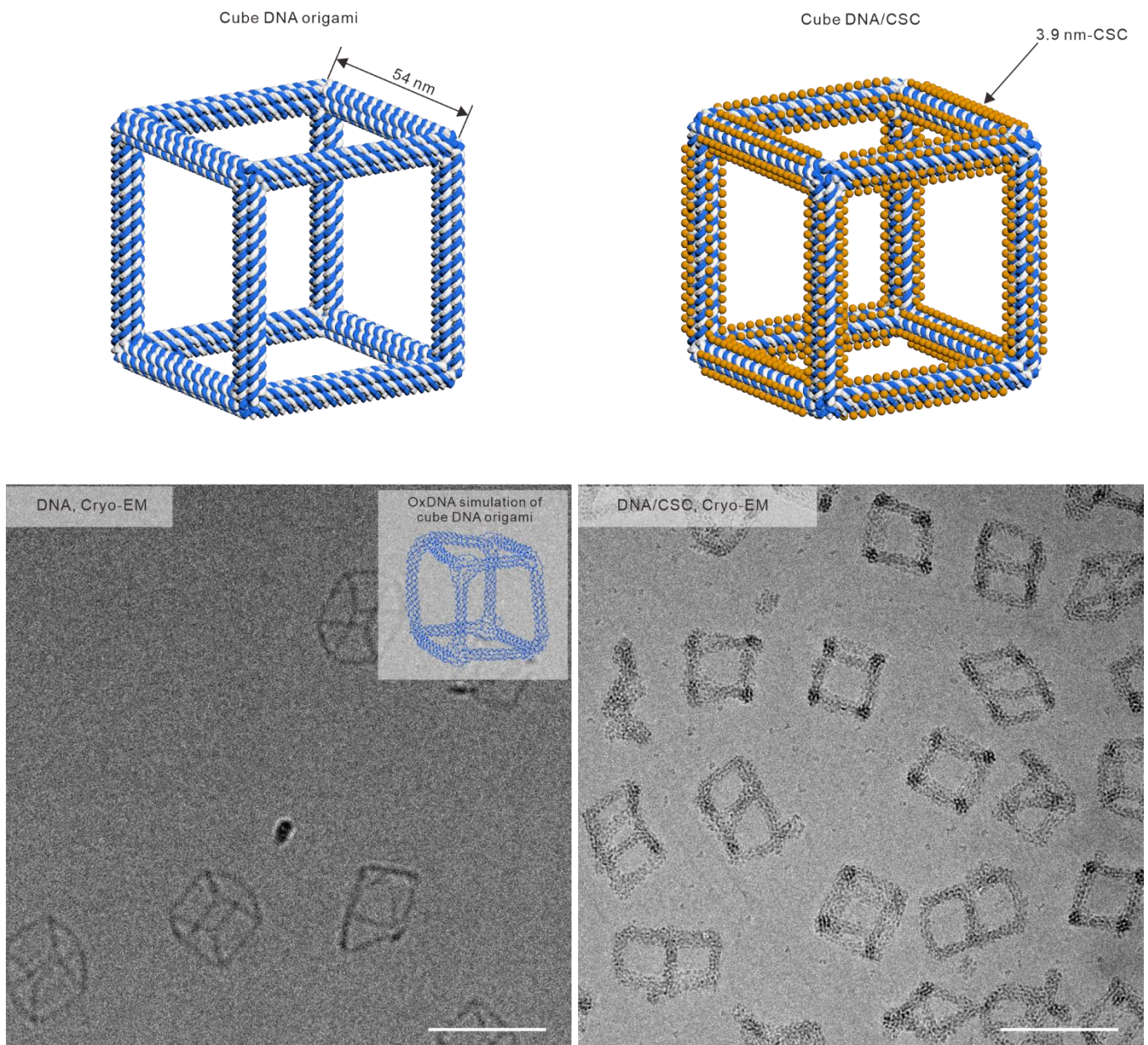
Supplementary Fig.14 | Cryo-EM images of tetrahedral DNA origami sample group.

Inset showed rigid conformation of tetrahedron DNA origami by OxDNA simulation, consistent with the cryo-EM images. Scale bars, 100 nm.



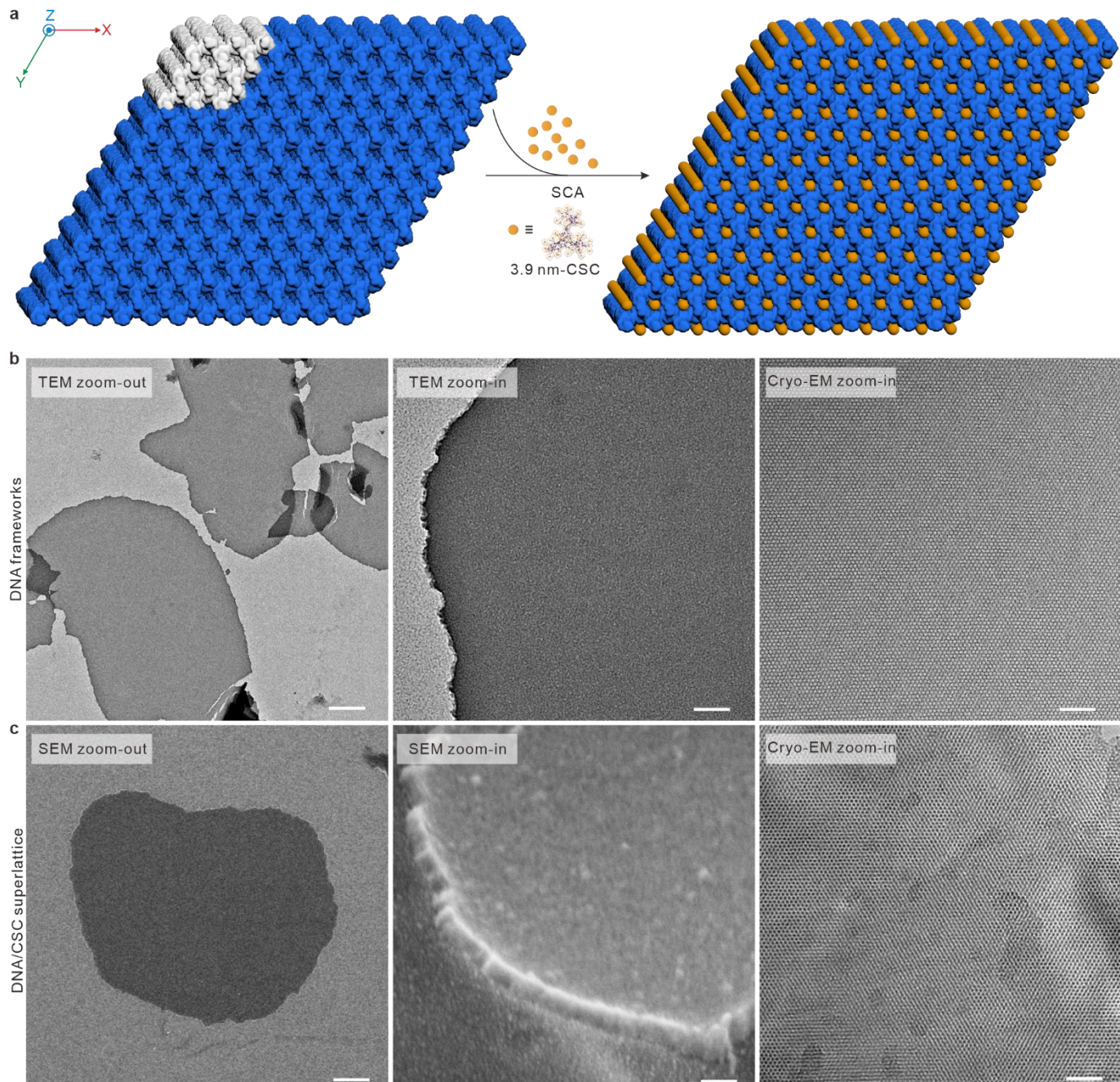
Supplementary Fig.15 | Cryo-EM images of octahedral DNA origami sample group.

Inset showed rigid conformation of octahedron DNA origami by OxDNA simulation, consistent with the cryo-EM images. Scale bars, 100 nm.



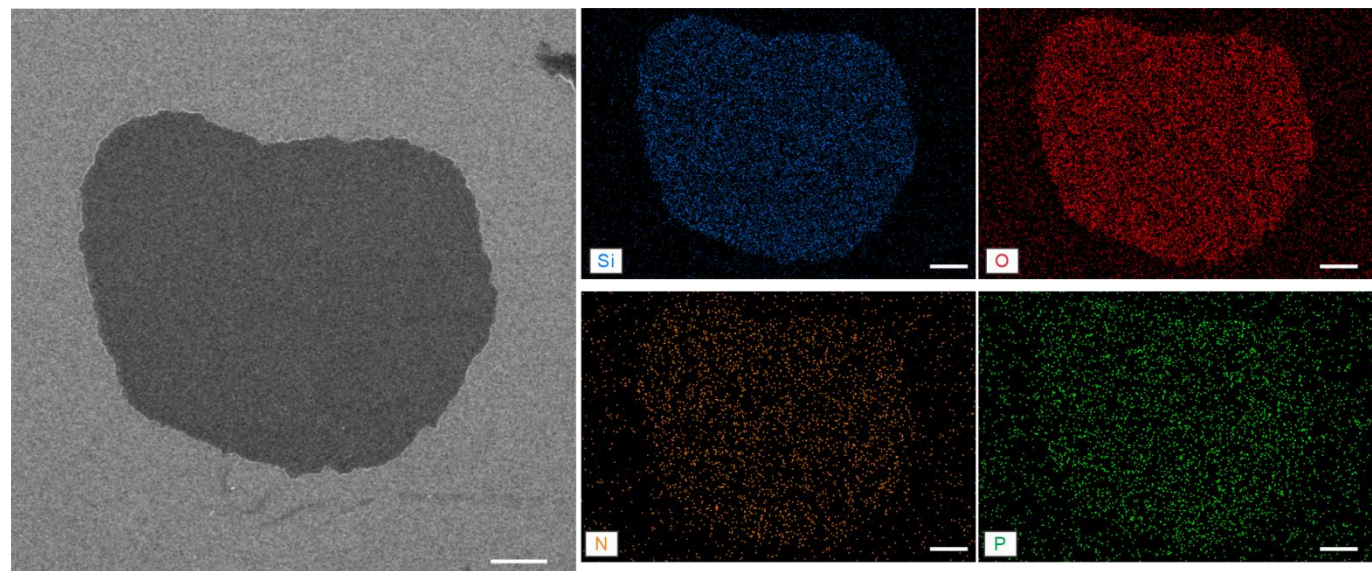
Supplementary Fig.16 | Cryo-EM images of cubic DNA origami sample group.

Inset showed rigid conformation of cube DNA origami by OxDNA simulation, consistent with the cryo-EM images. Scale bars, 100 nm.



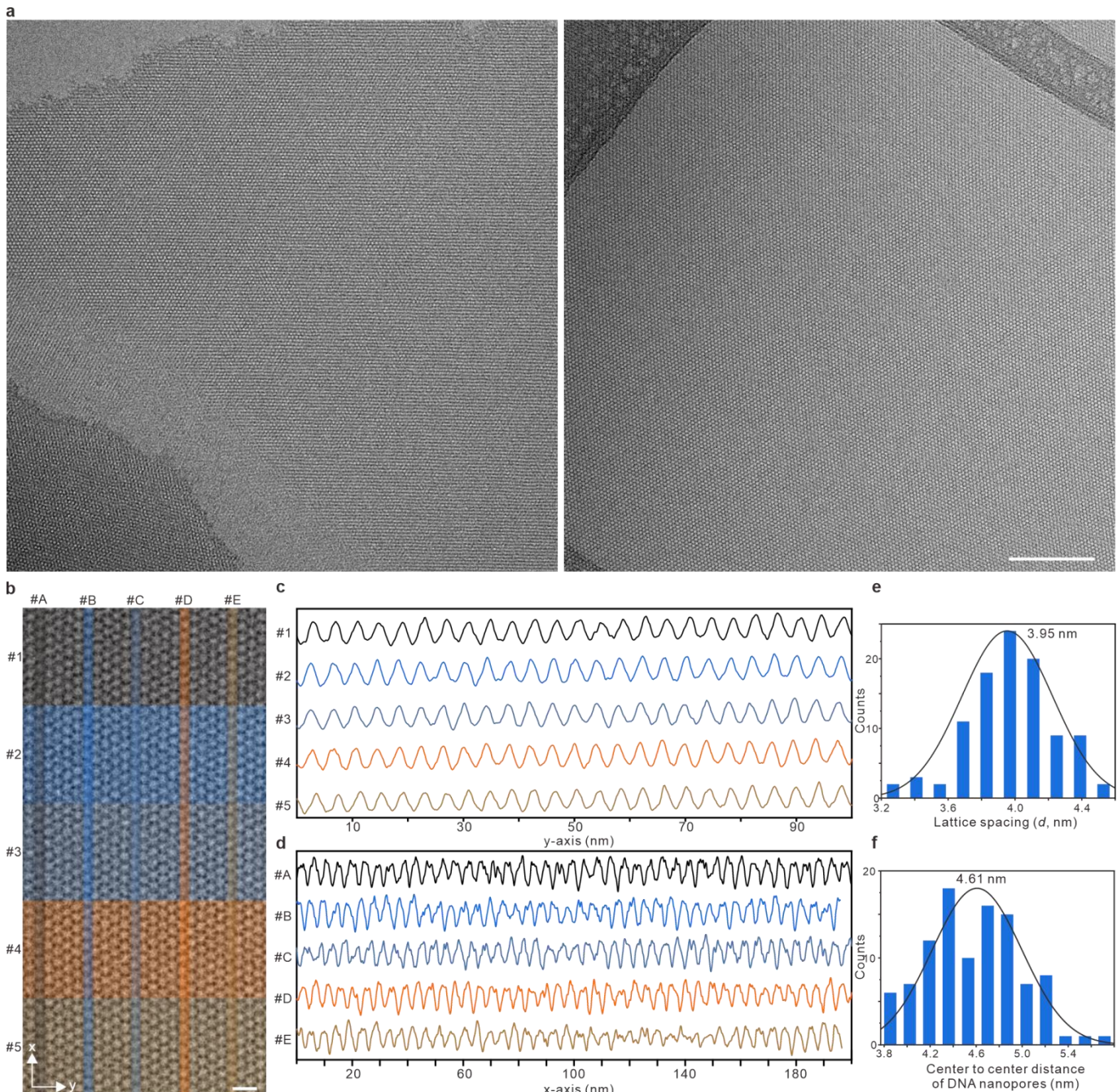
Supplementary Fig.17 | TEM/SEM/cryo-EM images of *p6mm* 2D DNA and DNA/CSC superstructure.

a. Formation of *p6mm* 2D DNA/CSC superstructure by silica cluster attachment (SCA). **b.** TEM/cryo-EM images of *p6mm* 2D DNA lattice. **c.** SEM/cryo-EM images of *p6mm* 2D DNA/CSC superstructure. Scale bars, from left to right, 500 nm, 100 nm and 40 nm.



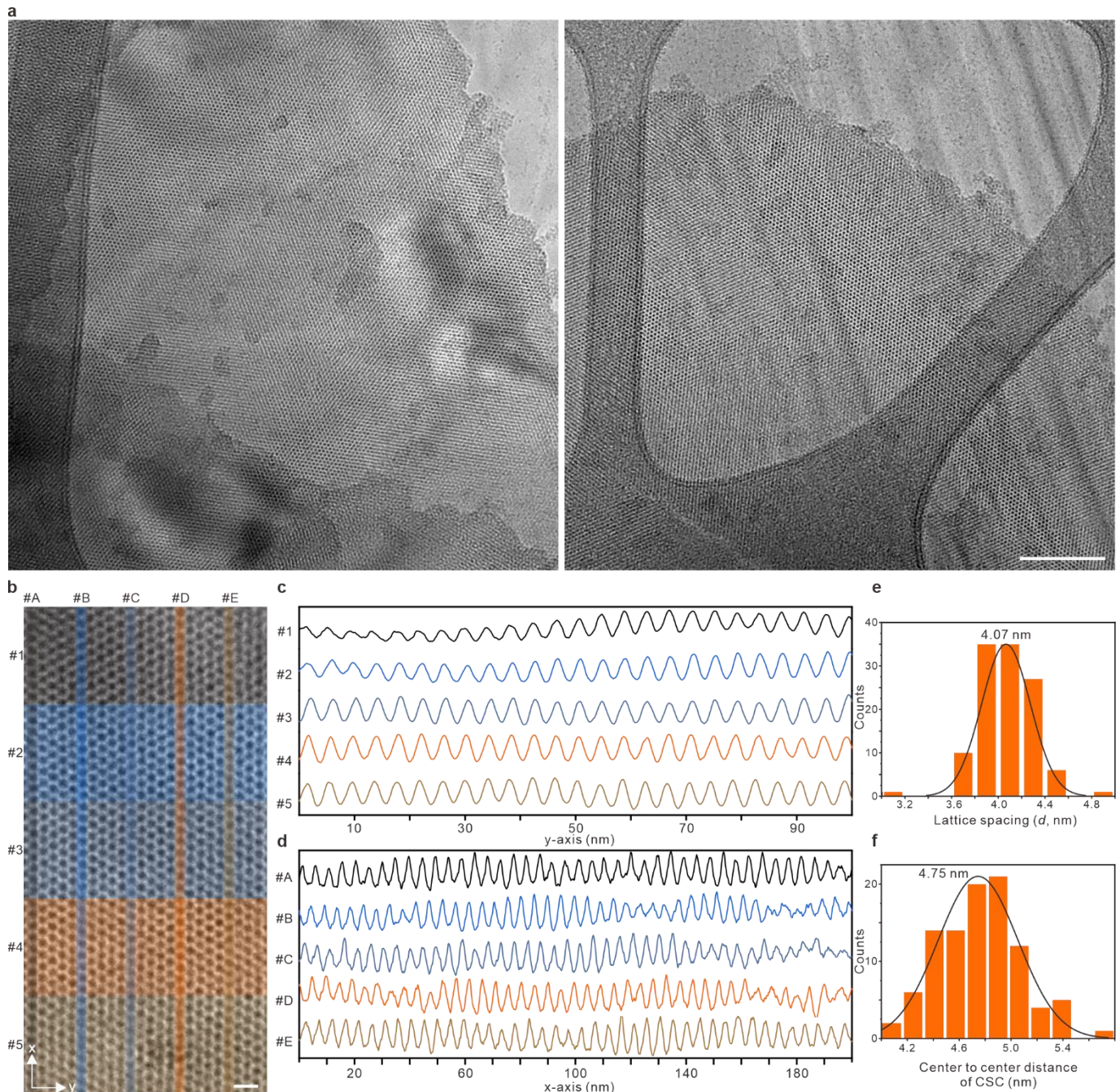
Supplementary Fig.18 | EDS mapping of *p6mm* 2D DNA/CSC superstructure.

EDS mapping showed uniform distributions of Si, O, N and P elements in *p6mm* 2D DNA/CSC superstructure. Scale bars, 500 nm.



Supplementary Fig.19 | Detailed characterization of *p6mm* 2D DNA lattice.

a. Zoom-out cryo-EM images of *p6mm* 2D DNA lattice. Scale bar, 100 nm. **b.** Zoom-in cryo-EM image section of *p6mm* 2D DNA lattice with labeled scan-lines. Scale bar, 10 nm. **c and d.** Corresponding cryo-EM line-scan profiles along the y and x axis. **e and f.** Histograms of lattice spacing (d) and center-center distance of DNA nanopores.



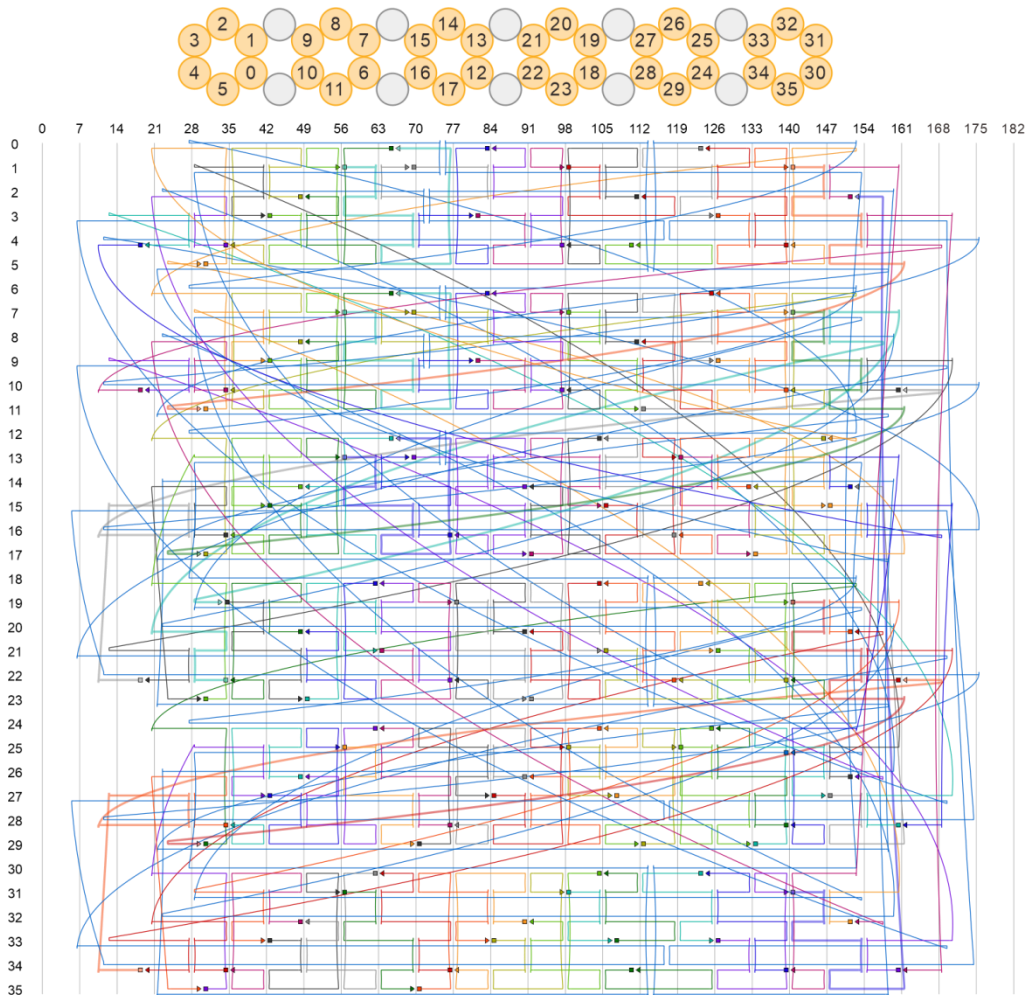
Supplementary Fig.20 | Detailed characterization of *p6mm* 2D DNA/CSC superstructure.

a. Zoom-out cryo-EM images of simple 2D DNA/CSC superstructure. Scale bar, 100 nm. **b.** Zoom-in cryo-EM image section of *p6mm* 2D DNA/CSC superstructure with labeled scan-lines. Scale bar, 10 nm. **c and d.** Corresponding cryo-EM line-scan profiles along the y and x axis. **e and f.** Histograms of lattice spacing (d) and center-center distance of CSC.

Supplementary Table 5 | Cryo-EM Data Collection and Refinement Statistics.

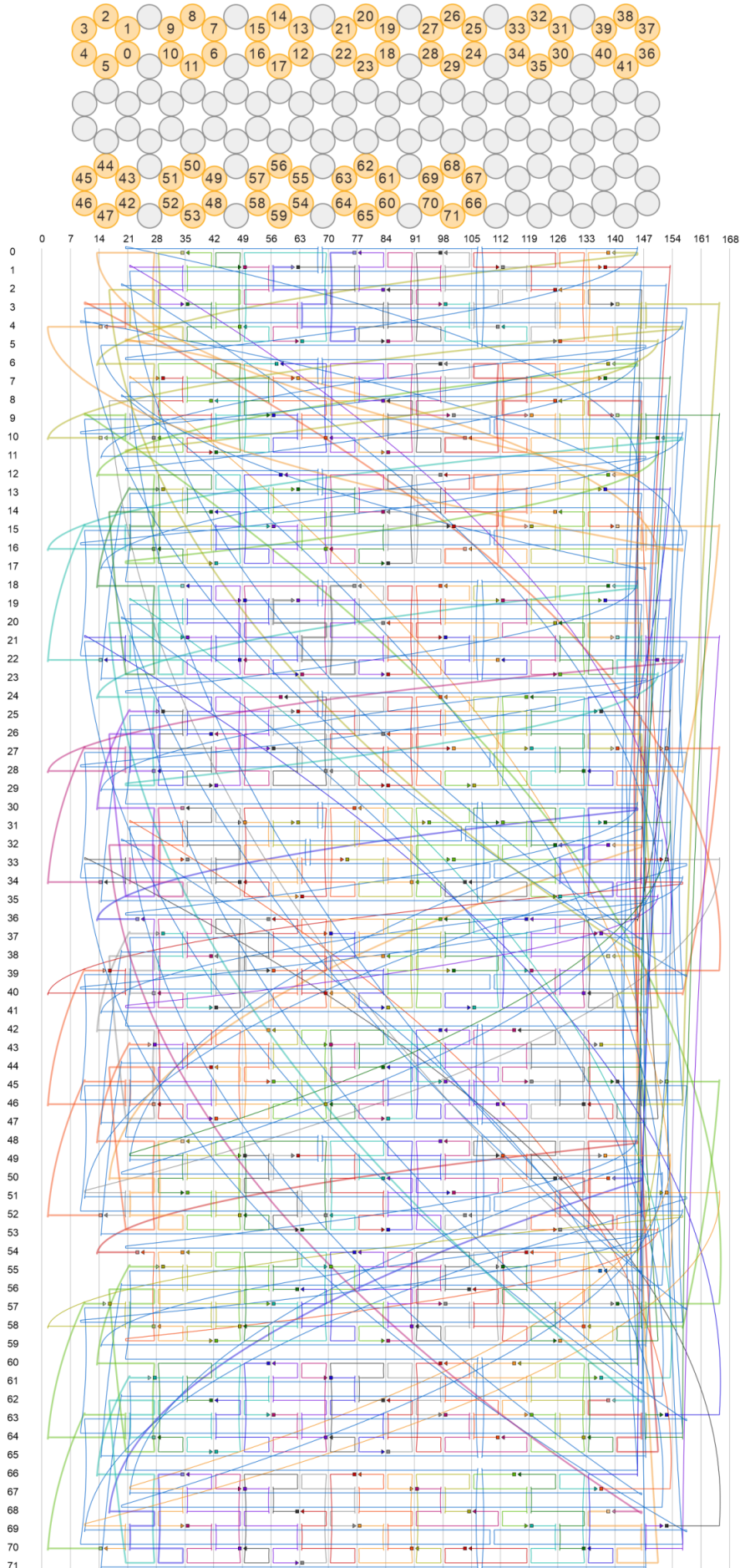
	CSC	DNA origami	DNA/CSC composites
Microscope	Titan Krios	Glacios	Glacios
Detector	K2	Falcon III	Falcon III
Voltage (kV)	300	200	200
Electron exposure (e⁻/Å²)	60	40	40
Defocus range (μm)	−0.8 to −2.5	−1.0 to −2.0	−0.8 to −2.6
Pixel size (Å)	0.822	2.500	2.000
Symmetry imposed	C1	T	C1
Initial particle images (no.)	316,325	199,847	140,554
Final particle images (no.)	32,564	62,638	38,401
Map resolution (Å)	8.1	17.0	22.0
FSC threshold: 0.143			

S3. Design of DNA frameworks



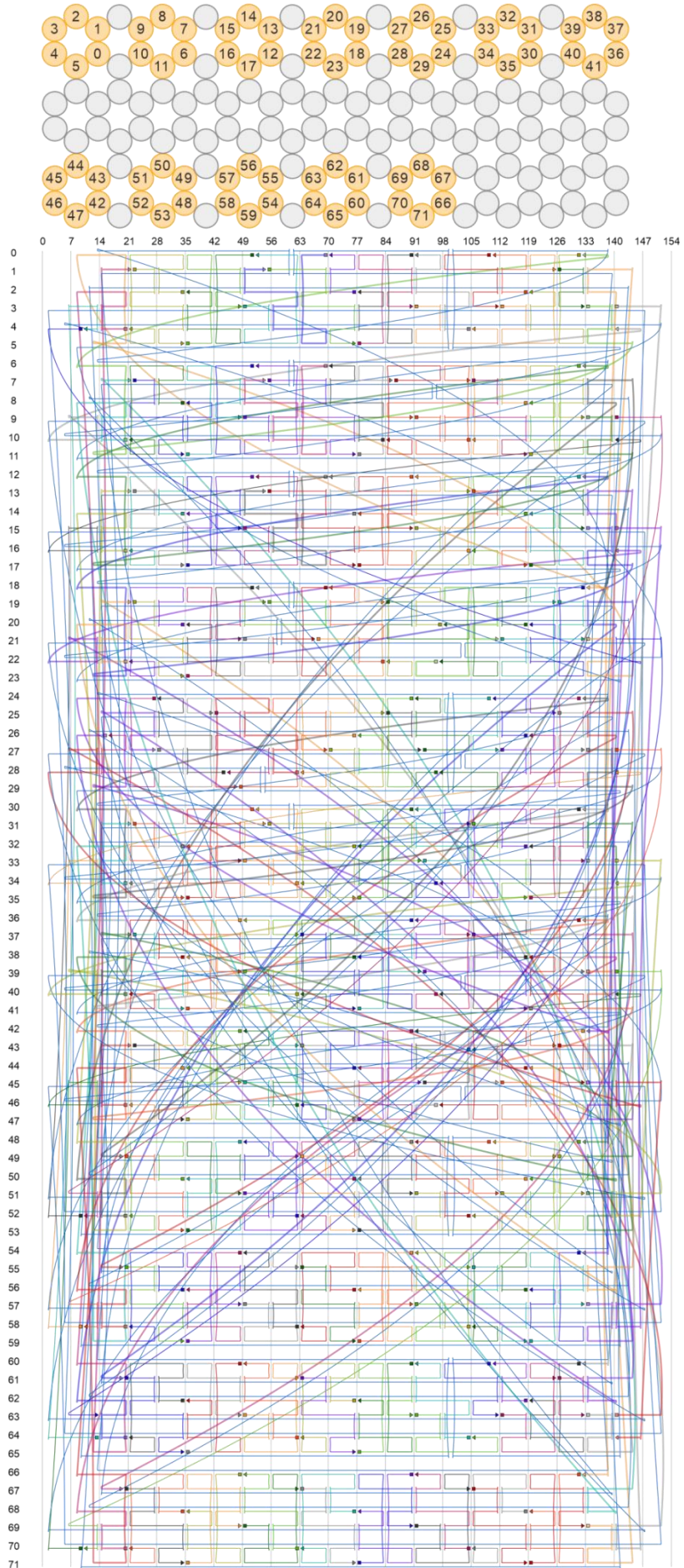
Supplementary Fig.21 | Strand diagram of tetrahedral DNA origami.

Top, cross-section view in caDNAno format. Bottom, strand diagram of tetrahedral DNA origami. The numbers on the left indicate the DNA helices. The numbers on the top indicate the position of the base pairs.



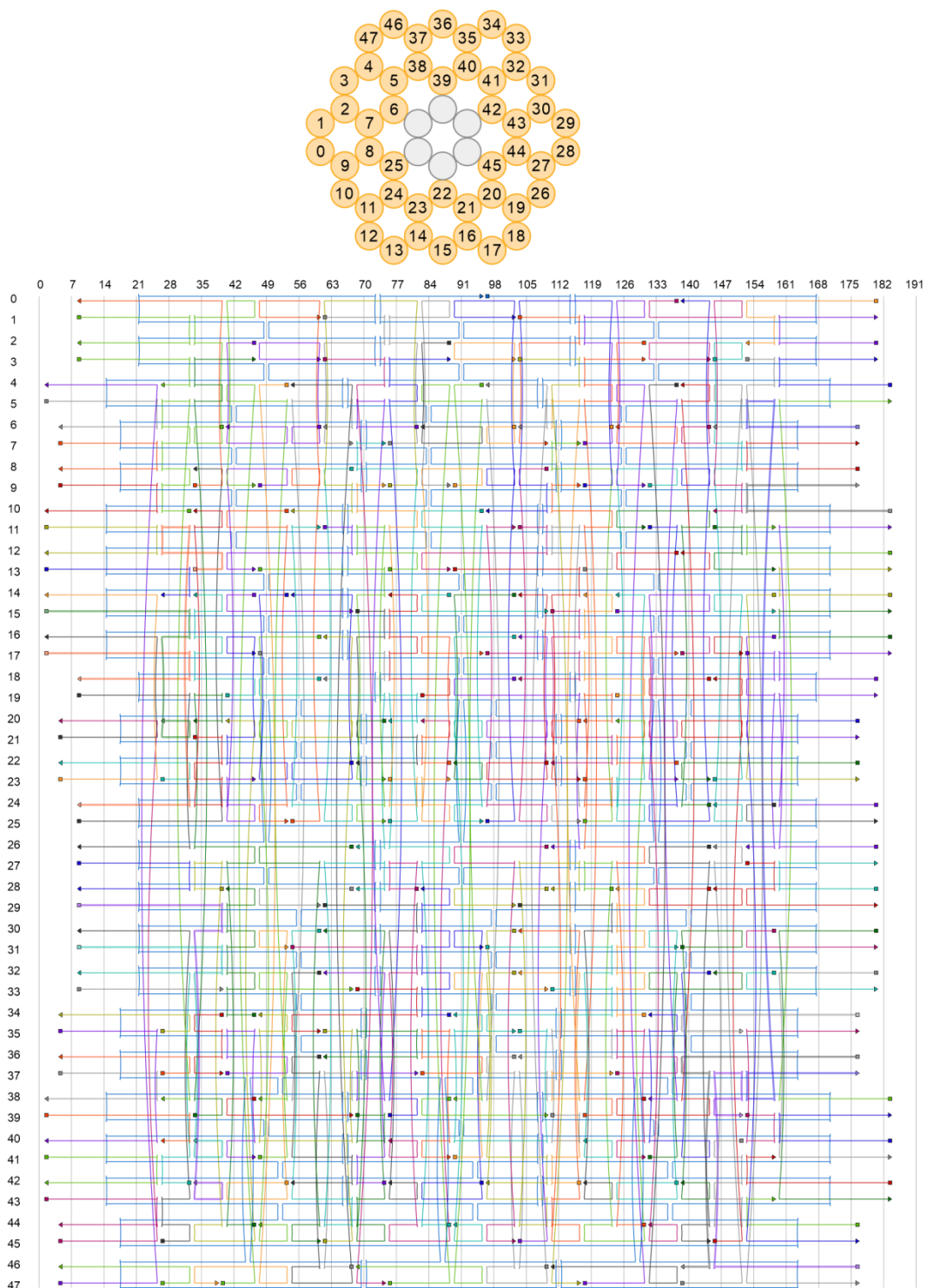
Supplementary Fig.22 | Strand diagram of octahedral DNA origami.

Top, cross-section view in caDNAno format. Bottom, strand diagram of octahedral DNA origami. The numbers on the left indicate the DNA helices. The numbers on the top indicate the position of the base pairs.



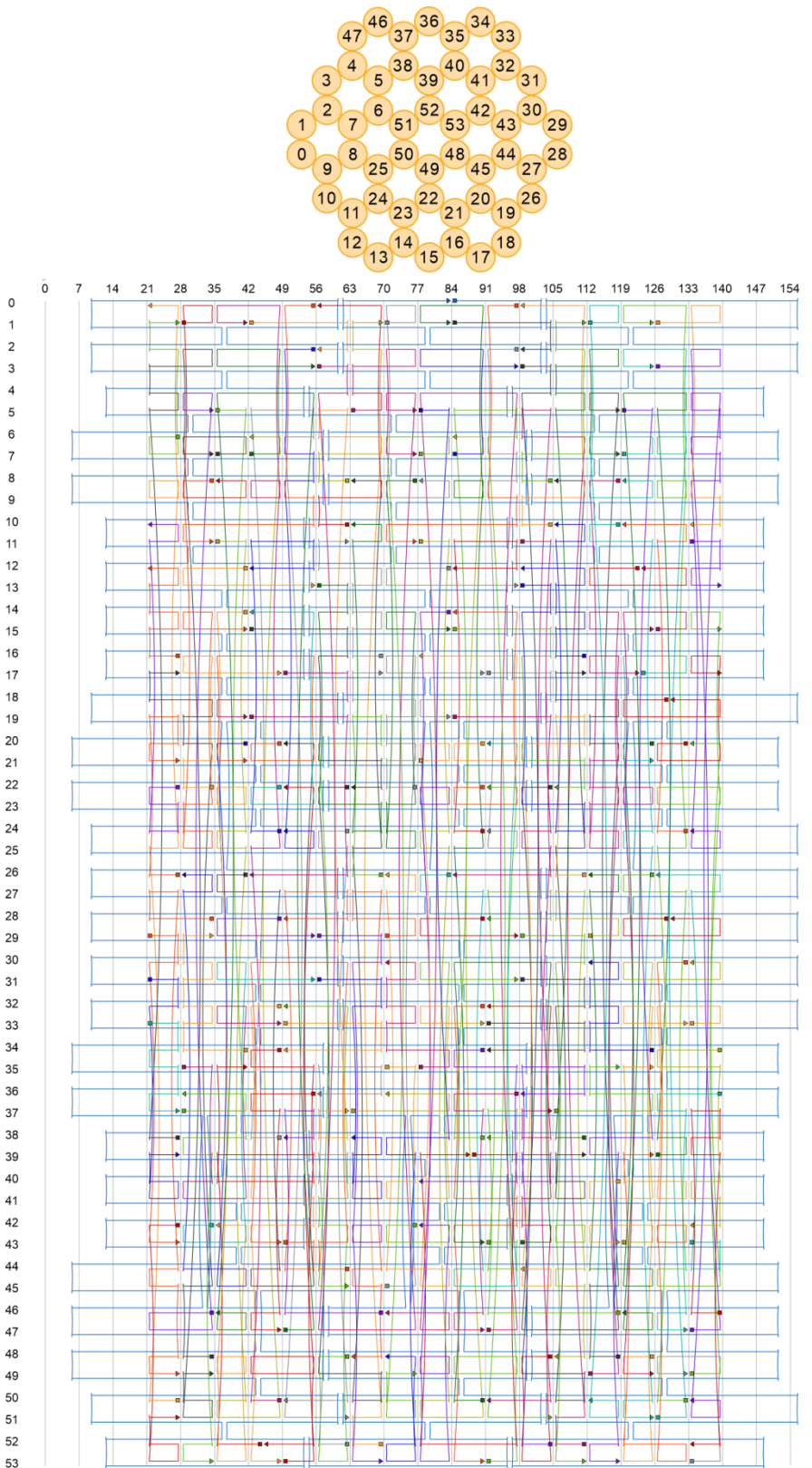
Supplementary Fig.23 | Strand diagram of cubic DNA origami.

Top, cross-section view in caDNAno format. Bottom, strand diagram of cubic DNA origami. The numbers on the left indicate the DNA helices. The numbers on the top indicate the position of the base pairs.



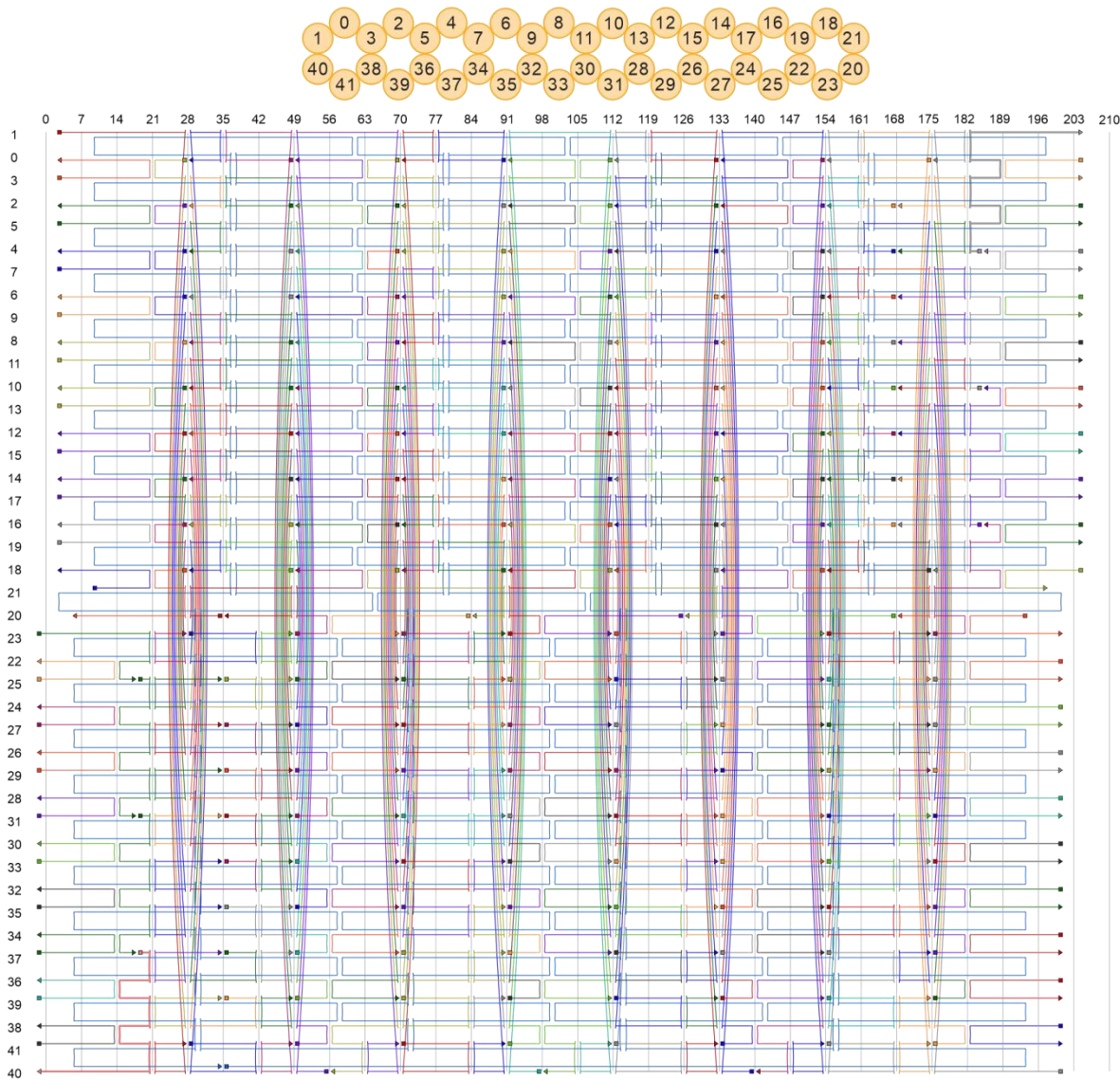
Supplementary Fig.24 | Strand diagram of 48-helix DNA origami.

Top, cross-section view in caDNAno format. Bottom, strand diagram of 48-helix DNA origami. The numbers on the left indicate the DNA helices. The numbers on the top indicate the position of the base pairs.



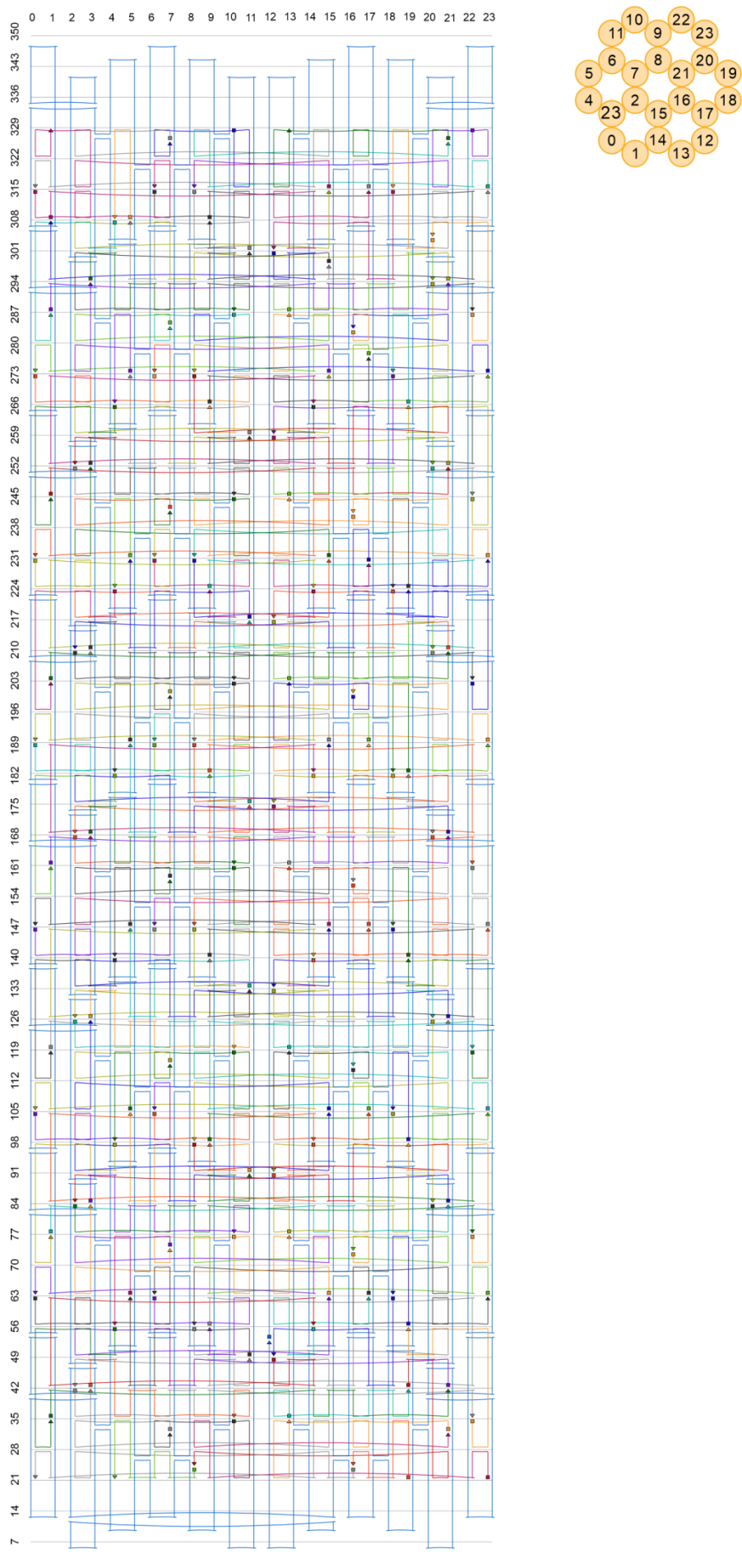
Supplementary Fig.25 | Strand diagram of 54-helix DNA origami.

Top, cross-section view in caDNAno format. Bottom, strand diagram of 54-helix DNA origami. The numbers on the left indicate the DNA helices. The numbers on the top indicate the position of the base pairs. Since 54-helix DNA origami belongs to simple $p6mm$ lattice with 7-nt domain. The SAXS data for the $p6mm$ DNA lattice with 7-nt domain (Figure 4, Supplementary Fig.16 and Supplementary Table 7) were obtained from this DNA origami.



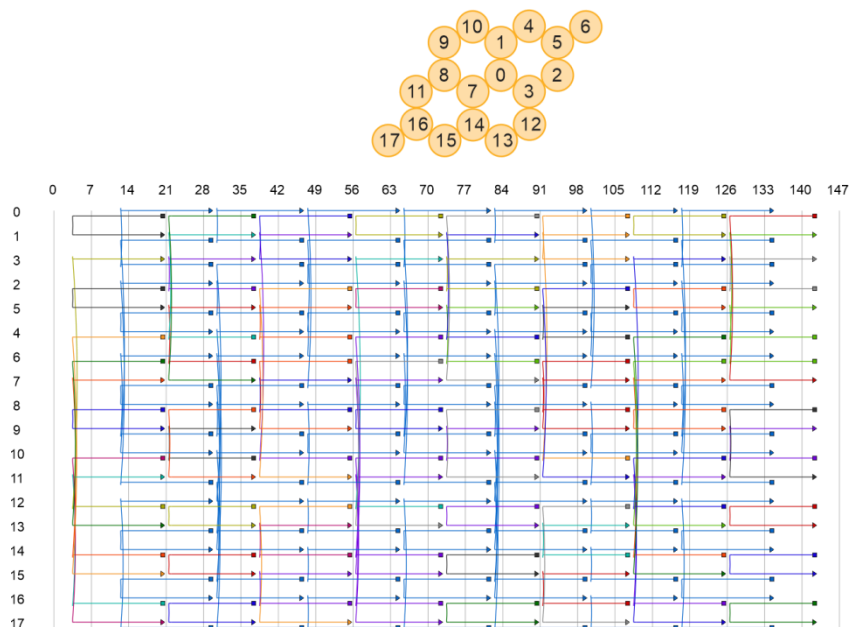
Supplementary Fig.26 | Strand diagram of 2-layer DNA origami.

Top, cross-section view in caDNAo format. Bottom, strand diagram of 2-layer DNA origami. The numbers on the left indicate the DNA helices. The numbers on the top indicate the position of the base pairs.



Supplementary Fig.27 | Strand diagram of 24-helix DNA origami.

Right, cross-section view in caDNAno format. Left, strand diagram of 24-helix DNA origami. The numbers on the top indicate the DNA helices. The numbers on the left indicate the position of the base pairs.



Supplementary Fig.28 | Strand diagram of *p6mm* 2D DNA lattice.

Top, cross-section view in caDNAno format. Bottom, strand diagram of *p6mm* 2D DNA lattice with 9-nt domain. The numbers on the left indicate the DNA helices. The numbers on the top indicate the position of the base pairs.

S4. DNA sequences

Supplementary Table 6 | DNA sequences of tetrahedron DNA origami (Scaffold 5250)

Name	Sequences
TDN-126-1	ACGGCGCGCTTGGTCAAATTGTTATCACGTGGAGCTC
TDN-126-2	GTTTATTCTTAGATCCCTTCATCCCGGGCGATAAAGATA
TDN-126-3	TTTAACATACCCGTTCAATTCCACACAACAGTCCACTGAAAAAC
TDN-126-4	CCGCCATGGATCCAAGTGAGGGTTAATTGCGCGATGGGGTA
TDN-126-5	TGAACATTCAAGGCAGTCCAGCTCCCTCGACGCTCCAGCGACCGCCTTCGCCACC
TDN-126-6	ATAGAAAAAAAGGGCATTAAAGAACGTGGCGCTCACAGCTGCACACAGTCGATTCAAGTGA
TDN-126-7	TCCCGGTGACATCGGCCGCCACCGCGTCAACGTCAAGTGC
TDN-126-8	GGAAAGAGTAAACTTTAAATTAAAAATGATATAATCATGCC
TDN-126-9	AAGGCGGACCTATCTTGGTCATGAGATCAATTCAATTATAA
TDN-126-10	CGAGCGGATTCGTTCATCCATATTGACTCCCCGTGTCGTCAAAATGCC
TDN-126-11	TCCGCCCTAGCATCACAAAAATCGTGCCTCCTGTTCTGCCGCTT
TDN-126-12	GCCTTTCCCCGTTGGCAGCAGCCACTTTAACAG
TDN-126-13	TCGTTATCGGCCACCGGAGAACTTCATTATCAAATTATCA
TDN-126-14	GACGCTTCGAGTTTTGGCAACACCGCAGGCTCCAGAACAG
TDN-126-15	AAACAATTCATCCCCAGCTGCATTAATTGAGCGGCACAAGA
TDN-126-16	GAACATTCCAGCGGGTTGCCTCACTGCTAGGGTGCTTCGA
TDN-126-17	CCACCACTACGGCAAATTGCGTATTGGCTTTCAATTGAT
TDN-126-18	GACTTATCTGGACAGAAAAATAACAAACCGCTTCGTTCC
TDN-126-19	TTTACTTAGTTATATTATTGAAGCAGAGCGGGATTGCCGAGAATTCTGGATA
TDN-126-20	GACAAACACCAACCCATGTCGTGGTTATTGTCTCAGAACGGCAAGGTG
TDN-126-21	TTAGTAGAGAAAACGAATGATTGGTCATCCCACGCCAACGC
TDN-126-22	ATGAGCTCGAGTCATTATCGGGCGGAATTGCCAGCCAGTCG
TDN-126-23	CCAGAATATTTTTTCGATCGCTGTTATTCACTAATTGCG
TDN-126-24	GAACCAGAACTCGTAGTCCGTTGATTGATATTGCTTCC
TDN-126-25	TTTGAATTGTCGTGTACCACCGAGATAAGGGTGTGAATAATA
TDN-126-26	ACATTCTAATTGCCTCCAGTAAGCCTTCTTCAG
TDN-126-27	CTCTTCCGCTCTCGCGCGGGCCAGTGTATTGCGAGGTGT
TDN-126-28	CGGGGGATTATCATGGCGAAAAGTCATTGAAGT
TDN-126-29	GGAAACCGTATTATGCAATTGTTATCTCTGAAGTAAAAC
TDN-126-30	TCGCTCAGTTGAATTCTGCATCCACCTTGCTCT
TDN-126-31	CGCATACTGAATGAATATTTTTACTATACATA
TDN-126-32	GTCACTGCATGCTTAGAATCCCAAAGGGAATATCCGCGC
TDN-126-33	AATGTGAGCTTCTTTATGAAACCATTGTTAGATCACTCA
TDN-126-34	AAATCCTCCCAGTAAACCCACTCGTCACACGCTCGCAGATT
TDN-126-35	CATTCAGCAGAAACTGATGGTAGTAGTAGCGGAATAAAC
TDN-126-36	AATATTAACTCGATTCACCGCGTTCTGCTTACCGATCTT
TDN-126-37	GGAATTGAAAAAGATAACCGCGAGACCCCCAACTATTGCAA
TDN-126-38	TGTTGGCCCGGCAAGGCCGAGCGCAGAAGGGCGAACAACTCTGGCTTTAGCTATC
TDN-126-39	TTCTCAATGGCTGATACGATACGGAGGGAGGGGTGAGACATTAA
TDN-126-40	ATGGTGCCTGACCATGATTGCGTAATCTGATGCTATGGTCA
TDN-126-41	TTTAATGCCATGTTTTTATTGAGATTGGACCTGGTCGCCTT
TDN-126-42	CGTCTATCCACTTAGGTGACGGTTAATGGTAGAACCGGAAGC
TDN-126-43	ACCGCGAACGCCGAAAGTCCTACGGTAGCAATAGATCTTC
TDN-126-44	TTGATCTTTGTTTTTCGGCGTGACAACCTACCTTGCCGGGA

TDN-126-45	TCTACCGAACCGGTGGATATTGAGACATTTACGACAAAAAC
TDN-126-46	CCAGATTCGATGTGACTGCAATTATTGGTTGTTGAG
TDN-126-47	CAGCCAGTTACCGCATGAGAGTAGATAGATCTCCGGACGAGG
TDN-126-48	CCCAGTGTACTTGACCGCAATGGTGTCAAGAGATCATAGA
TDN-126-49	AGCATCTCTGCAATAGGATCTCAAGAAGGTTGGTGAGCAATA
TDN-126-50	ATCCAGTTATCAGCTGGTTTTTGTITATAACCGGGTCCA
TDN-126-51	AAGGATCCCGGAAGACAAACCACCGCTGATCCATCCTAGAATT
TDN-126-52	TTCTCGGTGGTCTGCAACTTTCTCCATCCAGTCTATTGCTCCTCG
TDN-126-53	GCAAAAAATAGGGCGACACGGAAATCTGACTCGCTGCGCTCGGGCTGCGG
TDN-126-54	AGGAAGGAGATAACCGCTCAGTGGAACTTAAACTCACGTTAGTCAAGATTTTTTTGCAGG
TDN-126-55	CTCATT CGCAT GTGG ATT TT CCGCC GCGCA AGCA ACCGGCT
TDN-126-56	GCTTT CGGTGAG TTTTA CT TAGGTGTTAGGTCAACTCATA
TDN-126-57	GCGACTT CCGTCCAATCCAGCCCCAACATCCTTATCTGGC
TDN-126-58	CCTAAAGGTTAAGACATTCTGAGAATAGAAGATGCCTAAAGG
TDN-126-59	GCATTGGATTCAAAAATCAGCTACTCAACCAAGTCGTAATG
TDN-126-60	TATATTGTTCAAATCGGCGTCAATACGGTATGGCACGAACGT
TDN-126-61	GAGCGCGCGAACCTTTCTGTG
TDN-126-62	CTATAGGAGGTGCCTTTAACCAATATTGTTGTGGACG
TDN-126-63	CCAGGGTAAGCCGGGCACTGCATAATTCTCTGCCATGGAAC
TDN-126-64	GAGCCCCAACGACTGACCCAGCAAAAGCCTCATTGGCGACC
TDN-126-65	CACCTTGCCATTTTGAATTGTCAGATTCAAGGGGAGTTGG
TDN-126-66	GGCGAGATAAGTGGAAATGCTGCCAGCAACTAAGTCCGCGCC
TDN-126-67	CATCCGTTGATGCTCTAAATATGAAGAAACAACCGGCCAGT
TDN-126-68	ACTGGTGAGTCAGTAAAGCACTAAATCGTAATATACTCCT
TDN-126-69	AAATCCCTGTTAAAATTGTTTATTTCATAT
TDN-126-70	TCATGGTATAAAAGTGTGAAACTTGACTCAAGGTAAACG
TDN-126-71	GAGTTGCTCTTACTGAGCTTGACGGGATTCCCAATACTTT
TDN-126-72	GTAAATGCCGAAGTTTGCGGCGAATTGTTAGT
TDN-126-73	TAATATTTATAAAATCAAAAGAATGAGATAGGGTTGAGTGGTAAAGCCT
TDN-126-74	ACATAGCCGCAGTGGAAAGAAAGCGAATTGAGCGGG
TDN-126-75	AACCACAATCCTTCGACTCA
TDN-126-76	ATGATAACAGTTCGGGTACCTAAATGGTAATCAAATCGGCA
TDN-126-77	AAAAAATAGTTATTAAATCACTAGGCGAAAAAGAAACTCTC
TDN-126-78	TCATCAGGTACACAGTCACGACGTTGACGTTAGTCATGC
TDN-126-79	CAGCTTGTTCCCTGTTGAAACGCAGAACAGCACCAACGCGCG
TDN-126-80	CCAGGGAAACCCCTGACGCTTCAGTTACACGTAGAACGC
TDN-126-81	AAACAGATACGAGCCTTCCTGCATTGCCTTGTCAATT
TDN-126-82	ATTCAAGCGCTACATATGGCTTCATTCAATTGCTATAACTAC
TDN-126-83	TAATT CGTCTCCACCGGGTCAGCAGGTGCTACCTCATAG
TDN-126-84	CTCTCGTCACGCTTACATGATCCCCAGTAAGTATCTGCTG
TDN-126-85	TGCAGTCGGTGGCCCAGGCATCG
TDN-126-86	CGAGGGCGCAGAGCATCTCAGTTGGTACCTGTCGCTTGAGGATTGGTATT
TDN-126-87	GCAGGAATCTCGCGTTCGCCAGTTAATGGCAGTGGCGCGTA
TDN-126-88	GGCTACATGCCCTGGACTGTTGGAAAGGGACCCGCTCCCAA
TDN-126-89	GATTAATTAAGTTTTCGCCAGATTAAACGCCACTCAGCCCG
TDN-126-90	AAGCCAGGTGGAAAGCCAGCTGGCGAAAGGGCGCTAAAAAA
TDN-126-91	TGTTGCCGCTCCGGCGCCTTAATGCGCCTGCGACTGGAAG
TDN-126-92	TGGTGTACGTTAGAGTTCTGAAGTAACAATGATTGCC
TDN-126-93	CTCACGCCGGAAAGGCACCAATGAGCGTAAATGCCCTTTCA

TDN-126-94	AGCTAGATGTTGGGCAAGTGTAGCGGCTATTACCCTTCGC
TDN-126-95	CGATCAAAGTTGCGACAGTATTGGTAGTCGGCATGCGGGC
TDN-126-96	GTTTGGGGCGCGTCTCATCACGGCTGCGTGGCGCTCGTC
TDN-126-97	CTCCCTTGTAGGTGAGGTATGTAGGCGATGATATCTGACCGG
TDN-126-98	ACCGGATTAGGTCGTCGCTCCATGCTGTGCACGAACCTCCATAGGC
TDN-126-99	GTCCTCCGTTAGAAGTAAGTTGGCAGAACTTAAAAGTGCTTGGAAAACG
TDN-126-100	GCGGTTAAATTGTCGGAAAAAGAGTTTAGCTC
TDN-126-101	CGCTAGGGGGATGTTTTTGCTGCAAGGCATAAGGAAGTTATCAC
TDN-126-102	ACCACACGATCGGTATTGATCCGCCACCTAGAAGGCAACGT
TDN-126-103	TAGCTGTTCCCTTCTAGTTCTAGAGCGTGCAAAGCGGAAAT
TDN-126-104	GTAATCGTATTGGACAGCCAGCTTGGACAGGACTCTTGGC
TDN-126-105	AGGTGGCTTCCCCAGGGATCTGGAACCTGGACCAAGTCGATAT
TDN-126-106	GGGGTGCCTTGAGCTAACTCACATCCCAGAAAGTGCCACCTGTAAGCGT
TDN-126-107	ATAAAAGTTGTTCCATGGCCACTACGTTAACCAT
TDN-126-108	TTCCATCTATGCCTTTTCAGCAC
TDN-126-109	TTCGTCTTCTGATGAGCAAAAGGCCAGCTCCAATCTAAA
TDN-126-110	GCTTCCTTACACAGTTACCCACAGAATCCAATGCAAGGATC
TDN-126-111	ATTAAGGCCACCTGATCCAGGAACCGTAAAACGCCCTAAAGACAC
TDN-126-112	AACCAGAAGATCCTTGGTCTGACAGTTACAGGGACGCATCA
TDN-126-113	CATTGAGAAGGGATTCAAGCGATCTGCTTATCAGCAGATCCCTGAGCTTGGCGAC
TDN-126-114	GCGCCAGACCCGGTCCGGTAACTATCGAAAAGGCGGTATTGAACAGCAAAGTTCCAG
TDN-126-115	CTGCCACTTGCCAAGAAGTTAAATTGAGTCCATTCTTC
TDN-126-116	TTCACCTAAGAATGGCGTGGTCGCCTCGCAGTGGTTAACGCA
TDN-126-117	GACTTATCGGCTTGGTGAGCAGAGCCAATCACGTTGCTG
TDN-126-118	GTATATATGAACATGTGAGTAACGCGCACGCGAGAAACGAAAGCG
TDN-126-119	GTGAGGCTAATACGGACAGAGATTGAGCCTAAAATCACCTG
TDN-126-120	ACCGCTGAGGCCGCAAACACTTCGATAATGTACATTGGCTT

Supplementary Table 7 | DNA sequences of octahedron DNA origami (Scaffold 10004)

Name	Sequences
OCTA-126-1	AACGGCTGTCAGGGACTCCTTATTACGCACCGAAAAGAGTC
OCTA-126-2	CGAGGTAAACCGGCCGCAATAATAACGGGCCACCCATCCGTC
OCTA-126-3	CATTGCAGTATCTTAAAGAACGCAAAGTTCATCGGATGGCCATTGAAACCAT
OCTA-126-4	TCACTTCGCGTCAGTAGCAAACGTAGAACATCTTGTGGACTCCAACGTACTATC
OCTA-126-5	TCGTAAGAGGGTTGCCTCCCTCAGAGCCAATACCCTCAGTT
OCTA-126-6	GTCGAACGACTTTTCGAGCGTAGCGAGCCGGTGCCAGAAC
OCTA-126-7	AACTCAACAAAGGGTTATTAGCGTTGCAATACATCACCACT
OCTA-126-8	GGCCTTGTAAAGTAAAAGAACTCATAATCAAATCAGTATGTATTTCGT
OCTA-126-9	CCCAATTAGTTACCGGATAAGAAAATGTGAGTATTATCTTATCCATGCAAGCAAG
OCTA-126-10	TCCATACCGGCCCATTTTTTATAGCAAGCAAATC
OCTA-126-11	TTACCATTTTTGAAGGAAACCTCAGAGCCACTTTTCACCCCTCAGAAGCCT
OCTA-126-12	TAGCCGAGCATTAGGAAGACAAATTATTCTGCAATGTGCGCCTTA
OCTA-126-13	ATAGCTAGAGGGTAGAGTCGGCATACAATGAAAA
OCTA-126-14	CAGTGGCTTTCGAGTAATCTCTGCTCATATTCCCCTGAAC
OCTA-126-15	TGGACTCGTCTCAGACCGTACTCAAACGTGTTATGATAACCCA
OCTA-126-16	ATTATTGGAATGAAACAATAGATAAGTACAACATATAAGCT
OCTA-126-17	ATGGAAACGAGGGATCAATAGAAAATTGACATTAGCGTAA
OCTA-126-18	CTGCATATGATGAGTGTAAATTACGAGCATCCGACAAGTGATT
OCTA-126-19	ACGTGGCACATTGACAATTGTAACGGTTCAATTAA
OCTA-126-20	CGCTATGATAACCGGAGAATATAAAGTAGTAGAAATGCCTAC
OCTA-126-21	GATGCAACGACCAGTTCTCACGACGACGACAATAACCTGAACGCCA
OCTA-126-22	TGGCTGGACCTGAACATTGACGCTCAAAGGCAGTTACAGGCCCTG
OCTA-126-23	CTCACTTACGGGCGCTGGATTGCAAGCGAACCAATCA
OCTA-126-24	TTTGCCAAATAAAACAGATTACCACTCGACAAACAAGAAAA
OCTA-126-25	ATGCAGAACGGCAACAAGTCTGGAAAAACAGAGGAAATGG
OCTA-126-26	AAAAGGGCATATGGAACAGGGAGAGCGCATACCTAACGTAAGAAT
OCTA-126-27	TTGAGGGTGTACAAGCCGCCATTAAACGCTGACAGGAAATTGTTAACGCTC
OCTA-126-28	AGTAATTCCCATTCCAGGCGTGGAAATGAACGGTGAGTAT
OCTA-126-29	TTTATCCACCGGTAAACCGAACATCGTCTATAGAACCCCTCTGCCTGTTGAAAGAC
OCTA-126-30	ATAATCGGTAAATAATTATTGTTGGAAATTACGACATCATTTTTTACGCAT
OCTA-126-31	ATAATATCTGTCCACGGATTCACTCGTCGTTCA
OCTA-126-32	CCGGAACTGTCTGATTGGAGGTCAATGGACTCATGAAGGTAA
OCTA-126-33	TAACAGCACATTGGGGACATTCTGGCCAAATGCGTTAGCTA
OCTA-126-34	CTTCATTGAACTCTTACCACTAGTAAAAATGGTTAAATCAC
OCTA-126-35	TGCATGTATCCTGACTAGAAAAAGCCTGATTATTCCCGA
OCTA-126-36	TAACATATAGGTTGCCAACATGTAATTCACTCGAGATAGATGAATTACGCCTGG
OCTA-126-37	TTCAAAATACCAAGGCTAACAGTAGGGCGAGTAGTCCGGCGAGCTCGCACCTGG
OCTA-126-38	ATGCTGGACCGTTGAATTACCTTATGCGTTAGTAGGTATT
OCTA-126-39	AATTGGTTAATTGTTGGTTGTAACACAACCTTTCTACGT
OCTA-126-40	ACTGGTGCACTCATAGAACACCAAGAACCTTAATTGGAATCGC
OCTA-126-41	AAGAGTATGGTATTGTCGATCCAAATTGGGCTTGAGGCCAACGATCTTGC
OCTA-126-42	CCGAGATCCATTCTGGAGGAGCGCAGTCACCCCTGCCCGT
OCTA-126-43	CACTATTCTCCTGGCCCTC
OCTA-126-44	CAACGCAATGAGTTACCACTGCGATCCCCGGGAAGTCATTG
OCTA-126-45	CAACTGGATAATCCCGGCTTT

OCTA-126-46	ACTTTAAACAAATTGCCTCGGTGAAACAGCATTCCATCATAT
OCTA-126-47	GCTCATTCTATAATTATTCAAGGTTTATTGTTGACCGTACTCTTTTTCTGATGA
OCTA-126-48	GGCTTGCTAACACGTATTGATGTTGGAACAAGACGCACTGC
OCTA-126-49	GCGTTATTCAATTGTCGGTGGCAAAGCAATGCAGTTTTCTC
OCTA-126-50	GAATATACCAGTCAGTTTTTGACGTTGGGATAGGA
OCTA-126-51	GAGGCATTTTTTTTCGAGCCAGCTGTCTTCCTTTTTTATCAT
OCTA-126-52	CCATATTCTGACGTGTTGAGTGTGGTTATCAACCGTTAG
OCTA-126-53	AGAAGAAGTTACTCTTCTAATCAG
OCTA-126-54	AGACCGAATTCTGCGGCAGTTAACGACGAGTCGAGAATCG
OCTA-126-55	CATCCTAACAGAAAATGATATGAATAAATAAGTTCAAATTCA
OCTA-126-56	CCTAAAACGATCGCAATATATTAGTTCCAATCCTACCAT
OCTA-126-57	TTTAATGTCAGGCGCGTCACCGAAAAACTTTTAGTATTTC
OCTA-126-58	TTATGCCTCTCCGGTTGGTTGAAATACCGACTTAGGTAATTGCG
OCTA-126-59	CTGAGAGCCAGTTTTTCAGCAAATGAAAAATTATCAGAACGT
OCTA-126-60	CCAATGTCAGGTTTTAACCTCCGGCGTGTGGCAGTGT
OCTA-126-61	ACTGGCGAACCAACCATTATTGAATGCTGATGCAAAAATTTCATGTCCTT
OCTA-126-62	TAGATTATGTTACATCAAGCATTATTGCGCTGATAAATA
OCTA-126-63	ATCAAAAGCAGAACGATTTAACCGATTGTAATTCTCTG
OCTA-126-64	AGAACCGGAGCTGAATAATGGAAGGGAGGCCGTTGATAGC
OCTA-126-65	TTTGGGATTATCACCAATCAGAATGAAAATGGCTCAGTGCCACG
OCTA-126-66	AATCACCAAATTATTGGTTGATTTGATTTGACGCAACCGA
OCTA-126-67	CAACCATTTTTACCAATTAGCTAGCGTCAGACTTTTTGTAGCGCGTTACACCA
OCTA-126-68	TATAACTTTAATGCATTGATTCTGTACTGACGGAAT
OCTA-126-69	AGGTGAAATTAGAGGATTGTTGGATTACCTGCAAATTAGTC
OCTA-126-70	AGGC GTT GACT ACCT AAC GT CAG TTT ATAC AGT AGG CAA AGG TTT TTT TAG CG TT G
OCTA-126-71	ACCTAAAATATGTACACGTAAAACAGAACAGACTAA
OCTA-126-72	GTCTCGCCCGAACCAGTATTAACACCGTACTTCTGAGCCA
OCTA-126-73	TCCTGCGTCCGACCAAGATGAGATGGTCAATAAGATGGTTA
OCTA-126-74	TTAACACGATCGCCATAAAACAGAGGTGTTAGAACCGCAAGACAA
OCTA-126-75	CACCACCGATTAAGGGCGGAGCAAAACTGTCCTAAAAGAA
OCTA-126-76	CGCCACCGAGGAAAGCATGACTTTCTAACCAACTCTTTTTGAAC
OCTA-126-77	CGGT CATA CAT AT AT A TAG CCT GT CGG AT ATT AC GT TAG A AG
OCTA-126-78	GAAACATACAGTACAGTCAATAGTGAATTGCAAGATAAAACCAAAATTGAGAGGCT
OCTA-126-79	AAGAAGAGATTGCTCCTGAAAACATAGAGCAGTACATA
OCTA-126-80	TTAATTACATAGAATTATTCATTTCACAAATTAAATTAA
OCTA-126-81	TTGCTCCGGTCAGGCCCGAATAGGTGTGGTTGAATTAGA
OCTA-126-82	TTTGCGGATGTTTTGCTTAGAGCTTAATGTTAACAGAACCC
OCTA-126-83	GTGCGACCATAACCGAGGCATAGTAAGCGATAGCTAACCGGA
OCTA-126-84	TCGATTATGAAACAATTAAATGAAACAAACACTATAATCTA
OCTA-126-85	TCCAACATTGATTAGAGCGTCAATAGATAGCCCTTAA
OCTA-126-86	ACCGGATACTCAGGAGGTTGGCGGATCAAACAATTACTCGTATATCT
OCTA-126-87	TGCTTCTGTAAGATTAGAGAGTTAACAAATTGCAATAACCT
OCTA-126-88	CGCCACTTTTTCTCAGAACCGAGACGT
OCTA-126-89	GCCAAAATGAGAACGCTTACATCGGGACCAGAGTCATCAG
OCTA-126-90	AATCAATATATTAGAATTGAATACCAAGTTAACCGAAAACAAAA
OCTA-126-91	TTTCCCTGTGAGTATTGAATTACCTTACATCAATGAGCAA
OCTA-126-92	CGCTATCGCGCAGAGATACATTGAGGTATAAGTATAATCGT
OCTA-126-93	AAATCATTAGGTCTGAGAAAATAAGAATAATTACCG
OCTA-126-94	AAGACCGGAAATTACTCGTTACCAGACTGTCGGGTGTTCT

OCTA-126-95	AGTATTATAATAGAAAGAGGTCA
OCTA-126-96	TTCGCCCTGGTATGGGAAGCCGATCGGGAAACAATTAGATT
OCTA-126-97	AACCCTCAAAGAAATGCCTATTCGAACTTGAGTGGAACCC
OCTA-126-98	CTTGCTGGATTATCGATAGCAGTTAATGCCCCCCCACCAG
OCTA-126-99	TTAGTTTTTGAGCACTAACAAACGACTTAAAGTGCCGTCAGAACATCACCAGGAGCCGGC
OCTA-126-100	AAAGGAAATTAATTAGAGGCTGAGACTCATACAGGAGCCGGC
OCTA-126-101	TTCTTGATTATTTTGTAATAACATCACTCAGGGCGCATT
OCTA-126-102	TTTAGAGCGAGAACATGGCTTGATGCTCAAGATTGCC
OCTA-126-103	TATAATCAGCCCCAACGGGTCAGTGCCTATTATCATT
OCTA-126-104	CACCCAATCAAGTTGCCTAACGGCCGGATGATGGTTATCAATATAATCCTCCAGCAA
OCTA-126-105	GAACGTGCAGGAACAGGTTATCTAAAATTAAATCCGAAGGAT
OCTA-126-106	TAAAGGGAGTGAGGATCTGGTCAGTTGAACATTATTCTGAA
OCTA-126-107	CGTATAAACAGCGGTGCCGTAAAGCAAGTCTGAATATCA
OCTA-126-108	TCAGTAGGAAACCATCATATTCTGATCTAAAGTAGCAATAC
OCTA-126-109	GTAAGAGCGGGTTTGTGTTCTCAGTACCAAGTAC
OCTA-126-110	TGGTAATAGTATTAAAAGTTGAGTCAAATCAGTGT
OCTA-126-111	CTGGCATGGAACCGAGTGTGTTCCAGTAATCTCATGGAAA
OCTA-126-112	CGGAATTTTTTAAGTTATTAGGAAGGTAAATTGACGGAGTAG
OCTA-126-113	GGTGGCAAGCCCCCGAAAAACCGTCTATGCCTGACGCCAGC
OCTA-126-114	CACCAATCGACAGAAATCAAGTTTGAAACCCTGACATCAC
OCTA-126-115	TAGGATTCGTCATAAGGAAGGGATTTCGAAAGGAGGCCGATTTAAAGGGAT
OCTA-126-116	ACATGAAAAGTTGATTAGAGCTTGACTGAGAACAGTTG
OCTA-126-117	AAGGAGCAACCTCACCATCACGCAAATTGGTCGAACCGTAA
OCTA-126-118	GAACGTTTGAGGAGGTACGCCAGAACCGGGAAAGTGTAC
OCTA-126-119	GCAGAACATCAATCCACCGAGTAAAGCTAAATCAACAGTGCC
OCTA-126-120	ACTATGGCTTAATGTGAGGCAGGTCAAGAAAAGGAAACTAGCA
OCTA-126-121	GGAATATATAGTTTCATTGGGCAAGAGAACGTTGAA
OCTA-126-122	TTAGAATAGTAGGGATCCTCATTAAACTTCAAAGCCCCA
OCTA-126-123	CATCAATTCTATTTCTAATAGTAGTAGAGAGGTCTGCTTTC
OCTA-126-124	TCCCAATTGAAGATTGTTGCTAACACAAGCCAGAACTAGGGC
OCTA-126-125	CATTTCGATATGTAGAAAGGAACAACCGATTGGCCACACC
OCTA-126-126	AAAACAGCTCGAAGGAGCTAACACAGGAGCGGGCGTGGAAAG
OCTA-126-127	TGTCAATCAAATGGGACGAGCACGTATAGTAACCACCTGAT
OCTA-126-128	TAATAATAGGAGGTCGCCGTACCCGTATCACATCCGCCAG
OCTA-126-129	AATCTCCAGAGCCGATTCTGCTGACGCATCAGTGAGAAAAGGTGG
OCTA-126-130	CAAAAGGGCCCAAGCCTTTTGCCACATGAAGCGTCAGAAC
OCTA-126-131	TTAATTTTTGTATCGGTTAACACATAAATTAAACAGGGAAGCACAAG
OCTA-126-132	AGCGGAGAACGAATCGGTACGCTGCGACGTGCTTAGATA
OCTA-126-133	CATTGACTTTCATCGATGAACGGTAAAGCTATAGGCGCGT
OCTA-126-134	CACCAACAAAAAGTCTGGAGCAAACCGAGCTGCGAGGAAGC
OCTA-126-135	CGCAGTCGTATGGGTATAAGCATTAAATTGTATGTAACATTGTTGAT
OCTA-126-136	ATTCACATGAGAACATCCCCGGTTGATAATTGACCATTCTCG
OCTA-126-137	GCTGGCACAGAGCGCGAGTAGATTAGTTAGAAACAGTTTC
OCTA-126-138	CGCCCGTTGCTTCAATAACCTGTTCTGAAATTGCGAA
OCTA-126-139	TATAAAATAGGCCACAAACTACAACCGCGAACCCCAAAGCG
OCTA-126-140	TCATTCAAACGTTTGTGCTTCCCCACCCCTTCGAGCTTTGAACCAAG
OCTA-126-141	GTTACATTCTTACGGCTACAGAGGCTCGAACGCCCTCAT
OCTA-126-142	ATCATCATGATTAACTACAATAGTCTGCTTAACGTAAT
OCTA-126-143	CTGTAGCCCAGAACGACCAACCCCTCATTTCTCATATTAAATT

OCTA-126-144	TGTTTAGGGGGGGTCAAAATAGCAAGCCCAATACTGTAGCTCATTT
OCTA-126-145	TAGCCTTAACGGCGCTCGCCGCA
OCTA-126-146	GATTGACCGCTGGAATATCCAGAACAGTTCGCACATAAA
OCTA-126-147	GATGCTTTGCCGCGCATCTTCAGGATTGAAACCCAGAGC
OCTA-126-148	AATCAGGTGCACAATATTCAACGCAAGGATAAAACTCTGAT
OCTA-126-149	ACCATATAAAGACTTTCACTCAGCAATGCCGATTGTAGGTACCTG
OCTA-126-150	GATTGCAGGGGAAATAGCCGAGACCTAACGCTTCCAC
OCTA-126-151	AAACACTGAGTACCCCTGACTATTATAGTCAAAATAATCCCT
OCTA-126-152	AAGTTTTTTTCCATTAAACGGTAGCCG
OCTA-126-153	GCCACCCCTAAAGTAATATTTGTTAAAGGTGTCTCTGGTG
OCTA-126-154	ACCAGTGAATCGGCAAATTTAGAAAGGGTAGCATTGTC
OCTA-126-155	TAGTAATTTTTTATGAATTCTCTGAATTACCTTTTTGTTCCA
OCTA-126-156	TAACGATTCACTCAGAGCACTCAAATATCGCTGCTGAAGGAAGTT
OCTA-126-157	AGACAGCTCAGGGAGATTAAGAGGAAGCTCAACA
OCTA-126-158	ATATTAAAGCCTGATAAAAATAT
OCTA-126-159	TTTGTAGCAAATATGCAACTAAAGTACATTGCGGTTAGCG
OCTA-126-160	TTAACCAAAAGAACGCCACGTTGTCTCAGAAGATGTACCGT
OCTA-126-161	AAATCATCGGAGAGAACAGCTGATACTTGTAAAAATTAA
OCTA-126-162	TAATTTTTACTTGCAGGGAGAAATGCAGCGAAAGACAGCATTGAGGACAATCAA
OCTA-126-163	TTATGACAAGATTCCAGGGAG
OCTA-126-164	AAAGCCTCATCAACCATGCCAACGCATACAGCCATCTGTAC
OCTA-126-165	TATCTACACCGTGCACGTCAAAATGAAATTCTTGTAGCT
OCTA-126-166	GATAAATAACATAATCTTCAGAGCCTAGGCTTGAAAAGGG
OCTA-126-167	TGCAGCATGCCCTCTATTATTATCCCACAACATGATAT
OCTA-126-168	TTATCACTCCCGTAAGGCAAAGAATTAGTCTAGCTGCGCCG
OCTA-126-169	AAAACATTCTCGCGTAAAGCTAAATGGGGCCGGAATTTCG
OCTA-126-170	CGATTTCGATAGTTGATAATTGACAGGCATCGTAGT
OCTA-126-171	CAGAGAGATCAGCTTACAAAGGTTGGTCATTGCCTGAGAAGGCTC
OCTA-126-172	CGCTACCGCTTGCAGGTTTTGATCGTCACCTGAGG
OCTA-126-173	AAAATAAAACCAATGACAGTCAAATCACCAGAGCAGTATCAT
OCTA-126-174	ACAATGAATCCAAAGTGGAAACGATACTCTGGGGCAAGCAAT
OCTA-126-175	GAGGTGAAATAGCAGAGAAATGACTGATAACGGATCCAAT
OCTA-126-176	TTAAAGGACGAGCGCAATCCTCGTTGGGATTGGCTGGTTTTTATTGCT
OCTA-126-177	GTCGCTGAATTGCATTAAACCAATATTCTGGAGAAAACA
OCTA-126-178	ATTTTGCGTTAACGGAGTCAGGCAATGATCTTCTTTTGAGATCG
OCTA-126-179	TGAGAAATTGTACCCGGTGAGCGTGGATAGATGCAGTTAC
OCTA-126-180	TCAACCGCAAATTCACTGGTAAGCCGAGTACGTAAGAAA
OCTA-126-181	TCGCGTCAAGACGAAATAAGAGCAAGAACATCAGAGAGTAGATG
OCTA-126-182	ATCGGTGGGGGTGTATTAAACCAAGTTATTCTCCGGTG
OCTA-126-183	CAGGGCGGTTGCTGCCGAAGCCTTTAATGAACACATGAAGG
OCTA-126-184	TTCAACACACAGGAAGCGAACCTCCGAGGCGCATTATCAG
OCTA-126-185	GAGTTTATAGGAGTCGTGAAGACGTGTCAAGAGTAAT
OCTA-126-186	GACCACTGGCGGGTAAGATTAGTTGCTATGACCAATCAGGCA
OCTA-126-187	GTTCGCCATCCTTTGGAAAGACTCCTCGCATCCGTGAATAA
OCTA-126-188	ACTCAACGAAGCGGCTAAGGAAACCGAACCTTGATCTGAAC
OCTA-126-189	GGGAGTAAGAGGTTGGTACAGACCACTGCGGATGCACT
OCTA-126-190	TCGTTCGATATTCACTACCAATCAGAAGATTGGGTTCAATGTTGAGAATCGTAG
OCTA-126-191	CTGCGTGAGCAGCGGAGCTCGAATCGCTATTACCCAGCT
OCTA-126-192	TAAACAGAGCGTATCGAAGCGGAGAACATGATAAGAGGTTT

OCTA-126-193	CTGACCTGCGTTTGAATGGAATAATGAGTATCAATCTAAGA
OCTA-126-194	CTTGACACCGGTATTGAGTTAGAGTCTGACGCACATGTTCTGTT
OCTA-126-195	AACGTATTTTTTACAAAGCTGCTTAGGCA
OCTA-126-196	AGAGGACTTAAATCTTGTGAGTCAACGACTCGGAT
OCTA-126-197	ACCGAGTCATCAAGTTGCCAGGAGGATGCAACGAAGAGCCA
OCTA-126-198	GGCTTATAGAACCGGAGGGTTGTCGGACTGAAACCAACATTGCAAG
OCTA-126-199	ACAATTTCATCAAGAGCAGGCTTGACGACTACAGCAAATTTTATCAAA
OCTA-126-200	TGAAGCCAGATGAACGAAGTGAGCGAAAGTGTATCTGCTAC
OCTA-126-201	TCGCTACGGATGATTGAGTATTACGAAGTTAACTCCTTGAA
OCTA-126-202	TCCGAGTGAGTTATTGCTAAACTGGAAACTGGAACAGGCTGG
OCTA-126-203	GACTTGACGCCGATTAATTCAAAGAGGGGATTATTA
OCTA-126-204	GCTTGAAGGGATTGCTCCATGTTACTGTAAAATAACAGTTCATTCGAGAATG
OCTA-126-205	GAACGAGCGATTGTATTGTATCGCAAAGAGGGAAATCGT
OCTA-126-206	CTTGCTCTTAGACTCATCTTGACCCCCAGCGACGTAATAG
OCTA-126-207	ATGGGTATAAATTTTTGGCTCGCGATAAGACGATAACATAAC
OCTA-126-208	GTAATACATTCAACCTAAAACGCTGATAAATTGGTA
OCTA-126-209	TAAAATGGAGGCCGAGCAATACATCAAAATGAACGGCGAAC
OCTA-126-210	TTTGCACATCAGTTGAGATTAGAAAAAGCTGAGTTTTCAGATCACGCATCAGAACTG
OCTA-126-211	CATAAATAAGGGTCGCTAACAGTAGGGTCCATGAATTGTGT
OCTA-126-212	CAGGTAGACGAACCTGTTGAATAATCGTGGCAGAGCTGATTAT
OCTA-126-213	ATACCATTTCATTCAACTAATTATCA
OCTA-126-214	GCCACTACCGCGACCTGACGCAGACCTTAAACTGCATAAAC
OCTA-126-215	ATACACTAACGGAGGCTGGAACCTGCTGGCGCCCGGAAACGT
OCTA-126-216	ATTGCTGATATTTCCTAGCTGAAAGCAAATATAGAA
OCTA-126-217	TTTGGGTCTAACACGGGAGAATTAAACGAAAAGTCATTAC
OCTA-126-218	CGAAAATGTAGTCAGATATAATTGAGCGCTAACAAATGATCCGGGT
OCTA-126-219	AAAGTACAAAACACTGGATAGCGTCCAATCAACGGACCAGGA
OCTA-126-220	CCAAGCGGAAAGAAAGGACGGCGCTAACCGAACATTATA
OCTA-126-221	TAATAAAAAGATTAAAGAAGTTTGCCATGGATGCATTACGCT
OCTA-126-222	GAACGATTTGGCGCAGACGGTATCCTGAATTTTACCAA
OCTA-126-223	CGAAATCCGAAGGCGAATCCCCCTCAAATGCTTACGTGTTGA
OCTA-126-224	ACACCATGATATTGGTTATGAGCCATATTACTGCGCGAAAGA
OCTA-126-225	TCTTGTCTGTTCAAGATAACGCTTGTGGCGCAGTCATCGAGAGTTAAG
OCTA-126-226	TTTATAATCTGCGCAGGTTCTGAGCTTCAAATAAGCAGA
OCTA-126-227	AAGGTATAGATGATCAGCGATGCCAGAGATGTCTTAATAGCA
OCTA-126-228	CAAGAATTGAACAGACATCACGAAGGATGGGTCTGAATT
OCTA-126-229	CCGTTTACCGCACCGGTCGGACTGAACTTGTAATTACATAAAC
OCTA-126-230	GAATCATAGAACGGTCGTGCATTCAGCTGGTCAAAGGATTTTGAGTGAG
OCTA-126-231	AAAGTCATCTTACCAAGTGGTCTTGTCAACCGCCTG

Supplementary Table 8 | DNA sequences of cube DNA origami (Scaffold 10004)

Name	Sequences
CUBE-126-1	ATTAACCCCTCTCGAGGCATAGTAAGGATAAAATTAGTCCT
CUBE-126-2	TACGGGTTGATCGGGTTTGTTCACGCCAGGCACCGGA
CUBE-126-3	CGACATGAGTATCCCACATTCAACTAATTACTAGGCGCACG
CUBE-126-4	TGAGTGTGTCGAAAAGACGACGATAAAAATCTCTTCGTGA
CUBE-126-5	CAATCCTACGGTGTATCATAACCCTCGTTGACCACTGATTGAGCCGATCC
CUBE-126-6	GCACTTCCAGGAGAAAAAGC
CUBE-126-7	CAGCCTCAGGGGTTTAGTTAACCTACCAAAAAATGAC
CUBE-126-8	GTCCCCGACTCGCGTTGCCAATACCGACCGTGTAGCAACAGAACGA
CUBE-126-9	AGTCAGGAATAGCAAACAAGTCTGGAAAGAGTGATGAATGAA
CUBE-126-10	TAAGAACAAATAACAAGATGAACGGCTGGCCTGTTGCCCTTA
CUBE-126-11	AGGTAGAACAGCCAGTGATTCTCTTGATAACCAGTTCTTTGTTGTT
CUBE-126-12	GTGTCAGTGTCTTGCGACTTGTGCACTCATTGGACGGGA
CUBE-126-13	GAGAGTGGCGGCAGGACTCCTGTTATCATTCTCACTAAGAAA
CUBE-126-14	GCTGAATCAATCACTTGATGAC
CUBE-126-15	ATAAAAGTGCAGGCAAATCAACGTAACAAATCACTGGATGC
CUBE-126-16	GATTATGCAAAATTATCATCAAGAGTAAGAGCCGCAACGGGA
CUBE-126-17	TGATGCGCTGACATAAAGCCCTGACGAGAAAGTCATAGCGGGCA
CUBE-126-18	ACAGAGATTAGCTCTATTCACTGTAATTGCAATAATGGGCTCGCTGATT
CUBE-126-19	TATTTTGCTCGAAACCGCCTCCCTCATCTTGACGAGTTAG
CUBE-126-20	AGCATTGCGACAACATCGGCATTTGCGACCCAGACTACTG
CUBE-126-21	AGGTGAGAACCTCTATGGGTTCTTCATAATCAAAAGCTGGAAACGA
CUBE-126-22	AACGTCTGAATGGCGGAGATTCAACCGTATCAATAAGAAC
CUBE-126-23	ATCAGGTCCAGGTATCCTCGGCCGGTGGTATTATACGAGTA
CUBE-126-24	TGATTATGACCTGCTGGCCA
CUBE-126-25	AGAGCCACATTACCAAGTTATAATGAGTCACACGCAGACAA
CUBE-126-26	AGAACCGGCTGACCGATTGGCGTTCAATGTTGCAATCGTCTTTTGAAATG
CUBE-126-27	CCACCCCTTTTACCAACCGTAGCATTTTGACAGCCCACAGACCAGTTTAGGCTG
CUBE-126-28	ATTAGCGAAGGCTTCATTGCTGATACCGTAAATATTGT
CUBE-126-29	GGATATTCCACCGGGCCCGATTAAATCGTGGCAACCAGTA
CUBE-126-30	GTAAATTGCGTTTCTATCGATTTGGGAAGCCCGATCCCCTTTGGAAAAC
CUBE-126-31	AGTCTGATTACATTTAGTCTTAATCATATTCCACCCCTC
CUBE-126-32	TTTCTTGCACTGTTAGAAGAATATCCGATAATGCCCTT
CUBE-126-33	CATACATGGACATTAAAGCGTAAGAATATCCAACACCGAAC
CUBE-126-34	TGGACTCCTAATGAATAGTAAATGTTCATAAATGAATACA
CUBE-126-35	ACGCTCATGGCATGCAGCTGACCAACTTGAAAAGTTCTGTAT
CUBE-126-36	CACCCAATTATGTGTCATCAAGGGACATTGTATC
CUBE-126-37	CGTAAAGATTATACGTCGAAATCCCGACCTGCAATTGACC
CUBE-126-38	AGAGCTTGGCGAAAATTCA
CUBE-126-39	CTGGTATGCTAAATAGCGTAACGATCTAAGAGGACGGTGT
CUBE-126-40	ATTGCACAAGTTTAGTACAACGGAGGTAGTAAACCAGCC
CUBE-126-41	AGGGAGCTGGAGATCATCGCTAT
CUBE-126-42	TGCTTGTCTTGGAACAAAGAGTCCGTGCGAGTAGCGAG
CUBE-126-43	GTCGGGTGGATTATACATAA
CUBE-126-44	CCCAGCGCACTAAACAGGGCGATGCCCATATAGAACGCCGA
CUBE-126-45	CTAAAACGGAGCCAAAGGGCGAAAAACATTCCATATAGCGTCCCTCCATG

CUBE-126-46	GGGGTTTATATCCATACATTTGACGCTGCAGATCCAGATGA
CUBE-126-47	GAATCGTAGACTGGGAAGGTTATAAGTCACGTCCCATT
CUBE-126-48	GAATCCC GG GGTAAAGACAAATCTTTCTGCAACTATTAAAGGAGC
CUBE-126-49	TTTCCAGAACCGAAACATCACGAAGGTGATACAGGAAAA
CUBE-126-50	ATCGCCTGATGCAGACGAGATGAAGGTATAGACTACGTGAGGTGC
CUBE-126-51	ACGAGGCAAATTGTCAGCGCGAAACAATGGGTCGAACCAT
CUBE-126-52	TTACTTGT CGGCATAAAATCGTCTATT CGGAACCTAAAGACTCATCTACTGCG
CUBE-126-53	ACGGTGTTCATAGTCACATTCAATTTCAGCGAAACTATTTCGGCCTTG
CUBE-126-54	TTGTCTCAAATACCGAACAAATTACCGTAATTTCGTC
CUBE-126-55	CGAACGAATGTAACATCTGGTGCTGTAGAGGTATGCCACG
CUBE-126-56	AACAACTAATCCTAAAGGGATTAAAGTTGCGAAGTATA
CUBE-126-57	CTAAAAAATTGAGAGGCGATAAGTGCATAGGTGAGCTGA
CUBE-126-58	TATATTAAAGATGAATTACCTTTAAGACCGGAGGATC
CUBE-126-59	AAACAGGAACCATTTCGCGGA
CUBE-126-60	GCCAGAACTTAAACTATCACC
CUBE-126-61	CACGTATTG CAGGATTAGAGAGTACCTAATAATTACAT
CUBE-126-62	TACCGATGACAGGAAGGAGCACT
CUBE-126-63	GTCACTTCAGCAGCGCCTACATTTCGGCGCGTACTATGTTGCGAGCAAAC
CUBE-126-64	CATAACCTCAGAGCTAGTTGACCATTAGGTGTCTGTTTA
CUBE-126-65	TGGCTTAGAGATCCGACAATGACAACAGGGCGAAATTCTG
CUBE-126-66	GCCC GGAC GT CGAGT CAAT AGATA ACT AT CTTACGGTAC
CUBE-126-67	GTACTCACAGTACCGATTAGAATTAGACTTTAATTGAGGATTAGTTAT
CUBE-126-68	GGAGGTTTTTCGCCACCCCGCAG
CUBE-126-69	TCCAACACATTGATGAAACAAACATCAATAACCTTGACGAG
CUBE-126-70	TGATAAGCTCAACAGGAAGTTTCATTCCGTAGATTGGGAGCT
CUBE-126-71	TGCTGAAGTTGATT CAGATTAGAGCCGAGGGTTGATCTTAAT
CUBE-126-72	TTAACAAATTGGTCAGGGAGTTAAAGGCCGCTGCTGTTAGC
CUBE-126-73	AATATGCTTAATTGCGCTGAGGCAACGTGCTCGCAAATGGTCAAGAAAA
CUBE-126-74	CAAATCTAAAGTACGATACATTTCCTCGTTAGAAAATATCTCCTTT
CUBE-126-75	TAAATAAGGAATTAGTACAAAACGAGGTCAATGGGACATAAC
CUBE-126-76	ATCATAATGCAGATTTCAGGATGCAGGTATTACGGATAAAT
CUBE-126-77	CTGTTAAGGAATATGCATATGATTTGACGCTGGCCGTTAGTTTTAACTAT
CUBE-126-78	GTATCATATTTCACAAAATTGCTTTCAAAATAAAAGATTCAATTGAGATT
CUBE-126-79	ATTTAATGTTACCATTATTACCGAGCGAGATAGGGT
CUBE-126-80	ATGATATTAACATTGCCCTGCCTATTCACTGCAATT
CUBE-126-81	AAAGGGCGGAATTAAAAGGGCGACATTGAAATATTAAA
CUBE-126-82	TGGTCAGTTGTTAAATCAGTATTAAGAGGCTTGATGATCGGCA
CUBE-126-83	TCAGGTCCGTTAATAAGTAAATTGACAACCGAACCA
CUBE-126-84	AAAGCATTATAAACGTACATGGCTGAGACTCTCGACA
CUBE-126-85	CCCTCACATGCCGACAGCTAAAGTTAACGGGTCGAATTAAAA
CUBE-126-86	TTGTAAAATTGCCTGGCCGGAGACAGTCAAAGAATTGAGGGAGATAAAC
CUBE-126-87	AAATCCCTCACCTAACAGTTGAAAGGACAAACAACTCAAGA
CUBE-126-88	GTAAATGAGGGTATTCTAGCTGATAAAATTAAACCTTATT
CUBE-126-89	CAGTCCCCGTGGATTGTTAAAATTGTCTACACATCAAC
CUBE-126-90	TAAAGGTCAAAGACATCATATTGATTATCAGTAGGTAATTAGATTCA
CUBE-126-91	GAATTATCTTTCACCGACCAGATAGCTTAAAGTTACATTCAATGTTCCAGCGC
CUBE-126-92	AGTGTACACATGAACATTGCCGAACGTTATCAATATC
CUBE-126-93	AGTAAATCATTGCGGAAAAATCACAAGGCTA
CUBE-126-94	GAAGGATCAGTAAGTCAAAGAATTTCGAGACCTAGCAAATGTTTAAAAATCT

CUBE-126-95	TTCTGAATGGTAATTTTTAACCAATAATCAA
CUBE-126-96	GAAGGAGT GAGAAAGAGAGTCTGGAGCAAGCAAATTATTCAT
CUBE-126-97	ACTCGTAGCAAATCGCTAACCTCAAATGCCGAAATACAGG
CUBE-126-98	GTTTGAGTCACCGGCTATTTGAGAGCGCGTTACTTGAGTAA
CUBE-126-99	CTTTATTTAGAACATACATAAAGGTGGCCTTATTGATGC
CUBE-126-100	CCAAAAATAAAGATTATTCATCGTTAGATATATGGTA
CUBE-126-101	TATTTATAATCCTACGGAATAAGTTACAATAATTGTAAC
CUBE-126-102	GATATTGTCCTGATCAATAGCAAGCAAAAGGAATCCACGTAA
CUBE-126-103	TAACACGAGCATTAAACCGAGGAAACGTTTGTGCAATT
CUBE-126-104	AGAAACC GTTT CGGCATGATTAAGACCAACATAGAATAAT
CUBE-126-105	TTGATAACGCTAACGACCCGTAA TACTTATTGATTACCGCGCTAGA
CUBE-126-106	ACTGGCACATCGATTGCCTGAGTAATGTGATGATGACAATCA
CUBE-126-107	TCGATGAAGCAATAAAGGATAAAAATTACTTCTTAAAGA
CUBE-126-108	TGTTAGCAAACCATGAATAAATTGCAACCAGGAGAGAAGC
CUBE-126-109	CTTATCCAGCCGTTAATTGCGTATTTT CAGGTTGCTAAATTTTGGTTGTA
CUBE-126-110	GGTATTCTTT CGCGAGGCGACA
CUBE-126-111	TACCCAAAGACACCGATTGTTGGATTATTAGAACACGGAA
CUBE-126-112	GCCAAAAGAATAAAGGGAAACGCCCTGGT GCTACGGATAGATG
CUBE-126-113	AAAGATT TTGCCAGACCTCAAATTAAACAGTT
CUBE-126-114	AGGCTTAAATATAGCGGAGCCTATTAAAACGGCTGCTGACGTTT CACCGGTG
CUBE-126-115	AAATACCTACCATATCAAATTGCGGGAA CGAG
CUBE-126-116	ATAGAAACAGAAGGACGCTGACTTTGGGACGGCTTTCCATTTTGAATTGG
CUBE-126-117	AACGAAAAGAACCTAACAGAATTGGTTGGATGACCTCATA
CUBE-126-118	AACAGAAACATTATAGTAGGGAAACTGCTAAAAATAGAAGG
CUBE-126-119	ATCAATAATGCAATGTGCTGGA ACTGCTAATTGGAACGGAA
CUBE-126-120	GGAAGGGTCAACGCCATCAAACGCCCGGTT CATTACGCAGTA
CUBE-126-121	AACATCCTGATTGCTTACGAGCATGTAGATAAGTTACCAAG
CUBE-126-122	AGCTGAAATTATCGAGTGAATAACCTCCCTAGTTAACCG
CUBE-126-123	ATTAAGCAACAGTACTTATCATTCCAAGACATGTTGGTTGGA
CUBE-126-124	AAAACCGTTAGCCAATCCTT
CUBE-126-125	GGTCTCCGATAGT GACGACAATAAACAAACGGGTGATGAAT
CUBE-126-126	CCCTCCGCCAGTGGTTATCAACAATAGAAACCAATAACGG
CUBE-126-127	GCGCATGGCTCTGACATCAATTCTACTATACAAAATAATCGTCATCCC
CUBE-126-128	CTCAAGAGCGGTATCCTCAGAGCATAAAAACGTCAATTAAAC
CUBE-126-129	GGCTGCTGTATCGTCATACAGGCAAGGCAGAAACAAATCAATA
CUBE-126-130	GAAAATAATGCGACTAACTCCTCTACGGGGAGTAGCGTT
CUBE-126-131	TAATTTGCTTCTGCGCGCAGAGGCAGAAAGGTGGAAACGAA
CUBE-126-132	GAAAACATATATGTATTCAATTGGAGCAAAAGTCATTGGTTTGGCGCG
CUBE-126-133	TGCAAGAGTCTTCCCTTACATCGGGAAAGAATTGGTAAG
CUBE-126-134	TCCTAATTGAATACCAAGTATAGTAGTCAGGCAATCTTACTCAATATTAAT
CUBE-126-135	CAAGTACTCCAGACTACCGGATAATTGCAAGCGGTGGAGCCGGTTTGAGCGTG
CUBE-126-136	ATCGGCTCGCGCCTGTGCTTGCATGTGCCAGATAGCAA
CUBE-126-137	ATACAGTAATAAAGCATTGCAGCACTGGCTTCCGAGCTAA
CUBE-126-138	ATTGCCAATAAATAGTTATCTACACGAAATCAATCCTGAACAA
CUBE-126-139	GAATTAGATGGTCCCATTAGCAAGGCCAAGAGCAGCATCTT
CUBE-126-140	CATGTCAATCTGGCAATGCATGACGCTT GCGCTATCT
CUBE-126-141	TGAACGAAGCCCCATTGGGATTAGAGCCCTTTGAATA
CUBE-126-142	CCTGATGGAAACATGCAGCACCGTAATCATCAGAGGTTCAA
CUBE-126-143	GCAGACCGGCTTGTAAAGAA

CUBE-126-144	ATCTGGAAACTGGTCAATTGAGCGCTAATAGTAGGCCAGAGT
CUBE-126-145	ATTAAC TACGCAGATTAAGCCAAATAATGGAAACGGATGTTA
CUBE-126-146	TGATA CCTCCAGTTCCGCCACATGAAGGT CAGATGACCTAA
CUBE-126-147	TACTTGCCCAATATTTTATCTGAAC TCTCATCTTAAAGGC GT
CUBE-126-148	AATCGAAACTGGGGTAAA ACTAG
CUBE-126-149	ATCACCACTTATCAGTTACTCACCACTGCGATGCGACAGAAT
CUBE-126-150	CCCGACACTCAGGCTCCGACC ATCAAGCTGCCAATTCA CAA
CUBE-126-151	ATGAAATACCATTAAGACTAACATATGTACCCGAAATC AC
CUBE-126-152	TACCGAAGCCAGCAGTTGATAATCAGAAGTAATCGATTGAC
CUBE-126-153	AAGTAAGTTGAGCCAAAAACAGGTTATTGTATAAACAAAGATTTGAATCGA
CUBE-126-154	CCACAAGATCGATAGGCAAAGGTAGCGTATT TATGAGCGA A
CUBE-126-155	CAGTAGCAGCAATATGAGTTGAAGGATCCAGAGCAGCTGAC G
CUBE-126-156	TTAGCTTTACTGTAGCGGGCTTGAGTTTTAATT
CUBE-126-157	CAAGTTAGAGGGT GATCCCCGGTTGCTGCCAAGTTGCCTTTAGGAGG
CUBE-126-158	TGAAACCAATTGAGCCGTTCCGTGGCAATCGAAGTCCGTACT
CUBE-126-159	TGTTTCTATGCATGGTAAACAGAGAGGTAGCAAAAAGATAAC
CUBE-126-160	CAGATGATGCCCTACTGCGTGAAGCGGAGATCACAGAAAC A
CUBE-126-161	CAGAAGAAAAAATAGGAGGTTGAGGCAGAGCCCAATCACG TT
CUBE-126-162	CCCTAAAACAGTACCGCCACCAGAACCCCAGTACAATAGAA
CUBE-126-163	CTGCAACCACGTTGACGAATGGATCCTCCGCCACTTAATT
CUBE-126-164	AACATCAACTAAAGACTGAGTTCGTCAACCACCATGTCTGC
CUBE-126-165	TTTTATAATTATCACGCCACCCTCAGAAATTAAAGGGGGGGG
CUBE-126-166	ACGCAAATCCAAAATTTCAGGGATAGCAGTCAGACACATTGC
CUBE-126-167	AGGAACACTTGCCCTCATTAAAATACCATAAAACGAGCCGC
CUBE-126-168	GTATCGGT CAGTGACGCTGAGAGCCAGCGCAGGGGCCAGAAT
CUBE-126-169	GAAAATCTTAACCGGAGGTGAGGCCGTCTGATGTTGATTGGC
CUBE-126-170	CCATGTAATTGACATATCATCATGAACAGAACGAATAGTAAT
CUBE-126-171	AA CGCCTCTCAGAGATA CAAAGGGTTTATGAGCGCGAATT TTCTGATAG
CUBE-126-172	GCCACCATT CACAATGTCTAAAATCTCAGTATTAGTCCATC
CUBE-126-173	CGCCAGCCCGTAACGAATTGCGAATAATTTGATCCACCAG
CUBE-126-174	TCTCTTTTACCGTTCTAGGATTAGTTTTTGCT
CUBE-126-175	GGAAAGCTCAGAACGCTTGCTTCTTGATGAAATTCTGAGTTTAAGTGT
CUBE-126-176	CTTGATACCCCTCAT AAAAAGGCTCCAAAAGAGTCTACACCGC
CUBE-126-177	TTACATAAACATCGGAGTAGAAGAACTCGAGTGAGAAACTAC
CUBE-126-178	GGAAAGCAGTGCCAGGCCACCGAGTAAAAGGAGCCCTCAGA
CUBE-126-179	ACAAGATTAAAACATTGTAGCAATACTTAATT TTTAGGAAC
CUBE-126-180	TGTAATATGATGAAATCATTGTAATTG CATTATTGTGAG
CUBE-126-181	AAGAGTTCTAGATCGGAAACGA ACTAACGGATCCAACGGATTC
CUBE-126-182	TAACGGTACGCTTGGAAAGAAAAACTACTTGTAA ATAAGCTTTGCCAAGCACT
CUBE-126-183	CCGCAGTCCGTTCACTACCTTTAACCAAGCGCTAAAGA
CUBE-126-184	CCA ACTCTTTGCGCGTAACCACCACTAGCAAAGGAAGC
CUBE-126-185	TTTCGCGCAGTCGAAGAGTCATAGTACTCAAGCATCGG
CUBE-126-186	AGCGGAACCCCTGTTATGTAATGCTGAAATCAAATACGTA
CUBE-126-187	AATGCGCAAAGACAATATCGC
CUBE-126-188	GGCGAACGTACGAAGCGAGAATGACCATATGCAAATCGGCCCT
CUBE-126-189	GGCGCTAATGAGGAATTATAGTCAGAAGCTCCGCCAGGAAA
CUBE-126-190	AACGAGGCACCCGCTCTGAGCTA
CUBE-126-191	ATGCCACTGGCGAGTGTATCACATATTCTTGCCGCCAATCG
CUBE-126-192	CTTTTCGGCGCTCCGAGCGTAGCGAGCATCTTCTTAGGTT

CUBE-126-193	TCAAAAACGTAGAGGTAAGCCATGAACCGAGGTAATCAAAAT
CUBE-126-194	CCGAAAGGAATTACTGGCTTGGAGGAGAAGGTTCCCGCGCTT
CUBE-126-195	GTTTAAACGCTGAACCAAAACTTTCCTTCAGCCTGCATTTGGCGGT
CUBE-126-196	TTCGAGCTTTGCGAACCATGGAAACAGTTAAATCAATAGCGATATTGATTAAG
CUBE-126-197	TCTTACATAACTAAAGTATCTCCTGGTCAGTGAAGGAGCG
CUBE-126-198	CATAGGTGATTAAGCGGCTACAGAGGCTCACGCTCCGCTCG
CUBE-126-199	AAGAACCGCGTTTACTTTCTGCA
CUBE-126-200	CAAGACACAGAAAAGCACCAACCTTACGAAAGAGACGGGTTAAAGCC
CUBE-126-201	GGGTTATCCTGACTAGTTCCATTAAACAAGCGAAGCGAGGA
CUBE-126-202	CTCACTTATATCCAAAGGAAGGGAAAGAGGGTAAAATCAGG
CUBE-126-203	TCTCCGCCAACGAGGCAAGTGTAGCGGTTGAGGAGATTGCA
CUBE-126-204	ACATCAATGTCAGGTGCCATTAACTTACCGTACCCCGAACATC
CUBE-126-205	ATGGAATGACACCCCAGTATAAGCCAACGAGCGTGACGAG
CUBE-126-206	GGCTGCCATACAGATTTGAGCCAGTTGCGGGACTGCCTC
CUBE-126-207	AGCAACGTAATAGGTCTTACCAACGCTAACGCTCACCATAAC
CUBE-126-208	AACAGCAATTCTCCGAACCTCCGACTAATAAGAACGGGG
CUBE-126-209	GGTGTAGATACCAGATTAGTTGCTATTACGCCATACCCGG
CUBE-126-210	GGGAAATAAGTCCGCCATTCAACAGAGTAACGCGGACAGTAG
CUBE-126-211	GGTGAGTAATCAAATTGCTGATAAAATCTGGACTGAGAATATA
CUBE-126-212	GCAGACCTCTCGGATACGACCACTGGATAACTGCCACATGTA
CUBE-126-213	AATTTATTGAGAACGTGGAATGAGACATATCGAAACTGGAA
CUBE-126-214	AGAGCCTATTCTAGGTAAACCGTTGGCAGGAACGAGTCATTTTCAGGAGA
CUBE-126-215	AAGCCTTCAGAGGCTCCAGCTTGGAGCGGATGAGCTTACGAA
CUBE-126-216	GAGCGTAATGAAGTCTCGCTCAGGCCTCGCGTTATACC
CUBE-126-217	GGTCGTTATCCGATTAAAAACAGGGAAGACCTTATGTCTGTA
CUBE-126-218	GCCATCACTCATGTATTATTATCCAAACAACATCAAAG
CUBE-126-219	GCACTGGGTTGATGCAAATGCACGTAAAAATGAAACGTTGGTAAAAT
CUBE-126-220	GGCTTAATCCTGAATTGATTGATGTTGCTAAGCGGAGA
CUBE-126-221	AAAGGTTTTAATTCTCGCCACTCATTTTACAAGCA
CUBE-126-222	AAGTACCGTTTAGTCATTACAGTTCGGCTTGTGTTGATTTGCTTGA
CUBE-126-223	ATTTAGGAAATCAAGGATCTGCCATCCGTGAGTATCGAACATC
CUBE-126-224	AGCGGAATGGAGAGTGAAGACGGAAACCTTATTTCTTTCC
CUBE-126-225	GTTCGTGTGGTTAACTCAACGAGCAGCTATGGAAGGTTTG
CUBE-126-226	AACTGAGCGACTGCTGGAGTAAGCGTAGACGAGTCAGCTAC
CUBE-126-227	TGTGGCGCAGGTTAACAGCGATCGCTGCCAGAGCGATT
CUBE-126-228	AGTCGTCCTGGGAATTAAATCGAACAGACATTGCTTATTAC
CUBE-126-229	CAGAGAGTGGCTCACGTCTCACAGCGAGTATTCGACGCCT
CUBE-126-230	GAATTAACAACTTCCGTACTCATTTGGGTTGACATTGATTTTCCTGTT
CUBE-126-231	CTGAACACTTTACAAAGTCGCCT
CUBE-126-232	CGATTGTTAATATTGTAAAAGATATTGTGACCTGG

Supplementary Table 9 | DNA sequences of 48helix DNA origami (Scaffold 7249)

Name	Sequences
48h-pore-1	GATCACGGTGGTGGTGGAGGGGACGAAAGCTATTCAAGAGA
48h-pore-2	CCAACGTCAAAGCAATTGGAACAGATGCCCA
48h-pore-3	AAGAAAAGTCTTCCTTATAGTCCTTAGACTCTATGCCAAGTTAAGA
48h-pore-4	ACGCTCACTGAGAGACTACTTTTTTT
48h-pore-5	GCTTCTGGTGCCAATCAATAGAAACGACAGTATCGCGGCACC
48h-pore-6	TGAAATATTACTAGAAAAAGAGGGTAACTACGCCAAGTCAGGTCAGA
48h-pore-7	ACCTAAATTAACTAACTTCGCTAAGAACGCGAGATCTTCTG
48h-pore-8	TTTTTTTTTCCGTTACCAAGATGCAAAGAAGTTTTTTTT
48h-pore-9	TTTTTTTTTAACGCCATCAAAATAATTGCGGTGCAATCAGCTAGCCCC
48h-pore-10	TTTTTTTTTTCATTGAATCCCCCTCAACATAAATTAGTAGCCATTG
48h-pore-11	TCAAATATCAAACCCAGTTGAAAGGATTAATATCCAAAAACG
48h-pore-12	TTTTTTTTTAGTATAAAGCCATGTAATTAGGCTTTTTTT
48h-pore-13	AAAGAATCTAATAGCAAAATCAGGTTTTTTTT
48h-pore-14	CTAATGAGTGAGCCAAAAGAACATGGAAGCATAAAG
48h-pore-15	GCCCAGGGCGAACTGAACGAACCAGACAATATTTGAATGGT
48h-pore-16	TGTGATAAATTCAAACCTTTGGGAA
48h-pore-17	TTATCCTATTCTGTATCAACAATAGATAAGTCATAGAAAGG
48h-pore-18	GGTAAAATACGTGCCCTAAAGACTTTAGGCTTG
48h-pore-19	TAAGAGGTTCGAGCACAGGTCGATAAGA
48h-pore-20	ATGTGAGTGTAGCGGTACAACACTAGG
48h-pore-21	CATGACAAATTACCGTCCCCGAAAGCGCAGTC
48h-pore-22	CTTTAGCGTCAGACCGAGGCGCAAGCAAAGCCGT
48h-pore-23	ACCTCTGTGAAATGATTATTATGCCTATTG
48h-pore-24	GGTAGTGTAAATATCCATATAACTTTGCGGATGAGCTA
48h-pore-25	CGTAGAACCTTATTACGCAGTACTGGCACAATAATTACAGAAAGTAA
48h-pore-26	GAGCCACTCAGAACAAAGGAATTAGAGCCCAAGGCCGAAAGTGCCTTGA
48h-pore-27	TCAGTACCAAGGCGATAAGATGCCCTGCTGATTAG
48h-pore-28	TTTGACCGCCGAATTTCATTGCAACTAAAGTACGAGCATCGAACGAG
48h-pore-29	TGACAAGAGAGGCAAAAGAACACACTTTTTTT
48h-pore-30	TAACACCCAAATGATTAGTAATAAAAGGGACCTGAAAGCGTTTAAAAG
48h-pore-31	TCAGCATTGCAAAAAAAAGGCTCCAAAGGAGCTTATTCAA
48h-pore-32	CCAGACGTAATAAGTAACAACGCCAAC
48h-pore-33	TTTTTTTTGTACCTTCTAACCGAACATTTTTTTT
48h-pore-34	TAACTGAACACCAGCGCATTACACCGGACACGTACCAATGA
48h-pore-35	TTTTTTTTTGATGCAAATCCATATTCAACCGTTTTTTTT
48h-pore-36	ACCGCCTATCGTCGACCGAGCTCGAACATGCGTAT
48h-pore-37	CACCGGATCAAAATGACGGGAAACATAAAAATAGCAGCCTT
48h-pore-38	AACATTAAAAACCTAGTAAGAGCAACAAAAGGACGTCAGA
48h-pore-39	TTTTTTTTAGAGGCATTTCGAGGCCAGACGACAA
48h-pore-40	ATTACGAAGGAATACCACATTATTACATCGTTAACAGGACGGTGAATT
48h-pore-41	TTTTTTTTAAGAGGACAGGCTGACCTTTTTTT
48h-pore-42	AACCAGTTGCCTAACCAATTACCAATTAGAGCAAAACAGAGGCCACCC
48h-pore-43	CTAAGTATTAAGAGGCTGAAGACAAAAGAAATATTGAGCCACGCCACCC
48h-pore-44	TCCTTTAGGATTAGAGAGTACCTTTTTTT
48h-pore-45	AATCATTGGGAAGAAGGAACAACTAAAGGAACA

48h-pore-46	TTTTTTTTCTTACCCCTGACTATTATA
48h-pore-47	CAGAATTTTAAATAATATCTAGTGGCGCGCAATTCATCAA
48h-pore-48	TTTTTTTTTTAATATTGTATAGAAGGCTTTTTTTT
48h-pore-49	AGGCCGCGTCGCTGTCACTGAGGAAGTTATGCAACGGCTACAG
48h-pore-50	TCCTGTTGCTGGTGTCCACTATTAAGGACAGATAGGGTTGA
48h-pore-51	CTTTCACGTTGAAAATCTCACGAGCACGGGAGCTACCAAGCC
48h-pore-52	TTTTTTTTTCAATTACAGGTAGAAAGCAACTAATGCAGTTTTTTT
48h-pore-53	AACCCTACACAAGCGGTCCACTGATGGTGGTTCGA
48h-pore-54	TATCTTACAAGAAACAATGAATAAGCCCCCGGGTCTATTAA
48h-pore-55	TTAGAATGGGATTTACGTTGCGCTCACTGCCCG
48h-pore-56	ATTCGCCAGCTTCGCCTCAGGAAGATCGCTTTTTTT
48h-pore-57	AATAAACATACAGAAATCGGTTGACTATAGCGTAAACAGT
48h-pore-58	TTTTTTTTCTGAATATAATGTTACTTAGCTTTTTTT
48h-pore-59	TATAACGTACTATGGTTGCTTGCGCCGCAACTACATCAATAT
48h-pore-60	CATTAAAACGGGTACGAGTGTACTGGTAATCCCTATAAAGGCAAAA
48h-pore-61	AGTCAATTAGCTTAGATTAAGACTTTTTTTT
48h-pore-62	TTGACCGATTCTCCGTGGGAACATTTTTTTT
48h-pore-63	ATCAGAGATCCAATCGCGAAAAACCGGATTGCCAGCCAGGGTGGTT
48h-pore-64	TCACATTAATTGGACACCCTCGAGGTTATGTGTACAATTGA
48h-pore-65	GTGTTTCCAGGAAAACAGGTCACTCAG
48h-pore-66	GAGCGTCAATCGTCAGTCACACGACCTGCGGAACAAAGAATGAGTAAC
48h-pore-67	CCCGGAATAGGTGTATCACAAACTGCCGTGAGAGAAAATCCTGGTAAAG
48h-pore-68	TTTTTTTTTATGTAGAAACAGTACCGCACTCATTTTTTTT
48h-pore-69	TGAATTCTTAACCGCCTTAATTGTATAACAAACTTAATGG
48h-pore-70	TTTTTTTTTTTAATTGCAGTTGACCATTTTTTTTT
48h-pore-71	CAAAGTCGTAAAAATAAGAAACGATTATTATTAGTGAAC
48h-pore-72	TTTTTTTTTTAACATTCAATTGAATTCAAGCGC
48h-pore-73	ATTGTTGGATTAGAACTCAATATTACCAATCAACTCAATC
48h-pore-74	GTTTAAAAGCCGAAAGACTTCTTTTTTTT
48h-pore-75	TTAATTGGTAATTGAGCGTCGCCTGAA
48h-pore-76	TTTTTTTTAACGGCGGAAGCATGTCAATCTTTTTTTT
48h-pore-77	TTTTTTTTACTGGCTCATTATACCAAGTAAACGAAACATCGGTGAATAT
48h-pore-78	CATAGGTACAGTAGTCATATGCCTTATA
48h-pore-79	TTTTTTTTGCGCAACTGTTCAAATATTTTTTTTT
48h-pore-80	ATTCTGCCCTGTTAGACAAACAATTGACAAACAT
48h-pore-81	TGTAAAGCCTGGCTTCGTACTCCACACAAACATACGAGCCGTGCTATAG
48h-pore-82	AACAAAGAACGGAATAGCTGCAAGGCGAACGACGTTGTAACA
48h-pore-83	CACCGACTTCATTAGGAAGGTGGCGACAGGTTACGTACAAAGACACC
48h-pore-84	GACGGGCAGAGAGTTGCAAGGTGAATAATCGTCACAACCCAT
48h-pore-85	TTTTTTTTGTCAATTGCCTGAGAGTCTGTAAAAC
48h-pore-86	GGAGGTTGCACCCAAACCAAATCAATAATAGCGAAGTGAAT
48h-pore-87	CCGTATACGCAAGCGTCATACATCGTGGCAATTGGCAG
48h-pore-88	TATAAGGAATAGATTAGAGTCTTAGGAGATCAAAATTATTGAAACT
48h-pore-89	GCACACCAGCAGTAGATAGAACCCCTCTGACATTCTGAGAGTTGCTGA
48h-pore-90	CAATATGAATCGCAAGACAATCGGGTTATATAACTATCATAACCGACCG
48h-pore-91	ATTATCAAATAGAAGTATTAGACTTCTGAACCATGCATCA
48h-pore-92	TACCAAGAGCCGATATATTGTTGCGGGATCAG
48h-pore-93	ATCAGAAGTAATCGGAGCAAATTGAGAATTAATGAAGCGCCGGCGAT
48h-pore-94	ATTCACCTGAAATGACCTACACAACAGGAGAACAAACTATCGCACTTGC

48h-pore-95 TTCATAAACCGCCTCCCAGGAAGATTGTAATTTTCCAATATTTAGC
48h-pore-96 TTTTTTTTTTCATCAAGACAAATCAACGTATTTTTTTT
48h-pore-97 AAAAGATGTCAGAAGAATGACATGCTTCCAATACGTAAAATTAGCGAG
48h-pore-98 ATTTTTGAAGATGTTGCTTGAAATACCAATAACGAATCTACAGTTGAG
48h-pore-99 AGGCTTGAGGACCCGTGGCGGTGCTAT
48h-pore-100 TTGATACGCCACGCATAAACACCTTTATCAAGAAGCAAAA
48h-pore-101 TTTTTTTTTCTAGCTGATAAGATCTAC
48h-pore-102 ACGCAAACACCGAGTAAAAGATTAGGTACGCGATTAAACAGAGCG
48h-pore-103 TTTTTTTTAAATATCGCGTGAAAAGGTGTTTTTTTT
48h-pore-104 GTGAGAAATAGAAAAGATTCGCATTTCAATTAAACCAAA
48h-pore-105 TTTTTTTTATACATAACGCCATCATAACCCTTTTTTT
48h-pore-106 TTTTATTGGGTATTAGCTACAATTACTCCGACTTGCG
48h-pore-107 TTTTTTTTTCATCGCATTTCGGTCATCATTTCGCATTAATAAGCA
48h-pore-108 TTTTTTTTTAGTAAATTGGGCTTGAGAACCTTAT
48h-pore-109 TTTTTTTTGCATCAATTCTATAGCAAATTAAATTTTTTTT
48h-pore-110 TCTGAATAATGGAAGGGTTAAGTTAGACTCCTG
48h-pore-111 TTTTTTTTAGAACGCCTACAGTAACATTTTTTTT
48h-pore-112 TTTTTTTTAGATTAGTTGCGTCTTCTTTTTTT
48h-pore-113 TTTTTTTTATCCGGTATTCTCTTAAATCATTTTTTT
48h-pore-114 TTTTTTTTTCAGCTAATGCAGAACCGTAATTACAGGCTTTTTTT
48h-pore-115 TTTTTTTTACTCCAGCCATTCAAGGCTTTTTTT
48h-pore-116 TTTTTTTTAGATACATTGCAAATGGGGCGCGA
48h-pore-117 GTAACGAAGTTAAATACCGATAGCCCTAAACAGAATCAAAGAATA
48h-pore-118 GGTCAAGTTGATTGGAAGCAAACCTCATTCAAAGATATTATTAAACA
48h-pore-119 CCTCATTGAACCGCCAGGAACATCAGTGAGGGTG
48h-pore-120 CACCGGAATATGAAATGCTTTTTTT
48h-pore-121 GCCTGCAAGGTGAGGAAGAACGGCGAACGATTAGAGCTT
48h-pore-122 ATAACATTCAACAGTTCAGAGAAGTGTGTTCTGTATGGG
48h-pore-123 CTGCCAGAGATGGCGCATCGTATTTTTT
48h-pore-124 TTTCTTTCACCCCCGGAGAGGCGTCTGAGTTCTGCT
48h-pore-125 TCCTGATTATCAGATGATGCAGCCATTGTTGACCATCACCCAGCAG
48h-pore-126 AGAGCCGACCCTCAGAATTATTCTGAAA
48h-pore-127 CTGGAAGCGTTATTGTTGCTTAAATCAGCGAAAGACAGAAGAGTTAA
48h-pore-128 TAGCTGTTCTAGAATTGTAATCATGGCGCTT
48h-pore-129 CGATTGGAAGAAACCATACATAAAGGTGTAGCAAAAAAGGGG
48h-pore-130 ATGCTGTGCTTAGAGCTTAATTGTTTTTT
48h-pore-131 ATTTCAAAAAATCGCGCAGAGGCTTTTTTT
48h-pore-132 CATATATGTCGCTTCCAAGCTAACGATCTAAAGCTGCGGA
48h-pore-133 AATATTGTTGATATAGCCAGCTTCTTTTT
48h-pore-134 TTTTTTTTAATAAGAATAACAAATTCTACCTTTTTTT
48h-pore-135 TTTTTTTTACCGTGATAAAGGCTATCAGTTTTTT
48h-pore-136 ATTCAAACGCTCACAATTCAAGAGGTGTAAATTGTTACTAAC
48h-pore-137 TTTTTTTTGAAATTTCGCGATTAAAGATTTTTT
48h-pore-138 GAAGGGTAAAGCCAGAATGGCAACAAATGGTGTATAAGAAAATTG
48h-pore-139 TTTTTTTTGCAATAAAGCCTTTGCGGGTTTTTT
48h-pore-140 TAGTCTTAATGCGGGAAAGCGCCGAAATCGGAAAAAGAT
48h-pore-141 TTTTTTTTTGCCAGAGGGGTAATATGCGGAATAAGCTGCAAGGC
48h-pore-142 CTCCTGTCGTGCCAGCTGCAGCAATAGCGCAGATAGAACGA
48h-pore-143 ATAGGTTATGAACGAAGCCCCAAAAACTTCACCAAGTCACCGT

48h-pore-144	TTTTTTTTTATCAACATTAAATGTGAGCGAGTATATACTGGCCTTCCTG
48h-pore-145	TAGCGACAGAATCAAGAGAACATGAATCATTACCGCGGTATCTT
48h-pore-146	GGAACCGGGTGTACCGCGAAATTGACCCCCAGCGAAACGAAAAACAGC
48h-pore-147	AAAGTACCGACAAGCCGAAGGCCAATGCCATATTAGAATAT
48h-pore-148	CCAGTCGGAAACGGTACCGTCCACCAC
48h-pore-149	AAGGAGCAGGGGGAGGAAGGGCGGTCAAATAAGAATACGTG
48h-pore-150	ACGGAATCATATAACCTGATGAAAGGCCGGAGACGCTGGCG
48h-pore-151	AAACAGTAACCATCCGATAGTAAGGCACCAACCTAATTCCATTAAACG
48h-pore-152	TTTTTTTTTATATGTACCCGAAATTGTAAACGTTTTTTTTT
48h-pore-153	TATTCAGTAATACCAGAGCATCGTCATAAATATTTTTTTT
48h-pore-154	TGGCGTATATTAAATGAATCGGCCAACGCGCGGTGCTTC
48h-pore-155	AAAACAGACAGTGCCAGGCTTGATGATACAGCA
48h-pore-156	TCAATAAGAACGAGTCAATCACCGCGACATCGCCTGATAAAT
48h-pore-157	TAAAGTAGCAGGTCGAATCCTGAAAACATCGGCTATAATATAAATAA
48h-pore-158	TTTTTTTTAAAACACTCATCCAAAGTACAACGTTTTTTTTT
48h-pore-159	GCGCTGGAAGGGAGCGTAAAGCACTAAATTGGCAAGTGA
48h-pore-160	CGGCCAGGAGGATCAATAATAAACCACAAAGAATTCTCTAAT
48h-pore-161	TCTGTAAGGCCCTGAACAGCTCTATCAATCAAGTTAGTCAGAACGTGGACT
48h-pore-162	GGAAGGTAGTAATACCGTTGTAGCAATAGTCATCCCACCC
48h-pore-163	GTAAAACAGAAATAAAGAACAAAAGAACCTACCATCACTAACGAACCC
48h-pore-164	GAGAAACAAGTTACTTACCTGAAACAAAGAACATAAGGGATATT
48h-pore-165	CAATAGGCAGTACATACAGGGACACCCGCCGCGTACGCTGC
48h-pore-166	GTTAACAGCATTCCAAGAACATTCTACCGTAGGAAT
48h-pore-167	TTTTTTTTTCGAGAACAGCAATCAGATAAAATTAAACCAATAGGTTTTTTT
48h-pore-168	AACCTCGGAAATTATTGAGCCATTGAGCTTAATGCCCCCCACAAGTGC
48h-pore-169	AATATCTTCTAAAGGCAGATTATCATCA
48h-pore-170	CAGCCATTATCCTGAATCTACCAACGAGTTACACCCATCCCCTGTT
48h-pore-171	TTTTTTTTGAGATTGTATCCTGCTCC
48h-pore-172	TTTTTTTTTACAAAGCTGCTCCACCAGAACGAGTTTTTTTTT
48h-pore-173	AAGGAAACCGCCTGTTAGGCTTAATTGAGTTCTGCAT
48h-pore-174	CATAGTTAGCGTGAATTCCACAGACAGAACATTGCGAATAATA
48h-pore-175	AGAGCCGGAGGGAGAACGGTGAATACAACCGTCGGTAATGGG
48h-pore-176	TTTTTTTTTCAGAGCCTAATTGCCCTAACGAGCTATT
48h-pore-177	TTTTTTTTTATTAGTTAATAAGGCCTTATT
48h-pore-178	CTGAGTATTGATTATCTAACGAAATGCCCTGAGTAAGTACCG
48h-pore-179	TGACAACACATAAAACGCCTGTAGCAGACGGTTA
48h-pore-180	CATTACCGTAATCTATAGGCTGATGAACAACTGACCAGACGGTAGATT
48h-pore-181	TGGTTAGCCCTGACGAGAAAATTCACTTAAATTACATT
48h-pore-182	GGAGGCCAGAACATCTCCGCCACCCCTATTAGGGATAGCCT
48h-pore-183	GATTAGCGGGGTGTTATTTCAGCGCCACAGGACACCACC
48h-pore-184	ATCGCCACCAGAACGGTTGAGGCAGGGTTCATATTCAACC
48h-pore-185	GGGTTTCCCAGTCTAACGTTGAAACGTGATTAAGATGGTT
48h-pore-186	TATTCAGCATTGAGGATTAAGGCCGTCAATAGAT
48h-pore-187	TTTTTTTTGCTGAGAAGTAAACAAACATGTTTTTTTTT
48h-pore-188	TCCAATAAAACGAGCAAAGCGGAACCACCGAGAAG
48h-pore-189	TTGAAGCAAGAACGTGTAGCGCTTTTTTTTTT
48h-pore-190	AGGCTTCGACGATTGACCTACGCAAGGATAAAAGGTTAA
48h-pore-191	GAACCAGAGTTGCCTTATTAGCTCGATAGCAGCACCGTAGC
48h-pore-192	CGGTGCGGGCCTAGCGGAAACCGAGGACCCGGAGATCACCAC

48h-pore-193	GCGTAACGGTCGAGGTAAATGCCACTACGTGCGCCGTATTGCTTCGAGG
48h-pore-194	TTTTTTTTTCGGAACGAGGCGCAACTTGATTTTTTTTT
48h-pore-195	ATTTTGCTAAACTGGATTGCGTAGCTTAAATGAATCTCTGCAC
48h-pore-196	GATGTTCAAGGGTGAATTCACACAGCATTAAAGACTCCTCAAGA
48h-pore-197	TTTTTTTTCTTTAACCTCCGGCTTAGGTTGCAGCAAAAT
48h-pore-198	ACATGTTTCGAAATTAGTCACCCTCAGCCTCCCCA

Supplementary Table 10 | DNA sequences of 54helix DNA origami (Scaffold 8064)

Name	Sequences
54helix-1	AAAACCGGATTGCCCGGCCAGGGTGGTTTCACCCCTCAGGAGA
54helix-2	AGGCATGAGGAATGGTAGCAACGGCTACAGAGGTTGAAGAGCGAA
54helix-3	GTGGACTCCAACGTCAAAGTAAGTTGG
54helix-4	TAATAAGCCCACAAGAGCTTATCCGGTAAAGCCTT
54helix-5	CGGGAGAATTAACTGCGCTAAAACCGCGAAATAGCA
54helix-6	TACAGACAGGGAACAGAGGACTAAAGACAAATACG
54helix-7	GCTCCATGTTACTTAGCCGGGACTGAT
54helix-8	GACAGGACAGGAGGAAAGTGAGACGGGCAGAGAGT
54helix-9	CTTATTACTAAGAACTGGCATGAATTGAGTGGCGA
54helix-10	AGAAGTTGTAGCAAGCCGTTGCCTCCTACACCGGGCTATTAGCGGAAA
54helix-11	TCGGCCTGTCCTGAGTAGAACGCCGATTAAAGAACG
54helix-12	GTATGTTCCGGGTTAAGGCGAGAGGGGACGACGA
54helix-13	CATCGTAACCAAGTTATCAT
54helix-14	AGACAGCTAAATGCATTAGATGATATGAATCATATGTACCAAGAATA
54helix-15	GGCGGTTGAACAACAAATACCGCCTCCCGCGTAACCGTGCATCCTGTT
54helix-16	GCCAACCGCGCGATTCATGGAAACCTGTCGTGCCAGCTCGG
54helix-17	TCGAGAACAAAGAGAAACGCAGGCTGTCTTCCACCGCACTCA
54helix-18	TCACCCCTCAGAAAAACATTATTAGGGAGTTAAAGGCCGCTGC
54helix-19	TGGCAACAGTTATGTAGCACCGCGGCCAGGATCAGCAAACAAGACTC
54helix-20	AACAGGACTCAATCAACAAACAGTTTCAGATTGCGATCCAGAACAAACTA
54helix-21	GGAAATAAGAATAGTGTATGGATTGCGTTAAATCTAATGGGAATCAT
54helix-22	TTGCACAATAACTATAGTGAATCACCATAATGCAGAACATGAATATTAA
54helix-23	CGCTCACTGCCCTGTCACAATAAGACAATAGTGTGCGGCCAGGGTTT
54helix-24	AAAATAACAATCAATAACCGCGCCTCACGGTCGGGCCT
54helix-25	ACCGATATATTCCGAAATGGGACCAGTTGGCTTCCAGACCTAAACA
54helix-26	AGCGCCACAATAGCGGAATAATAAAAAAAATACATACATA
54helix-27	ATAACGCTACCACAAGATTACCGAACAAATCTAC
54helix-28	GTCACACATTATTTTGACGAAACGCATTACGCCAGCCAGGTAATA
54helix-29	GTGAGGGCGACATACCGAACATAAGTGTAAAGCCTGGACGCCCTC
54helix-30	CATGTTCAGCATAAGCCTGAATGGCGGGCC
54helix-31	AATGATAAAAGGGACCTTCTTAAACAGCTTGTACCGATTATTCTGT
54helix-32	CAATAACCGGAGCAGCGCAAATAAGAGAACATACGACGACGA
54helix-33	ATCACACAACATACGAGCCGGACACGCCCTGTAGCATTCCACA
54helix-34	AACTTGCTTCGAGGTGAATGTTATATGTGAGTGAATAACC
54helix-35	AAACAAGATGCCCAACCGCCTGTATAAAACCGAGC
54helix-36	AAATTGTCTAAAACCCATTAACATCTTCTTTTC
54helix-37	AATTCAAGTTGTGAAATTGTAACTAACACATTAATTGGA
54helix-38	GTCACTGAGGCAAATTATAAACAGTTAACCACTTGGATTAT
54helix-39	CCAGTGTGTTAACAAACGCCACAATAGTAATGCA
54helix-40	CGTCGCTTCATATAATGACCCCTGTAATAGATAGCGAAAAGAA
54helix-41	ATCAGATTCCGGAGCCTTAATAACAAACAACCATGCCACTGAGAAGAG
54helix-42	AATGAATTAGCGTTAAATTGATTATACTTCTATTAGTCGCACAGA
54helix-43	TTCCTTCATTCGTAATCATGTTGCTTCCAGTCG
54helix-44	CTGCCCAAGTTGGGAAGGGCGTGGCGAATTAAACCGGAATA
54helix-45	AAATCATTAGGTTAACCAATTGGGAACGGCT

54helix-46 TTTATCAGACGCTGCAGATACGAGCAACACAGTTGCCCGAC
54helix-47 CAAAAAAATAGAAAATCTCCAAGTGGTCGCTGAGGC
54helix-48 ACTTTAAATAGGAACGCCATCAGCTTCAATTAAACATC
54helix-49 GATTTGGTTAGTATTACCAGCCAACAGAGGTGCCTAATGA
54helix-50 TCGAAAGTGCCTATTGGGCCAAAATTAATGAATCG
54helix-51 TTACCGATTATTTAGCAAATCAGATAT
54helix-52 ACGTTGATCGGAACGAGGCTTTGCGGGATCG
54helix-53 ATAATAATGACCTAACATCAGAAAAGCCCC
54helix-54 GACAGTGTGTTCGTCACCACCTATTATTAGCTTCCGGCACGCTCAC
54helix-55 CACCGTCAAATTATGTGCACTCTGTGTCGGCTCTGCCSTAT
54helix-56 CGATCGTGGAACCGTTAACGGTGGCGGGCAGCGGATCAAATTCGAG
54helix-57 GTTTGCATAGCGAAATTTCAGATTAA
54helix-58 TTGCTGCTCTAACGGAAACAGCTACCATTATTGTAAACGTTGGTTT
54helix-59 CAATATTAAAGCGTTAAAGTTTGCTAAATATT
54helix-60 CCGTAACACTGATATTAAAAATAGGATAGCAAGCC
54helix-61 GTTCAGCAAAACCATTAGCGCTGGAATGGGTACACTGGTGT
54helix-62 ATACTGCGGAATCGTAGACTGCTTTGCAATTAGTTAGTAATGCGGAGAC
54helix-63 AATTACCTTTTCACAGTTCAAGAAATTAAATTACA
54helix-64 CAATACACCACTAGCCAATGACTTGAGTTAAAGACGACGT
54helix-65 CACCATTAGAGCCAGCAAAACTTGAGTCCCCCTGGTGCCGCTGCGC
54helix-66 TCAAATGAAATCAAGTTGTAC
54helix-67 TTTAACCCCTAAAACCAGAAGAATATAATTACCGGCGGA
54helix-68 ATCGCCAATGCGCGACTGATAATGGCTGAATAATTGTTAAATTTAA
54helix-69 TCCAGCAAGTAAGCGACACCCTCAGAGCCACCACCCCTTTACCCCTAA
54helix-70 GTTTAACGTCAAAATAAAACACCCAGTGCAGGAATTACTACAAATT
54helix-71 ATCGCGAAAAGAGTGAAACAACTAATAGATTAGAGGAGGCCAAACGAAA
54helix-72 CTGCGAAGTACATCAGGCGGCCAGTGCCGATAACCTCACCGAGCGTCCG
54helix-73 GAGCCCCATCGATATTGCCTCATGGCTATTACCCAGAAT
54helix-74 TATAGTCGAGGAAGAAGGCAATTAAACATATCAATT
54helix-75 TGAAAAAACAGAGGGTGCCACCAGAAGGTCAATTAAATTAAATC
54helix-76 CAGAAAACCTCTCAAGAGAAGGGTATTAAGAGGCTATAGGTC
54helix-77 TGAGCGCAGAAATTGCGTAAGGCCGTAACAGAATGAACGG
54helix-78 CGCCACCCCTCAGAGCGTCAGATAGCCCCCTTATTACTCAGGA
54helix-79 CAGCTTATGCAGGCCTTTAAGTGATGCCGCAAACCGAGATAATCA
54helix-80 TTTAATTCTCCAACCTTTGATAATTGCATATGCA
54helix-81 GGCAGATTATTCTGAGAGCCACTGAACCTCAAAAGTTACAAA
54helix-82 GGTTTCTCATAGGTGTATCACTAAGGATTAGGATTAGCGGGT
54helix-83 GGCATTTCGGTCACTGTAGCAATCAAGGCAGCACACGTCA
54helix-84 GTGCCATCCCCTCAAGCAACCGCAAGATGCCGTTAAGGGTAGCCGCAC
54helix-85 AGACCGGAAGCAAACGAGCTTAGATTAAAGAAGCATGACCATCTTAAA
54helix-86 ATGCCCTGTGCTTGAATACAAGATTTCAGGTTAACGGTCATT
54helix-87 TAAGAGGAGTAGCAAGAATTAGCAAAACAAAGCGAAGCAGA
54helix-88 AATCAATAACATTAAGCGGAATTATCGACACCGCCATAAAAAGTAC
54helix-89 ATCTGGTAAAGCATCACCTTGGCAGCAATGCAACATGAGGCCACCAG
54helix-90 TATAGCCCGGAAGTCGAGAGGAGTATTATAGATAA
54helix-91 GTCTGGTCAGCAATGGAACGTGGTTGAGCCGCCAC
54helix-92 GATTGCCCTGATCGTCGGAGCAAATGGTAGTTG
54helix-93 TCCCTCAGAGCCACGATTGACCACCGAACAGAGTC
54helix-94 ACTAATGTTAGCAGATGGCTAGAGCT

54helix-95 AGGTTATCTAAAAACAATTGTGGCAAATCAACAG
54helix-96 ATAAGTGAATCCCTTATAAATGCGAAAATCTGCCAGTTGGG
54helix-97 ACAAACACAAAGTTAAGAAAATAGCTATCTTACCAGAAACAATAAGAT
54helix-98 TTGGGGCAGTGAATATCAACGCAAGAACCGGATATCGCATAGGACACT
54helix-99 TACCTTCCAGCGATTATAGTGAGGCAACCGGTTGATAATCA
54helix-100 CAGTACCATCTTGGTAGATGGGCATAGGAGGTTTGCT
54helix-101 TTTTTCATCCTCAGTTACAAATAAGAACGATAGCTCAGAGGCAGGTC
54helix-102 TCTCTGATTGATGATACATTGCGACAGGCCTTCAGCAAC
54helix-103 AGCCTCATGGAGCAGCTATCAAGCTATT
54helix-104 GCAATAACAAAAACATTATCAACGAGAAAAGCGGATTAAAAGAAGATGA
54helix-105 ATTCCTGCCTGATTGTTGCTGAACGAAGTCAGTATTCCGCCACCCCTCA
54helix-106 GAAAGGGTTCGGAAGTACAAACTACACGATGGAACCCATGTA
54helix-107 TCAGTGCAAACCACCCCTCATTTCAGCCAAACAT
54helix-108 CCCGTGTGCCGGACGTAATCAGCGCACTCAATCCTGTTGCC
54helix-109 GACATAACAGCAGTCATCAGACCCCCCTGCATCAGA
54helix-110 TTGCAAATTAGAACTACATAAATCAATGAGCAATTTCATTG
54helix-111 GGAAGGGTTCATCATACAAACATCAAGAAAACAAAAAATTAT
54helix-112 ATTCGCAAACGATCAAGAATATAGAACCCCTCTGACATTCTG
54helix-113 AGGCCACCCCTCAGAACCGCGGATTAGAGTTGATACCGCGG
54helix-114 GACAGGAGCCGGACAGAGCACGTCGTGGGAACG
54helix-115 CCAGTACGGTGTCTAATTCTGCGAACGATAACCCAAACATCT
54helix-116 TTTAGGAGCACTTACATTGAAACAATCGAACAG
54helix-117 TACATTAGATCAAAGAATAGCCCGTCCGTCAAGACTTACAATATC
54helix-118 CAGAACCAATCCAAAATAAACCAACGCTCGAACGTGAGAGA
54helix-119 ACCATTACTCCAAGCGCGAAACAAAGATGTAGATTCAATAA
54helix-120 AACTGATCCCAGTCTTTAACCGTCATATTAACCGCCACCC
54helix-121 CATTCAAGGAAACCCCGCGCCTTCATTAAGAAGGTAAATATTGTCACCCG
54helix-122 CATTGCCGACGGCCTGGAGTGTACTGGAACAGTG
54helix-123 ATGCCTGAGAACCCATTAATTGAGGCTTCATAACCCCTCGTTAGTAA
54helix-124 CCAATAAGAACAAAGATGATGAAACCACGCATTCAATTACC
54helix-125 ATCGGTGCATACCGGAATGCGGTTACCATGAGGGAAA
54helix-126 CCGTGGTAGAACGCCATTGAGTATAAACGCCATAGAAACTATCCCA
54helix-127 TTTGCCATAGCCTTGATATTGGAAAGCTTAAGTTGTAAAA
54helix-128 TTGACCTACTATATTTCATCTACTAATACAAAGAACAAAGA
54helix-129 GCAAATTCCGAGTAAGTGTGTTATAATTACGCCAGTCAGC
54helix-130 TCGGCAACCCGACAACCTCGAAAAGTTAACAAACTGACCGAGCTCAT
54helix-131 CAGTATGGACCGTGGGCCCTGAACAGCTTCTATCAAGCTAAACAGAAC
54helix-132 TAGACTCAATCATAGGTTGTTCAAGTATCAGAGAGATAAGTTAGA
54helix-133 TTCTAGCACTTTGTTAATGATTTCAGACGGTCAATCATAACAGACCT
54helix-134 AAAAATTAAATTACGGGTATTTTCAGACGGTCAATCATAACAGACCT
54helix-135 CAATCGGAACGAGCTATTGCGAGGGAAAGCGCAGAGATT
54helix-136 GCCAGGGATTAAAGGTTCCAGCGTAGCGTTGCCACCAACCGGAAAG
54helix-137 GGGTAACGGATGTGGAAGGAAACCGAACAGAGCCAAAATAATTACCGCC
54helix-138 GCATGTCATCTACAGATGAATATACAGTAAGTGTAAA
54helix-139 ATTCTCCCGTTATTGCGGAACCATATCAAACCCCTCTGAAAGGAATT
54helix-140 CCGTCGGACATTAAGTTGAGCAATAAACCATCACCTTGCCAAGAGGA
54helix-141 ACGTTTCGCACTCCAGCCTGTCTCGGCCTCAGGATAGCTGT
54helix-142 AAGCTTGAGACGCAGAAAGCCTTTCT
54helix-143 TAATCGGGCAAATTTAATTACAGGAAGATTGTAAGGCTC

54helix-144	CTTGGCCGGCTTGAGCTGGCTAACGGTG
54helix-145	GCTGGTTGTCCACTATTAAGGCAAGATAAGGGTTGAGTGTGT
54helix-146	TAGTTGCGTCTTCAGAGCACTGCAAGGCCAGC
54helix-147	ACGAAGGCACTAAAACACTGGTTGAGATCAACCGAGTCAAA
54helix-148	CACCAACGTCGAAATCCGCGGTCTACAACGGAGATTGTATC
54helix-149	GGTCCACTGATGGTGGTCCCATGTGAGTGTAGCCAAAATA
54helix-150	CCCAATCGCGAACGCAATAATGAAATAGCCCAA
54helix-151	AAATCAAAGAATAACACAGTTGTTCTGACACCAAAATTCAACAAGA
54helix-152	TAATGTGCAAATATTGATGCAGGGTTATGGTAGAATTCAACTAAGCATA
54helix-153	ACTTGTGACTTCTTGATTAGAACCTGATTAA
54helix-154	TGCAGAACGGTTGTAAAGGACGGAGTGCCTACATACATTGGCACGTTG

Supplementary Table 11 | DNA sequences of 2-layer DNA origami (Scaffold 8064)

Name	Sequences
2layer-1	GACGGTCTGTTACTTAGTAAATGAAACTTGTGTCAGTTG
2layer-2	GACCAGGCGCATCGCTACCAACTTGATAGCCGATCCAAT
2layer-3	AACGGCGACCCGTCTAGAAAATTAAAAACAGGCAATAAATC
2layer-4	CGACAGTATCGGGTAGGTACGTTGGTGGTGGTGCCTGCC
2layer-5	TTTTTTCATCTGCCACTTCCGGCTTTTTT
2layer-6	TTATCAGAGCGGAAGGCCTAGTAACCACCCCTGTC
2layer-7	ATCAAAATTATTATTATACTTCTGAATAAACCGCGTTTT
2layer-8	ACATAAAATGTTAGCGCCCAATAGCAGTCAGTAGGACGTCAA
2layer-9	AATCAATAGAAAAAACGCAAAGACACAGTCCACAACGATC
2layer-10	TTTTTTCATCAATATAATCCTGATTGAAAGCCGAAAGG
2layer-11	CACTACGATTAACAGGAGCCTTAAAAGGAAAAAGGCTC
2layer-12	AAAATCTACGTTACGAAACTGGCTCATTCAATTAAATTG
2layer-13	TATTTAAAAAACAGAATGCAATGCCTCCTGACCCTCATATAT
2layer-14	TGAAGATTCGGCGAACGTAATCCCCGACCGTG
2layer-15	ATAATGTTAGAACGGAGCTTCAAGGGTTCAAGGCGGGGC
2layer-16	TTTTTTGAATTGTGCAGAAACAGTTTTTT
2layer-17	CAAACCCCACCTCACGAGTAATAACATCTTA
2layer-18	TTTCATTGAATCTAAAAACATCAAGAACATGCCACATGTA
2layer-19	AGAAACATGAGTTATTATCCTGAATAGCATGCACCCAGCTA
2layer-20	CAGAACATCAAGTTATTCTGAAACCATCGACAGTACCGGATTAG
2layer-21	TTTTTTGGTCAGTGGCATCTAAATATCTTTTT
2layer-22	AGGAAGTTTGAGGGCTTGCCTTCAACTGTTGATCGGTTT
2layer-23	AGAAAGATTCAATTATAATAAACGAACAACCTCATTCAAAG
2layer-24	GAAAAGCTCATATGAAGATTCAAAGAGAGAGTAATGTGTA
2layer-25	CGCCATGGTGGATAGCTCTCATTACGCGCCTGT
2layer-26	TTTTTTCGGATCAAAATAAAAAATTTTTT
2layer-27	TGAGAGCAACACCGACTTGCGGTAAATATCACCGG
2layer-28	ATGTGAGTGAATGTAACCTTTTAATAATTGAAAAGCCA
2layer-29	CCCACAATTGAGCGAGCGTCTTCATGACCTTACCAACGCT
2layer-30	CATTTCGGTAGATATGCCCTTAGCGTAGTATTAGGAACCT
2layer-31	TTTTTTAAAAATCTAAAGTCATCAATATCTTTTT
2layer-32	GCTACAGCAGCATCAGCTGATACCGTTAGGTGAATTCTT
2layer-33	AGATACATAACGGTACCAAGTTGAGATTAAAGACTTCAAAAA
2layer-34	TAGCATGAATCGATGACAGTCAAATCTTAGGGTGAGAAAGGC
2layer-35	TAGTGTGTCAGTGGGGGGCATCAGCATCAGA
2layer-36	TTTTTTTCCCGTAAAATTGCCGTTTTTTT
2layer-37	AAGATAAAAAATACGAACAATTGAAATTAA
2layer-38	TTCCCTTAGAATCACAAACCTTGCCTCTCATATGATTACTA
2layer-39	TCAGAGGAATTAACCTACAAAATAAAATCCGAGCCTAATTG
2layer-40	CAAAATCACCGGTGCATAGCCCCCTTATGTATAAAGTCAGTG
2layer-41	TTTTTTGGTCAGTATTCACTGAGCAAATGTTTTTT
2layer-42	GCAGCGACGCTTTGACAACACCAAGTTAGTTGCGCCG
2layer-43	ATCATAACCCCTCTGGCCAAAAGGAATTACTATTAAATCAA
2layer-44	GCAAACATCAGGTCTAACCGTTATCTCACCACATCAATATG
2layer-45	TCGCTGAAATGAAGGGTAAATACACTGGGCTGGT

2layer-46 TCCGATGCTGAAAAGCCCATCGACCTAAATAGAGACGAGAG
2layer-47 TTTTTTCCGGCAAACCATAACGGATTTTTT
2layer-48 GCGAACTTGAAATGCCTACATACATTGG
2layer-49 GAGAAGAGTCAAACTACCCTGAAAACATGCGTAAAAATACC
2layer-50 TTAGACGAATAACACCCAATCAAATTTGCAGCCATATTAT
2layer-51 CGCCACCCTCAGGGCAACCAGAGCCACCAGGAGTGCCTCAT
2layer-52 TTTTTTACATGCCATTAAACAGAGGTGAGTTTTTT
2layer-53 GAGTTAAGGATTCGGTGCGCTGAGAGAAGTTTGCTAGCGTC
2layer-54 GGCTTTGCAAAGCCGGTTACCAAGACGTTAAACAATTCA
2layer-55 TACAAAGTAAGGGTAGCTATTGTCTGGTCAGCACCAAGCTT
2layer-56 AGCGTGGTGCTGTGGAGGCAGCCTCCGGTGCCTACGGGTC
2layer-57 TTTTTTACGTGCCGGGCAACGGC
2layer-58 AGCGTAAAGAGATATTCAACAGTCACACGACCAGTAA
2layer-59 CCTTTTTAACCTGGTTAGTGAATTATTTCATCACTTTTT
2layer-60 TTTACAGTACGTAAAAATGAAACACCAGAGCCGCGACGATT
2layer-61 CACCAGAACCATAGAACCGCCACCCCTAGCGCAGAACCTC
2layer-62 TTTTTTCAGACAATATTGATAGCCCTAAATTTTTT
2layer-63 GACCTGCCCTGATATTGCTAAACAACGCCATTCTGTATGG
2layer-64 GAACCGGATATTGAAAAGGCTGGCTGACCATCAATTGGGG
2layer-65 AGCGAGTCCAGCTGCATAAGCTAAATTGGCAATAAGCCT
2layer-66 CGCCATTCCCCTCAGGAAGATTACCGCTGGTTTT
2layer-67 TTTTTTACCGCTCTGGGAAGGGTTTTTT
2layer-68 CATTTGATTTAAACCCGCCCTGGTTGCTTAGAAA
2layer-69 TTCAGGTTAACTACATGCACGTAAAACCAAGTACATCATT
2layer-70 TATTACGAAGAACTAAGGCTTATCCGGAGGAGCAAATCAGAT
2layer-71 GACATTCAACCGAAAGATTCATATGGTGCAATTCCACCAAGTA
2layer-72 CAATACTGCGGACCGATATAGGTTGAGGCCTCGCCCACGCAT
2layer-73 ACGGCTGGAGGTGCCGGAGAAATGTTACCGCTGATAATT
2layer-74 GTGGTGCCATCCCGCTTTCGCACTTTTTT
2layer-75 ACAAGAGAACCTCCGGCTTAGGTTAATCCAATCGCAAG
2layer-76 GGCCTTGATATTGTTAATGTAATGCATAAGAAACGATT
2layer-77 ATTCTGGCCAACGAATACGTGGCATT
2layer-78 TTTTTTTCAATCCGCCGAAAGGTTCTTTTTTT
2layer-79 AAATCGTCATAATGTTAGAAAACGAAGCGGGATTGCAGG
2layer-80 GAATCCCGACTGGAAGAGGGGTAATAGGAAAATAGCGAGA
2layer-81 ATGTCCAGCATCAGTGAGCCGGTCAATATTGCCTAGAGATC
2layer-82 ATTGCAGCACGCAAGCAACCGCAAGAATACTTGTAACATCCTGCGG
2layer-83 CAGAACCGCGAGAAATTCTGACCTAAATAGCTATTACCTGAA
2layer-84 TTTTTTCTGAAATGGATTATTTTGACGAAAA
2layer-85 CAAATATTGATGCAGGGTTATATAACTAAGTCTGAGAGACTA
2layer-86 TTCACAAACAAATATCTCTGAATTAAATTAAAAACAGCAGCC
2layer-87 ATTAAAGCAGGTACGCCAGCATTGACAAGCCTCAGAGCCGC
2layer-88 TTTTTTGCTCGTCAAAATTACCTGCAGCCTTTTT
2layer-89 ACAGAATGACCATAAGTCAGAAGCAACGGAACGAACCCCTCA
2layer-90 AATCAGGAAATGCTACGATAAAACCTAAGAAGAGCAACACT
2layer-91 ATCTGTTGCCCTCGTGTGTTCAGCAGAGAACGGTGTCTGGA
2layer-92 AATGGGTGCGCGGTCCAGCGAACCGT
2layer-93 CGCATTACCGCCTGCTGAGTAGTTGATTAAATTACAGTA
2layer-94 TGGTTGATAAGAATAAACACGAACGATTAATGC

2layer-95 TTTTTTGCAACAGGACTCAATCGTTTTTT
2layer-96 GACC GTG TAGTTAACAAAATCATAGGAGGGGATTAAGACGCT
2layer-97 TTCC GTT CCAGTAAGTACTGGTAATAAGTGAACACAAGCGCA
2layer-98 ACATGGCAATGGAACAGAGGCCACCGCAACTCCCTCAGAGC
2layer-99 TTTTTTAGCGGTGCCGGTGTGGTGCCTGGTTTTTT
2layer-100 AAAAGCGGATTGCACAAATATCGCGTCAACTAAAGAGCAACG
2layer-101 GATTAAGTACCCCTGACGAGGCATAGTAGTCCTCAACTAATGC
2layer-102 CGAATCGTTAACGGACGATCCAGCGCTATACCCCGTAAAAC
2layer-103 TGCCGGGCATCCCTGTTAACGTTTTTCGTCTCG
2layer-104 AATCATACGTTACAAATTCCCTGCAACCAGCAG
2layer-105 TTTTTTAACTATCGGCCAGCCATTTTTTT
2layer-106 GAAAAAAGAAAATAAGAGCGATAGCTTAAGGTATTAAATTAAATT
2layer-107 CCAGTTTAACGGGCAGTTAATGCCCGCTAATATAACAAAG
2layer-108 CCTTGAGGATGATAACCCGGAACCGCGAAGTCTTCATAAT
2layer-109 TTTTTTCCAGAATCGGGCTTCGCGTCCGTGTTTTTT
2layer-110 ATTTTAATTGAGCACAGGTCAAGGATAAGGGTAAATTTCATG
2layer-111 CGAACCAAGCCCGAAGGAATACCAACAAACCATTATTACAGGT
2layer-112 GGAGTGTCACTGCGGTACATACGGGGTAGAAGATTATAATCA
2layer-113 GCACTCTGCCCTTGTGTAGCACAGCGGCCTT
2layer-114 CCA GTATGAATGCCATATCATTGCTGAGCCACGC
2layer-115 TTTTTTAATACTTCTAACGAACTCATTTTTT
2layer-116 ACGCTCATTTAGTAGTAAATCGTCGCAAGAATAATCAATAT
2layer-117 AACCTGCCTATTTCAGAGGCTGAGACATAGCCCAAGAGATAA
2layer-118 ATTATTCA GTGCCCTAGCGTTGCCAGCTCGTTTCATCGG
2layer-119 TTTTTTACCA CAGAAGGATGATGGCAATT TTTTTTT
2layer-120 TTTTTTAGCCTCCTCACATTCTGTGTGAATT TTTTTT
2layer-121 CATAGAGAGTACCTGCGGATGGCTTAGTCTAAAACGTAATGC
2layer-122 CTCCTTGGAAAGCATAACGGAACAACCAATACGTTGGAAAGA
2layer-123 TTGTTTCTGCCAGCGGTACCGAGCTCTATAATATTAAAGCAAA
2layer-124 CCTGTTGGGCCGTGGAAAATTCTGCTCATTGC
2layer-125 AAAGTTTTAACGGTACCCGATTAATCAGAGCGTATAACGTA
2layer-126 AACGCCAAGTAATAAGAGACTCAGTTGACAAATAT
2layer-127 TTTTTTAGGCCACCGCGTTGTAGCTTTTTT
2layer-128 ATTTAGGTAGGGCTTGGAAACAGTACATATTACATTAAACAA
2layer-129 CATCCTCAAGAGAAAGCGGATAAGTATATAGCTAAAGAGCA
2layer-130 GATTAGCACATGAACAGACTGTAGCGCAAATCAGTAGCGA
2layer-131 TTTTTTATTGTTATCCGCTGCTTAATGAGTTTTTTT
2layer-132 ACGAGCTTAATTGCATATGCAACTAAAATCATCTTGAGGCAA
2layer-133 AATGCTGAAGAGGTATACCAGTCAGGTGAATGAATTACCTTA
2layer-134 GAGAATT CGTAATCACACATACGAGCCGAATCAGCTAAAATT
2layer-135 TAGCTGTGTGAGGCAGCGCCGACTTCTCCGTGG
2layer-136 AAGTACCGACAATAAACAAAAATAGATAATTGAG
2layer-137 TTTTTTTAGACAGGATAATCAGTGT TTTTTT
2layer-138 GGTAAAGGGATTTAACAAAATTAATGATACTGAGCAAAAGA
2layer-139 AGGCCGTCAGAGGCACCGTACTCAGGCAGCAGATACCGAAG
2layer-140 TAAGTATTTTGCTTAGCAGCACCGTGGCATAGCAAGGCCGG
2layer-141 TTTTTTGAGCTAACTCACCAGCTGCATTAATT TTTTTT
2layer-142 TAAGTACGGTGTCTAATTCTGCGAACGCACAAAGTCCCCAGC
2layer-143 TCATT CCTCAACATCTTAATCATTGTTGAGAGTAGTAAATT

2layer-144 GCGGAAGCATAAAGGCTCACTGCCCGAAAAAAATAATTTTAA
2layer-145 CCTGGGGTCACAATGTGCCAATAACCTCACCGGAA
2layer-146 TCAGCTAAAGTCCTGAACATGTACAAACGCCGTCA
2layer-147 TTTTTTCTCGTTAGAAAGGGATTTTTTT
2layer-148 ACGCGCCTCTGCCCATTCAATTACAGGAATACCAAGTTAC
2layer-149 TTGAGGTTTAGTACCCACCTCAGAGCGAGGAAACGAACAAA
2layer-150 CTCAGAACGGAATACACCATTACCATCTCCCCATTGGGAAT
2layer-151 TTTTTTTGAATCGGCCAAACCAGTGAGACGTTTTTT
2layer-152 CAGAGTAGATTAGATAACCTGTTATTAAATTGTGCGGAGAT
2layer-153 ATTAGATAACAGTTAACACACCAGAACACGTGCTGCTCATTCA
2layer-154 AACTTCCAGTCGGCGGTTGCGTATGATCATCAACGTCTGG
2layer-155 GTCGTGCATTAATTGTGCTGTCCCAGTCACGACG
2layer-156 CTAGCGCTTAGCTGCGCGGGCGCTAAGAAAGGGCGAACGTGGCGAGATTTTT
2layer-157 AATAATAATCAATACTGGACAAGTTGCGACAAC
2layer-158 TTTTTTTACAGGGCGCGTGCTTCTTTTT
2layer-159 CTAATTATCAACTGATTGCTTGAAGCCACCTTACATC
2layer-160 CGCCACCACCCCTCATGTACCGTAACAAGGGCATGATAATAAC
2layer-161 GGATAGCCACCCCTCCACCGACTTGAGAAATGACGGAAATTAT
2layer-162 TTTTTTGGCAACAGCTGATTGCCCAAGCATT
2layer-163 GAGCTATATTTCATCTACTAATAGTCGTAGCCGAATCCGC
2layer-164 CGCGAGCTTCGCAACAACGTAACAAAAGAATAATCTTGACAA
2layer-165 CATGGCGCCAGGGCTGCCCTGAGAATGGATTCTAAATGTG
2layer-166 TCTTTTCCCGCGCGGCTGCGCTTCGCTATTACGCC
2layer-167 TTTCCTTCGCACTCATCGACGTTATCATACTATT
2layer-168 TTTTTTAGCGGTACATGCGCCGTTTTTT
2layer-169 CAAGAACGCATGTATACAGTAACAGTAACAATTGCGTAGATT
2layer-170 ATCTGAGTTTCGTCACAGACAGCCCTCGCAAACGTGACTCCT
2layer-171 CAAACTACCAATAGAAGGTAATATTCTCAGACACAAAGGGC
2layer-172 TTGTATCGCGCGAAGGAGTGAGAATAGCAATTCAACAGTT
2layer-173 GTGAATAAGGCTAATCCATTACCCAAATATGGTCATTGACC
2layer-174 CCTTCCTGCCATCAACATTATGACCCATACATCGGTTGTACC
2layer-175 AGCTGCGCATTGCCATTAGGGAGAGGGAAACCT
2layer-176 CTCAACTGTTGGTCCGCAGCCAGGTTGAGGCGCATCGTAACCGTTTTTTT
2layer-177 TTTTTTGATCGGTGCATTAAGTTTTTT
2layer-178 TCGTATTAGACTTACGAGCACGGGAGCTACATGT
2layer-179 GGGAGAAACAATTAGGTCAAGATGAATAGAAACCATCCCAC
2layer-180 GGAATACGAAACCGAGGCCTTCTACGTATTCTAAGAA
2layer-181 TCATTAAGGTGAATTATTGAGGGAGGGAAACCCATTTCAG
2layer-182 GAACAAGCACGGAATAAGTTCATAAAGGGTTGTTCCCTTCCA
2layer-183 AAAAGAAAAGAGGACAGATTGACCGTAATCCCTAGGCAA
2layer-184 TTTTTTGGCGAAAATCCTGTTGATTAGATGGGGGACGA
2layer-185 AGGGCGAAATGGAAGGGTTGGCAACATGACTCCAAATCATT
2layer-186 GAAGTAGCATTAAACAGATAGGGTTGAGTAACCGAAAGGCGCA
2layer-187 AAATCATAAGGTGGCTTCATCAAGAGCAGAGAACGGTGTACA
2layer-188 GAGAGTTGCAGCAACCGAAATCGGAAATGGGATGGGAACAA
2layer-189 ACGCTGGTTGCCCTCGCACTCGAAACCAGGCAAAG
2layer-190 AGGAACAAGCAAGCTCTATCATGACGGGGTTGGATTCCCTGA
2layer-191 TTTTTTAAGGAAGGGGGCAAGTGT
2layer-192 ATTTTCAATTAAACAGAAATAAGAAGTGGAGAACCTACCAT

2layer-193	ACCATAGTTAGCGTTATTAAAGAACGTGATAAAAGAACATACAT
2layer-194	TAAAGTTGCCTGTATACCAGCGCCAACAAATTATTTGTCAC
2layer-195	TTTTTTCGAACGTTATTACGGAACAAAGAATTTTTT
2layer-196	GATTATAAAAACACGGAATTGCGAATCCCCGAAAGGAACAAAC
2layer-197	GGGCTTGAGATGACACTGCCCTGACGAGGATTCCCGGAAGTT
2layer-198	CCAATAGTTGTTAGAGAACGCTTAGCATGTAATACTTTT
2layer-199	TTGTAATTGCGAAAGGGGGAGCGTTGCTGTAAAG
2layer-200	TTTTTTGGTAACGCCAGGGTGGAGTTTTTT
2layer-201	ATAGATAAAACAACTCAGGAGGGCCAGAACATATA
2layer-202	AAAATCGCGCAGGAAAAACGGATTGCCAATAGATATGCAGA
2layer-203	GTTACCAAAAAGTAGGGAGGTTTGAATTGGAACCTCCGAC
2layer-204	TAGAGCCAGCAACCGCAATTATCACCGTAGAACCGCGCCACC
2layer-205	TTTTTTATTAGAAGTATAAATCCTTGCCTTTTTT
2layer-206	AAGAATACACCAACTGAAAATCTCAGGAGAATAATTTTC
2layer-207	TGCGATTAAAGAATGGTTAATTCAAGTTTAATGAATAT
2layer-208	CGCATTATAAACGTAAAATTTAGAATTATTCAACGCAAG
2layer-209	ACAATGTTCAAACGACGCCATCCACACATGGTCA
2layer-210	TTTTTTCCGCCACGCCAGTCCGTTTTTTT
2layer-211	GAAGGTTAAATCAAGAGAACGTGAGTCTGTCTTAAC
2layer-212	AGATGATGAAACGGTAAGGCATTATTAGACGACGACAAAA
2layer-213	CCCTTTAATAGCATAGTGCTATTGATAAGCCTAAATCA
2layer-214	AAACGTCACCAATTAGAACATCACCAGTAGGGTGTATGTTGATA
2layer-215	TTTTTTTTAGGAGCACTATACATTGAGGTTTTTT

Supplementary Table 12 | DNA sequences of 24helix DNA origami (Scaffold 8064)

Name	Sequences
24helix-1	ATCACCGAGCGACACATCGATTAGCGTTGCCTTAAGGTCA
24helix-2	TAGACGGCAATAGCATAAGAGGAAACGCAATAACCTTCCAGA
24helix-3	ATCCCATTTCATCGCGAGAACCGAGGCCTTCTAGAACCGGTA
24helix-4	CTTAGGTTTGAAATCATCTTGTCTAGTACTAGATTAC
24helix-5	TTAGAACACGGATTACCTTTCAAAAGAAGATGCAGAATTTC
24helix-6	GAAGATAATCAATACTGAACCTAACAACTAACCTAACATATC
24helix-7	AGCGTCAATTCTGACCCCCGCCAGGCGGATAAGATAGGGGT
24helix-8	TAGAGCCATTAGAGCGGAAGCATTGAGGATAGCG
24helix-9	AAGTCAGTTAAATAAAAATTGAAGCCTCTGTTA
24helix-10	AATCAATGGAACAAGTAACAATTTCATCCATGTCA
24helix-11	CTGATGCTCACGGATTCTCCGTCCCAGGCTCT
24helix-12	TAAAACATTCTTGCCCTGCCGGCGGTATCACATCC
24helix-13	AGAGGTGTGCCGGTACCGGTACACTGGTGTGTTACGATCC
24helix-14	TTTCTGTAAACACTACGAAAGGCCACTAACAAACCA
24helix-15	TGTACTGCGAACAAATCTACTACCAGTCTTCATC
24helix-16	AAGGAACCGCCTCCATAATCAGTGAGGCAAAGACATATT
24helix-17	TGATTACGCAGTATCAAATTAAACCGTTGAAACGATAGTT
24helix-18	CCAAGATTAGTTGCATCACTGCCTGAGACAATAAATAT
24helix-19	AAAACAGTAGGGCTGGTAATATCCAGAATAGATTAATTA
24helix-20	CCAATTTCATTGAAAAAACGCTCATGGTATTCTTTT
24helix-21	CAGTATTAGACTTCTGAAATGGATTATGAATGGCTTCT
24helix-22	GAACATGGTTCTAGAATCAGAGCGGAGTTCTCA
24helix-23	CCTGTATCACCGTATTAGACAGGAACGCCCTGAGCCG
24helix-24	GTCTGTCCGCATATGGTTACGATTGAGGGATAGCCGAACAA
24helix-25	TGATTAGAATTATCCAATCCAATGAAAATGATATAGAAGGC
24helix-26	CTATCGGAGTAATTCTGCCAGCAGAACGCTAACACCGGAA
24helix-27	GCCATTGTGTAAAACATAGCATAGTGAATGCAGAGGCGAAT
24helix-28	TGACGCTGCAGGAGCGGAATTATTCAAGAGGA
24helix-29	CCGATTAAGCCCATTGTACCGTACGCCGTAGAAGGATTAGGA
24helix-30	TGAGAACGCTGAGGCAGGTACAGTCCTCATTATTCATCGGCA
24helix-31	AGTGTGTTCTCCGGTCAGGAGCAAAATACCGAATTAACTTAATTGC
24helix-32	AAAATCCGTAATGTCATATATAGGGTAATTGAGTAATTACGAGTCAAA
24helix-33	CAGCAGGACCGTAACCTCGTGAATCGGCTGTGGTTATACCGTGCA
24helix-34	GCCCTGAAGAACAAATAGCTAACTCCAATCGCACCATACTAAGTTGGG
24helix-35	CACCAGTCATCCCTAAAGGTGAAATAAAGAAAAC
24helix-36	GATGGCCCCCAGCGTACACTAATGGGATTTCGCATGGCTTTATCATC
24helix-37	GTGGACTGGTAGAAGAACTAAGTAATAAGTTTACCGACTTGTAAATGCA
24helix-38	CCTTTAATTCCAGTAAGCCGGATTGCTGACTATTATAGTCCCTACTG
24helix-39	TGCCTGACTTATAAAACATTAATAAAAGCAAATTAAAGCAATAAAGATT
24helix-40	CGGATTGCGAAAATATAATTCTAACCAAATTGGTTAAATTGATGTA
24helix-41	GAGACCGCGAGAGTTATCGGCGGGAACGGAGCTTCAGAGGTGTTTACG
24helix-42	TCATAAAAGAGACGGCGCTTCCCAGCATGCAACCAGCTACGATACGGA
24helix-43	TTTGACCCACTACGAAGTTCTGAGGACTGGGTAGC
24helix-44	TATTACACCAACGTACCTTATATTCAAAGTAAATTGGCTTCTTAATC
24helix-45	TGAATCATTTGATAAGAGGTCCGAGATAACTAAA

24helix-46	TCACCCCTGTAGGTAAAGATTGTTCCGAATTAAATG
24helix-47	TCTGCTTGGGATAGGTACGACGCTGGGGAAAGA
24helix-48	CGGTTGGCGGATCAAACCTTACCCCTCAAGCCGCACAGG
24helix-49	GCCTGAAATTATACCAAGCGCCCGTCTAGTTACTT
24helix-50	GATACACAGATTCATCAGTTGCACTATTAGCAACA
24helix-51	GGAATGAATGAAACGAATCAAGTTGCGGAAATCA
24helix-52	CTCAACGCCAATATATCTTACCGAAAATAACAAG
24helix-53	TTCAATGCACTCATTAGGAATCATTAGATAAGTAA
24helix-54	ACGACGAGTTAATTACCGACC GTGTTGAGAGAGA
24helix-55	ATAAACATAACAGTCGCTGATTGCTGATTATAAG
24helix-56	TAATCACGTCAGATGAAGAACAAAGTTGAGTGCCCAGGTGCTG
24helix-57	TGCCGCCACCTGTCTGGTCAGTTGTAACGAACCCAGTATT
24helix-58	GAAATGGGTTAATGAACATGAAAGTACAGTCTCCT
24helix-59	AAATAAGAGGTTGGAACAAAGAGTCAGATTAGGAATT
24helix-60	TTCTACCAAAATCAAAGAACATAGCCATTTGCGGAAA
24helix-61	ATTAATCAAAACCTGTTGATGGTAAAAGGGTGAGAGG
24helix-62	TTTATAATCAGGAACAACGTGGCGAGAAATCATAGTCA
24helix-63	TGTGGAAACAGCAGCAAGCGGTCTTGGTAGATGAA
24helix-64	CGGTTGCAGGGCAACAGCTGATTGAATTCTGCTCACG
24helix-65	ACGGTGAATTCAAAGGGCGAAAAAGAACAAAGTACAT
24helix-66	CTATCATGCTACGAGGCATAGAATAGTACAAAAGAACATGA
24helix-67	GTACGTGAACATGTTAAATATTCGCTAGATTCCAATAA
24helix-68	CCGGACCAACCGTTCTAGCTGGAACGGTGTCTGGATTGTAAA
24helix-69	TCGCACCCGAGACAGTATCGGCTGGGAAGTCGCCACCAGTCA
24helix-70	CCAGTAAAATCCCGTAAGCTGGCAACGCCGGITGCCAAC
24helix-71	AGCGCGGTTGTGCCCCCTGCATTCTGCCCCCTTGTTCCT
24helix-72	AGCCGTTTCCCGCAGCTGCTCAGCGCGAGGACATAAGGCT
24helix-73	CCTCGTTTACCAAGATGGTTAGCGATTAAAGAACAGAAC
24helix-74	TGGAAGTTTCATAAGCAAAGCAAAGACTTCAAAGCAGGGTTG
24helix-75	TTTGCCCTCAGAGCTGACCCCTGTAATAAAATCGGC
24helix-76	TCCGGGCTCATTTCGCTCTGGCCTTCATTGCC
24helix-77	TTAGTGATGAAGGCCGCCACGAAACGTACAGCGAACCGCCTG
24helix-78	CACTGCGCGCCTGGAGGTGTGCACTCAATCCGAGTTCTTT
24helix-79	AGGCGCAGACGGAGAGGCTTCATTAAACGGTATTAGGGC
24helix-80	ATAACAGTTGATTCCAATCATAAAATCGGTGTGTC
24helix-81	TCTACAAAGGCTATCAGGTTAATAGGAACGGAGGGTAGCTAT
24helix-82	GGTTTATCAGCTGAAAGACTTCTAGGCTAAAATTACTT
24helix-83	CTTCTGGTGCCGGAAACCACAATAACCTCATCCAGCCAGCTT
24helix-84	AGTTAACGATGCTGATTGACCAGCGGGTGGCCT
24helix-85	AACGGCTGGCACGCATTGGAAGTCTTCGAGGTGCCGACCACA
24helix-86	CATAAGGGAACCGAACTGAGTCTTAATCAGAACG
24helix-87	CGATAAAAACAAATAGCCATCAAAAGATAAC
24helix-88	CGGAAACTCACAATGACACCATGGCAACCCCTCA
24helix-89	AGAATTGAAATAATCCAGAGTCTTACCATCAATT
24helix-90	TAAACCAAGTACCGACGAGCCACATGTAAAAACAGG
24helix-91	TCAAATAAATTTCCTCTGTCAATATAAGGCGAT
24helix-92	AGTGAGAATAGCAAAGAGCCACGCCACCTGCAGGG
24helix-93	TGCCCGTCCAGCATACCAAGAACAGAGCCAATCAAC
24helix-94	CGTCTTACGAGAGGCTTGTAAATGTTAGATCTTCATAAA

24helix-95 CAGAATTAGTCTGCGAACGAGAAATGGTTGTAACG
24helix-96 CCTTCGCATCATTGCCCTGAGAAATCGTAGAGCGAA
24helix-97 CCCCAGTGCAGGCCAAAGCGCCAGGCATCCGTATGC
24helix-98 ACCCATCCCCCGTTCCGGCAAGCCTCCGATATGAA
24helix-99 GTCGCGTGCACTCTGTGGTGTGCCGCATCAAAGCCTGGAGTGT
24helix-100 TTAGAACGACCAACTTGAAAATAGGCTCAGTGCCGTCGAGA
24helix-101 TCCAATACGCAAACAATAGAAAATTAGCAAGAAAAATAATGCTGTAG
24helix-102 GCTATAGGCGTCTTCAGCCATATTATCGAAGCAAGCCATCAATATGATA
24helix-103 ATCATCGGCATTTCAAAAGGTAAAGCCCTGACCTGACAGTTGAGGGG
24helix-104 CGCTACGAACCTTGCCTAGAACATCGGAGGTGTACATCGAC
24helix-105 TCATAACTTAAAAGAAACCACCAACTCAAATATGTGCAGCCAGCGG
24helix-106 ACACGAAGGCCATGAGGTGAACCACCACTAAATCGGTC
24helix-107 CTGGCCCGCTTGCCTAATATTGGGCGCCAGGCAGCAAATCGTTCA
24helix-108 TCGCCTGCACCCTGCCAATAGGAATACCTATTAGATAAAATTGTGTC
24helix-109 AAGAGAGAGCCGCTGACAGGAGGTTAACGAGCAAAATAACGCCAAA
24helix-110 AATGCTTCAAAAATCAGGAATCGTCATAAATATAAGTTGAAGTCCAT
24helix-111 CTAATCAGGCAAGGAAATTGGGGCGCGAGCAAGCAAACAAGAGAGA
24helix-112 AAGATTGATTTGTTAAACCGGTTGATAATCATCTTCAGGCCACACCG
24helix-113 TAAGTTGGTAAAACGACGGAGCTGGCAAAGGAAACCGTTTGAGGTAA
24helix-114 GTCTGGTCCGTCGGTGGTGGCCTGACTTGACTCACG
24helix-115 CGAATTTCATTGTTAATGAATGCGCGGGAGCACGCACGATTA
24helix-116 AGTTAACGAAAGACAGCAAACCGATATTCGAAGATGAACACTCAAT
24helix-117 GTAACAAACGAGAAACACCGACAAGAACCGGATCGAGTTGGAGACGA
24helix-118 CCATAAATAAACAGAGAGGCCACCACCGGCGGAATATAGACTGCTTC
24helix-119 ATCATACTAGTTAACGACTCCTAACCTAACCTAACATTCAATAACTTAT
24helix-120 CGTTAATTATAAGCAAGCCTTAAATCAAGTAATAAAACTAGAAC
24helix-121 TCAGCAGGGCCGCTTACAGGGCGCGTACCCACCCCTAACG
24helix-122 CGACGTTGGTAACGAAGCCAACGCTCATAAACCTGTTGCGGAATT
24helix-123 GGCAGCACAGCAGCATTACATTAACTTAAACATTGCCAGAGGAGC
24helix-124 GTGTGAAGTAATCAGAGGATTAGAACGAGATAGAGTC
24helix-125 TGCCCTGAGCTGCTGCCCGGAATAGGCTCCACCACGGCTGACCAGG
24helix-126 TTAGCATGGAAGGTAAATATTTCACCCAGCGCCACCGAGATAACATA
24helix-127 ATAACGTCAGCCTTACAGAGCGTAAAAATAAGTAGCAATTTCATCC
24helix-128 GAACGATCTGTTATCAACAAAGCTAATGACGACGTAGAAGAACACG
24helix-129 GAAAAGAATCAAATCATAGGAGAGTCAGATAGCTCAATTAGTACAT
24helix-130 GTTTAAATAATCCTGATTGTTGATGGCAATCATCAAATACCAATTAAAT
24helix-131 GTTTCGAATTCCACAGACAGCAACTACAAACACTGAGCTAAACCCCTCA
24helix-132 TGAGTGTGCCAGAATGGAAAGAAATAACGATTGGTACGCCACCGCCA
24helix-133 AGCAGAGGAAATAGGAAGTAGCACCATTACTATTCAATTAAAGTGGGAAT
24helix-134 AATCAAGTTTATTCCGCTAATATCAGAGTAAAAACAGGGACTGAACA
24helix-135 AAGAAGCTTAATGGTGTCCATTACATTCCCTGAACAAGAAAGAAAC
24helix-136 ATCGCTTAACAATACTAACGAAAGAACGCCAACCTTTAACGTTAAATG
24helix-137 GAATTAAACCTCAAATTGCGTAGATTTCCTCTGAATAATTGCACG
24helix-138 CAAGAGCACCTATTATAAACAACTTCAATAGCGTAACGATAATGAAT
24helix-139 GCGCGAAAATCAGTTCAACGGGGTCAGTGCTGAATTACCGTACAGGAG
24helix-140 TTTTCAGGGCGACAGACCTTACCGTCAGACTGTA
24helix-141 AGTTATTGTTAAAGGCCCTTTAAGAAAAGTA
24helix-142 TTATCAACATGTTCTACCGCGCCCAATAGCAAGCA
24helix-143 TCATAACGCTGAGATCGATAAAAGGCCTTAAAT

24helix-144	TATTCTTATCAGATTGTTGAATACCAAGTTACAAA
24helix-145	AGGTTATCTAAATTAGTCTTATGCAAATCAACAGTTGAAAG
24helix-146	TTAGCTTCACAAACCGTTAAGAGGGCTGAGACTCCT
24helix-147	TAGCCCCGTCTTCAGAGCCGCCACTCATCAC
24helix-148	AGGAAACCACATCACGGTTAGCAAACGTAGAGGAAC
24helix-149	TTCTAAGTAATAACTATTTGCACCCAGACCGGG
24helix-150	TAGAAAACCTTGCTTAATTGAGAATCGCAGCTTAC
24helix-151	AATTACCCAACAGGATTACCTTTAAGAAAAAC
24helix-152	TTTAGGACAATCGTACAAACAATTGACTAGATAA
24helix-153	TTTGCTCAAGGGATCTCAGGAGGTTAGCCGATAT
24helix-154	TTGGTCACCAACCAGACAGACCACATTCAACAGCCATTGTGAATT
24helix-155	ACAAGTTAACAGGATGCTGGCTTAGAGCTGAACACCAGCGCAT
24helix-156	AAAAGTACCGTGAGCGAACAGGCCGGAGACAGCATGTAAATAAT
24helix-157	ATTTATTTAGATAGACAAGGCGCATCGTAAACTATATCCTCCGG
24helix-158	GCGTATACAGCTGTTGCCCTTGCCGCCAGCAAATTATGGAAGGG
24helix-159	GGGATAGAAAACCTAACAAACCTAAAGGGTTAGTACTAAAGT
24helix-160	GACAAAGCATACTCGGGCAACGGCATCAGAAGGCGGTACCAGCA
24helix-161	CCGATAAACAGAACGAAACACGGAGATTGTGATGATTCCAGTA
24helix-162	GAATACCCAAAAAAATAGATACATTATCGCGTTAAAACCTCCAAAGGC
24helix-163	CCTCCCGACTTGGAAATCGATATACTTTGCCGGATTAGAACCCCACA
24helix-164	CCAGTAACCTTCCAAGTGCTGGACCAGTACACCGGAAGGGAAGAA
24helix-165	GTTATACAAATTAGCAACTGTCTCTGTAGCCAGCCCCGTCGAAGGTAT
24helix-166	ACAAACATCAAGATTCTCGTCAACCATGTTACCACTGGTGAGACTTT
24helix-167	GAGCCGTCAATAATCGGGGTTCCCGGGCGCGTTCTGG
24helix-168	GGGTTGCTACAGACCCAAAATACGTAATAGGCAAACGAGCGG
24helix-169	TCAAAAGAGGGGGTTAACTGGCTCATTAGTTAACCAACAG
24helix-170	GGCATGAAGCATTAAACATTCAATTGAATCATATAAAAAAAACTAAAGA
24helix-171	GGTTTGAAATATTTATGAAAAGGTGGCAACGCTACTACAATACTTCTT
24helix-172	CAGTATACCAGGGTTGAAAAGCCCCAATTAGGCCATATTTACTCAA
24helix-173	AAAATTAAACCGCAAGGGATGTGCTGCATGTGAGTTGAAACACCGCCA
24helix-174	TACATTTGGTCATAGGAACGTCAGCGTACGTTATAACTCGTTACATT
24helix-175	AAGTATACATTCACTGGCGCTGAGGCTCTCAGAATACCGCCCAGGAGG
24helix-176	CGGAACCTTCAGAAAAATTCAATTACCAACCACCCCTCAGAAGAATCC

Supplementary Table 13 | DNA sequences of *p6mm* DNA lattice

Name	Sequences
XY9-IN1	GGGCTCCTGACACTACAGTCAGATGTAGCCATAT
XY9-IN2	CACTTTCATTGGGAGAGCTATGCGTTCGAACG
XY9-IN3	GTTCCGACTATGCAACTACGTCACTGTGCACATA
XY9-IN4	CCAGTCAGGGTGTGGCTAAATTATAGGCCAATCC
XY9-IN5	CTGATCGGACGAAGCCTCAGAATCCTAAACACAC
XY9-IN6	ACTCAACTTTCTTAGCGAGAGGGTCCCTCTCA
XY9-IN7	TTTAATGAAAAGGTCCCCTGTGCGAGATGTA
XY9-IN8	AGCGTGCACTAAAGAGTGTCATCAGACGTTCTTC
XY9-IN9	GACCCGGCACGGTTTGAGTTACAACCTCTCATAA
XY9-IN10	GTTTCTGTCAACTTATATCGGCCGGATACCGGG
XY9-IN11	AAGGTCGTTCAATATTAGCGGATCGGTGCGAAAAA
XY9-IN12	CTGGCACCCATTGGAGAAACGTATCTGTTCATGT
XY9-IN13	GGCCATTCTAATGTAGGTGAATGGAGCATCCGTC
XY9-IN14	TTCGTGCCGTTCTAGTTAGTGCTCCTAGTGAT
XY9-IN15	GTTACTAAGTTCAGACCCATAGGCTCAGCTGGGT
XY9-IN16	CTCCCTACCTCTCCTGGCTCTATGAAGTCAGTCT
XY9-IN17	GGCAGTAAGGGAAAACGTAGTACACTCGAGAGT
XY9-IN18	AAGGCCTTGACTAATCGAGTTGGATGCATCG
XY9-IN19	GGTATTAAACCGCATTAAACGTGAATCCGACCCGTT
XY9-IN20	TAGCCAAACGTAGAAGGGTCTCATGTATTGCCA
XY9-IN21	GATCCCTGAGCCTTAATCGCGTTAATAGGGACCA
XY9-IN22	ATCAAATGGCGACGTCAAGGGCCTTGATTATGC
XY9-IN23	ATGTTGCTCTACCGGTATGCGTACGATGTCCTC
XY9-IN24	TTCTGAAGTGTTCAGTGGTGGCGTACAAACGT
XY9-IN25	GTCGGATTATTACCCACACGGGACATCAAACAGC
XY9-IN26	CCGGCTTGCATTATGTGGACGTGGAACAGATTAA
XY9-IN27	GGGATGTTGACTGTACGATGACTCTTCCGACTC
XY9-IN28	GTAGCAGCGTTACCATGGATTGCGTATTGAATTAA
XY9-IN29	TATGGACTCTCGGAAAGTTAGTGTGCGTCTATCAACG
XY9-IN30	CCTTCTCCTCGTATCCGTAAAGACACATCAGTT
XY9-IN31	GTCCATCTACTGTCCGGTTCTGTACTCTTGTAC
XY9-IN32	CAGTTAGAATTGTTATGCGTGGAGGATGGCGTAAG
XY9-IN33	TCTTATGAATGACAGGAGGCAGGACTTTGATTGT
XY9-IN34	CATACATCGAACATCTTGTACGACCTGCAAACACTCC
XY9-IN35	GCTTATTGAAAGACTGGTTCTCACCAATTCCGGTC
XY9-IN36	TGTGCTATTCACTCGTTGCGTACCTATAACTT
XY9-IN37	TCGCGCTCAATCTTACATCATATTGGACTCTGGATC
XY9-IN38	AACCTCCGGATCAAATGTCAAACACTACACCGTAC
XY9-IN39	TCGCATGTTGCCTTATACCCGAATAACAGTACTGT
XY9-IN40	TGGTACCTCTCCGAATGATCACACACTACAAGTAA
XY9-IN41	GGAACCAACCAGATACTGTTAGTATGGGGAAACGAAA
XY9-IN42	TGAAGTTAGGAAGTCGCGATCACTAATCTGAAGGC
XY9-IN43	CCATTACGTAGCCAATGTGTACAGCAAACCTCCAATG
XY9-IN44	TTCTGCAAGTGTTCAGTTAACAAACGCGCATCTTTA
XY9-IN45	CAGGATCAAGAGACATTAGCATTGCTACTCCGAA

XY9-IN46	CGATTTCGATTATGTCGGATCGGTAAAGGTTACGGT
XY9-IN47	CCAAGCTGTGATAGGCTTGATTGAATTAGCCGAAC
XY9-IN48	GTACAGTAGTATGTCGTGCCCTCGCGTATCTACTAA
XY9-IN49	CTATCCCTCACGGGACCATAATTGTGTAGGGTATCTC
XY9-IN50	GGGACAGCGATAACAATAAAGCGGAGGTGTTCTATAC
XY9-IN51	CCTAGCAAGTCTACCGTAAGTGTCAATTACACAGTG
XY9-IN52	GCAGTCCATCTCCGAGGGTCGGATAATTATTCTG
XY9-IN53	GTGGCTATATGCCGTAAAGGACTATGACAACATCC
XY9-IN54	GCAGGTAAATCTAGTCAAGCATCGCTTACTCAGCT
XY9-IN55	ATGTTATTCGTCGTGGGACGCTAAAACACTCTATGG
XY9-IN56	GCACGAAGCAGCTGACTATTGACGATCTCAATTG
XY9-IN57	GTCTTAGGAACGGAGGTCTCAGGAACGGTCATTAA
XY9-IN58	GACCGAGAGTCAATGGAGACTAATGTTACCGTTT
XY9-IN59	GTCTCAATCGCTTAGAGTCCGAATCCGTTACGATC
XY9-IN60	TTCAGTACATCTTCGCGAACCTATCGCGCTAATC
XY9-IN61	CGACCTCGTATTCTCAAATCGGTTGACTCCCTGT
XY9-IN62	TCCCAATTGAAATCTAATGGACAAACTGTAGCGGCA
XY9-IN63	AGTTAATT CGC GACCCGGTTAAAACGATTGACAAGT
XY9-OUT1	TTTTTTTCCATAGAGTGATTGAGACTTTTTTT
XY9-OUT2	TGGTGAGAATTTTTTTTTTTCTCTGTCA
XY9-OUT3	GATTCA CGGGATGTTGTCTACTGTACATTAAGGC
XY9-OUT4	GGATT CGG ATGGTCCCTATAATCCGACTTGAGAAAT
XY9-OUT5	TCCATT CAGC CTCAAGGTTGGTCCACTAGGAA
XY9-OUT6	TCGTTTAAGCTGTTGAGTTGGCTATAGTCAGCT
XY9-OUT7	TGTACTACTC GGGAGTCTAACTTCAGGTCTGAA
XY9-OUT8	CGGCACCAGTATAGAACGAGGGATAGTGACGTCG
XY9-OUT9	AGAGTCATCACTGTGTATAGCCACACATAATG
XY9-OUT10	CACAAGGCCTTACGCCAGGAAGAAGGAGTTGCAT
XY9-OUT11	TACCGCAATT TTTTTTTTTTTAAACGACTG
XY9-OUT12	TTTTTTTTGCCGCTACGAATTAACTTTTTTT
XY9-OUT13	AGCACTAAACAGTACTGACGTAATGCCAGGAGA
XY9-OUT14	ATGCAATGCTGAGAGGGAGTGCACGCTAACTGAACA
XY9-OUT15	TCATAGAGTAAAGATGCCAGGTACCACTACATT
XY9-OUT16	GTCTTACATT TTTTTTTTTCCAGTCTT
XY9-OUT17	TTGCTGTACCGTTCGAAATGCCGGTCTAATGTCTC
XY9-OUT18	GT TTTAGCGGAGGACATCCAACATCCCCGGT CGC
XY9-OUT19	TTTTTTAAACCGTATGTACTGAATT TTTTT
XY9-OUT20	CAACA ACTCATT GGAGTCCGGAGGT TAATATTG
XY9-OUT21	TTAACCGCGAGAATAAACGCTGTCCCTACCGTA
XY9-OUT22	AGTCCTCGCTTTTTTTTTCGGATACGA
XY9-OUT23	AGTTCTGAAACGGGTCGCAAAGCCGGATTAGATT
XY9-OUT24	TTTTTTGATCGTAACT CCTAAGACTTTTTT
XY9-OUT25	ACCTCCGCTGACGGATGCCTTAGTAACACGGTAGA
XY9-OUT26	TTTTTTTACTGTCAAACGAGGTGTTTTTT
XY9-OUT27	TCCTCCACGTTTTTTTTTTAAAGATGTT
XY9-OUT28	TATAATTGGAGTTGCCAATAAGCCACTCTTA
XY9-OUT29	AGTTTGTCCGAGTCGGAACTTCAGAACGGAAGAGA
XY9-OUT30	TTATT CGGGTACATCTCGTCCGATCAGACGTATCTG
XY9-OUT31	CCCTCTCGGACCGAAATAAGCACACAAACCG

XY9-OUT32	TTGTAACTTAACCAATTCTAACTGAGGCTTCG
XY9-OUT33	TACACAATAAGACTGACTCTTACTGCCTACGGGCA
XY9-OUT34	TCTGATGAAACTGATGTCGCTGCTACTGTAGTGT
XY9-OUT35	CATCTGACC GTT GATAGTAGATGGACAGCCACAC
XY9-OUT36	GATACGTTGATCCAGAGCTTG CAGAAGTTCCC
XY9-OUT37	GGATTCTGGTACAAAGATT CATAAGACTAAAGAA
XY9-OUT38	ATTCAAATCCGATGCATCGGTAGGGAGCCCTCGGAG
XY9-OUT39	CGATCCGCTTACTTGTATGAGCGCGAATAAGTT
XY9-OUT40	AGGCCCTAACCGTAAACACAGCTTGGCCTTCTAC
XY9-OUT41	AGTGACGTACAATCAAAGAGTCCATATCTCCAA
XY9-OUT42	TTTTTTTTAATGACCGAATAACATTTTTTT
XY9-OUT43	TTTTTTTCAATTGAAGCTCTCGGTCTTTTTTT
XY9-OUT44	AGCCTATGGTACCGTATAACATGCGATCTCCAAT
XY9-OUT45	CATGAGACTTAGTAGATCTTGCTAGGCTTGAAAC
XY9-OUT46	CCCATACTATTATGAGAGCAGGAGCCATGTAAGAT
XY9-OUT47	AATGACACTACTCTCGAGCAAGGCCTTTGACTAGA
XY9-OUT48	AAGCGATCCCCGGTATCCGGCACGAATTATTGTAT
XY9-OUT49	CCACGTCCGAGATACCCATGGACTGCGTGGTAA
XY9-OUT50	AGGTCGTACTTTTTTTTTTTCCCGGACAG
XY9-OUT51	ACGACACTATTTTTTTTTTTCCATGGTAA
XY9-OUT52	TCCAATATGGAAAAGAACGAGTCGGA ACTATAAGGCA
XY9-OUT53	CGCATAGCAAGTTATAGCGATGTATGGGACCTT
XY9-OUT54	TTTTTTTACAAGGAAGCAATTGGGATTTTTTT
XY9-OUT55	GTACAGAAATT TTTTTTTTTTTT CATAAACAA
XY9-OUT56	GTACGCGACTTTTTTTTTTTTACTTCGCA
XY9-OUT57	GTGTGTGATATGGCTATGAAAAGTGACATTGAT
XY9-OUT58	TTTTTTTGATTAGCGCGCTCGTGCTTTTTT
XY9-OUT59	CATAGCCTACATGAACAGACAGAAAACCGACATAA
XY9-OUT60	ATTAGTGATGTGTTACCTGACTGGCATT CGGA
XY9-OUT61	TGTCCCGTGTTCGGCTATTACCTGCCGTACAGT
XY9-OUT62	CTTACCGATTTTCGCACAGAATGGCCTGGTCCCGT
XY9-OUT63	ATCGTCAAAGCATAATCAGTTAACCTCCCACGAC
XY9-OUT64	GTAGTTGGTATGTGCACAAGTTGAGTCGCGACTTC
XY9-OUT65	ACCGAGGGACCCAGCTGAACGACCTTAAGCCTATC
XY9-OUT66	GCGTTGTTGGATTGGCCTTCATTAAAACATTGGCT
XY9-OUT67	CGGCCGATTTCGTTCTTGATCCTCGGATTAGT
XY9-OUT68	GATAAGTTCTGGCGAATATCAGGGATCGACCTCCGT
XY9-OUT69	ATTATCCGAATCACTAGGGGTGCCAGCACGACATA
XY9-OUT70	AACATTAGTACGTTGTAGAGCAACATCTCTAAAGC
XY9-OUT71	GTACGACAAGCTGAGTATCGAAATCGTTAATGCG
XY9-OUT72	TCAACCGATTAATCTGTTCCATTGATCTCCATTGA
